A Neurobiological Investigation of Visual Target Detection and the Optic Lobe of Dragonflies

Joseph Mahandas Fabian

Discipline of Physiology
Adelaide Medical School
The University of Adelaide

August 2017

A thesis submitted for the degree of Doctor of Philosophy

Table of Contents

i. Thesis Abstract

For many decades the insect nervous system has provided novel insights into the mechanisms of visual processing. Despite commonly being labelled as ‘simple’, recent evidence suggests that some insects have remarkably complex brains. Guided by a brain the size of a poppy seed, dragonflies detect and pursue prey amongst cluttered backgrounds with high success rates (Olberg et al. 2000; Combes et al. 2013). These pursuits are not simple reactionary processes, instead the brain uses internal models and selective attention to maximise performance in challenging conditions (Wiederman and O’Carroll 2013; Mischiati et al. 2015). However until now we have no detailed and up-to-date description of how the dragonfly optic lobe is organised, and little understanding of the strategies optic lobe neurons use to detect and track visual features.

My initial work describes the morphology and organisation of the dragonfly optic lobe, the most complex optic lobe of any insect studied to date. I demonstrate that in contrast to recent reports, the dragonfly lobula complex differs substantially from its dipteran counterparts. Furthermore, both the second and third optic ganglia contain approximately twice as many synaptic layers as any other insect.

Next I performed a series of electrophysiological experiments that investigated the effects of target trajectory on the responses of target-detecting neurons. A small feature drifting across the retina generates a weak and variable signal. For this reason the human brain has adopted a strategy where target movement is integrated across a trajectory in a predictive manner, improving signal strength while ignoring distractors (Watamaniuk et al. 1995). I demonstrate that a facilitation mechanism modulates gain across the receptive field of target-detecting neurons, maximising responses to targets presented at a predicted location and suppressing responses to targets elsewhere. This modulation of gain results in large improvements in local contrast sensitivity, and also induces strong direction selectivity that matches the direction of stimuli in the recent past. I then investigated how different parameters of a targets trajectory affect the intensity and spatial spread of gain modulation. Targets of differing velocity, contrast, size, duration and trajectory length were drifted through the receptive field, before quantifying the strength of gain modulation. I show that gain modulation is gated by target contrast, and that the magnitude of modulation is dependent on complex interactions between the parameters of a primers trajectory and the probe that follows.

Finally, I investigated whether this gain modulation was a mechanism underlying the selective attention previously reported in target-detecting neurons (Wiederman and O'Carroll 2013). When presented with two targets simultaneously, target-detecting neurons select and respond to one, and ignore the presence of the other. With the use of a novel frequency-tagging stimulus, I demonstrated that when presented with two competing targets, both the selected and unselected target trajectories induced an increase in gain ahead of their path. This result suggests that predictive gain modulation is not a mechanism of selective attention, but a parallel processing strategy that acts to improve signal strength in challenging conditions.

Finally, I characterised the physiological responses of a population of neurons sensitive to the movement of larger features or patterns. Controlling flight at high-speed would benefit from the detection of low frequency patterns in the environment. We show that bar-sensitive neurons in the dragonfly lobula complex have highly abnormal responses to stimulus velocity. Our data describes the diverse physiological properties of these neurons, including their tuning for motion direction, height, width and velocity, and their sensitivity to contrast of different polarities.

Together, my thesis provides a significant contribution to our knowledge of the visual system of dragonflies. In a broader sense, these findings build our understanding of the structure and function of nervous systems, and the strategies implemented to efficiently solve challenging sensory tasks such as small target detection.

ii. Thesis declaration

I certify that this work contains no material which has been accepted for the award of any other degree or diploma in my name, in any university or other tertiary institution and, to the best of my knowledge and belief, contains no material previously published or written by another person, except where due reference has been made in the text. In addition, I certify that no part of this work will, in the future, be used in a submission in my name, for any other degree or diploma in any university or other tertiary institution without the prior approval of the University of Adelaide and where applicable, any partner institution responsible for the joint-award of this degree.

I give consent to this copy of my thesis when deposited in the University Library, being made available for loan and photocopying, subject to the provisions of the Copyright Act 1968.

I acknowledge that copyright of published works contained within this thesis resides with the copyright holder(s) of those works.

I also give permission for the digital version of my thesis to be made available on the web, via the University's digital research repository, the Library Search and also through web search engines, unless permission has been granted by the University to restrict access for a period of time.

Joseph Fabian

iii. Acknowledgements

I wish to thank my supervisors, Steven Wiederman and David O'Carroll, for their efforts and contributions in the past three years. Their input has been invaluable in all aspects of my candidature, and as friends.

In addition, I would like to thank the past and present members and collaborators in the Wiederman and O'Carroll Labs for their aid throughout this project: Basil el Jundi, Elisa Rigosi, Benjamin Harvey, James Dunbier, Zahra Bagheri, Bernard Evans, John James, Benjamin Baden, Bo Bekkouche, Samuel Polacek, and Matthew Schwarz. Together you have made this project a very enjoyable time.

Finally, I would like to thank my family. Mum, dad, Leo, Shona and many others.

iv. Common Acronyms

STMD	Small Target Motion Detector
CSTMD1	Centrifugal Small Target Motion Detector 1
SF-STMD	Small-Field Small Target Motion Detector
TSDN	Target Selective Descending Neuron
LMC	Lamina Monopolar Cell
LPTC	Lobula Plate Tangential Cell
EMD	Elementary Motion Detector
ESTMD	Elementary Small Target Motion Detector
RGC	Retinal Ganglion Cell
LA	Lamina
ME	Medulla
LOX	Lobula Complex
LOP	Lobula Plate
LO	Lobula
PLO	Primary Lobula
ILO	Inner Lobula
MLO	Medial Lobula
SLO	Sublobula
LCD	Liquid-Crystal Display

v. Author's Comments

This thesis is presented in the format of thesis by combination. This means that the results presented include a combination of published articles and traditional results chapters. Publications within this thesis are in the exact form of the original article as published, or as submitted, except that font type and size has been altered to allow a consistent format throughout the thesis, and figures have been inserted into the text at the appropriate places.

In text references to figures are as they were in the published or submitted manuscript, but are captioned based on their chapter and figure number eg. Figure 1 in Chapter 2 is captioned as Figure 2-1.

1 Introduction

A significant portion of neuroscience research ultimately revolves around one central question: What strategies do neurons use to efficiently encode information? The human brain is the most complex biological structure on earth, containing approximately 86 billion neurons (Azevedo et al. 2009), each forming an average of 7000 synapses (Pakkenberg et al. 2003). Limited by current technology and knowledge, insight into such questions may be more readily observed in organisms with smaller, less complex brains.

Consider a small insect such as a dragonfly encountering a swarm of prey. Armed with the limited resolution of a compound eye and a brain the size of a grain of rice, dragonflies can select and extract tiny visual prey from backgrounds cluttered with distractors. These pursuits are highly efficient, with dragonflies successfully capturing their meal in over 90% of attempts (Olberg et al. 2000; Combes et al. 2013). However the neuronal computations that allow such robust and accurate performance in a system with limited resources are poorly understood.

In the following introduction I will describe the current state of knowledge regarding the structure and function of insect visual systems, with an emphasis on dragonflies. In doing so, I will describe the known physiological and neuroanatomical pathways involved in motion vision, target detection and tracking, and some of the higher-order physiological properties of these pathways. Finally, I will review work that investigates the detection and extrapolation of small moving targets in vertebrates. Together, this background information introduces the central focus for my thesis, which presents a novel and detailed neurobiological investigation of the dragonfly visual system.

1.1 Behavioral strategies for tracking and pursuit

Many organisms must detect the motion of targets in order to see potential food, mates or predators. Animals have evolved behavioural strategies that maximise their chance of success, while minimising their own energy expenditure and risk of predation. Some of nature’s most spectacular examples of target tracking and pursuit are observed in flying insects.

During aerial pursuits, most insects keep their target in a fronto-dorsal position on their eye. This behaviour has two purposes; it maximizes target contrast by displaying features against the bright sky, and it holds the target in the area of the eye with the highest spatial resolution (Kirschfeld and Wenk 1976). Flies pursue small targets, often with the intention of capturing mates (Land and Collett 1974). During pursuit male blowflies use body rotations to fixate targets in the frontal visual field (Wehrhahn et al. 1982). This allows the fly to simply copy the track of its target, a strategy commonly known as smooth pursuit. This is a simple strategy, however it is energetically expensive because capturing your target is only possible if you fly faster than them (Boeddeker et al. 2003).

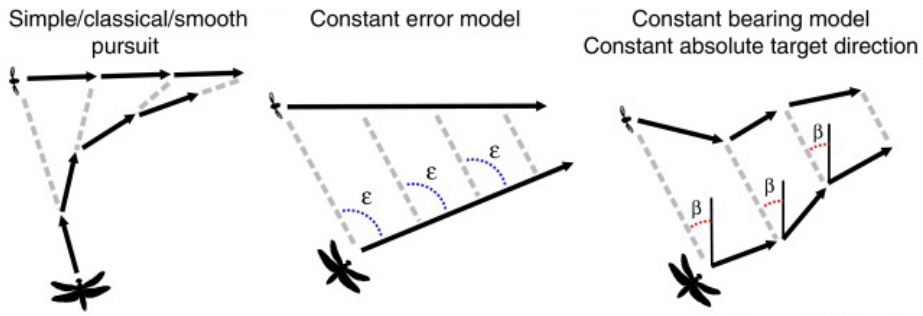

Figure 1-1: Three common pursuit strategies employed by animals to capture small moving targets. Reproduced from Figure 2, Gonzalez-bellido et al. 2016.

Larger hoverflies, small predatory flies and even humans use a more advanced tracking behaviour, the constant bearing angle (CBA) model (Collett and Land 1978; Diaz et al. 2009; Gonzalez-Bellido et al. 2016; Wardill et al. 2017). This model postulates that by maintaining a constant bearing angle, the pursuer is guaranteed to eventually intercept the target. This strategy is favourable over the smooth pursuit strategy of blowflies, since interception flights can be performed while covering a shorter distance at a slower speed.

Until recently it was thought that dragonflies use a similar CBA model to guide visual pursuit of prey (Olberg et al. 2000; Olberg et al. 2007), driven by a reactive neural autopilot (Gonzalez-Bellido et al. 2013). However recent work by Mischiati et al (2015) demonstrated that dragonfly prey pursuit was inconsistent with a CBA model.

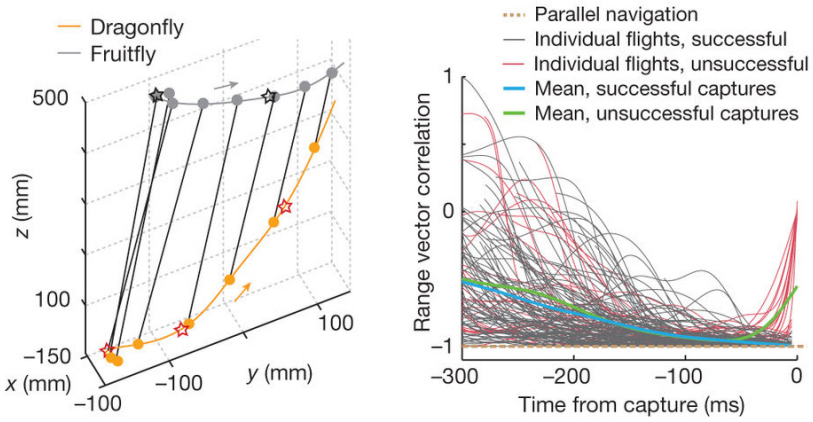

Figure 1-2: Reconstruction of a dragonfly's pursuit of prey. Reproduced from Figure 1, Mischiati et al. 2015. A) Black lines represent the range vector, and stars represent major turning events. B) The correlation between range vector and its derivative, plotted over time for a series of prey pursuits. The CBA model proposes that these values should be perfectly anti-correlated, with range vector correlations close to -1.

The authors demonstrated that prey-image drift is minute and poorly correlated with the angular velocity of prey. This means that reactive control strategies are unlikely to be effective for controlling dragonfly steering during pursuits. During pursuit target movement across the retina is not only dependent on relative prey translation, but also on rotations of the dragonfly's body and head. Mischiati (2015) found that rotations of the head were equal to the combined effects of the dragonfly's body rotations and relative prey translation, but with opposite sign. This suggests that dragonflies use head rotations to cancel prey drift across the retina, keeping targets 'foveated' on the dorsal acute zone of the eye. The latency of these head movements relative to prey movement was just 4 ms, much too fast to be driven by visual input. Therefore, these head movements must be driven by an internal representation of predicted prey movement and body position.

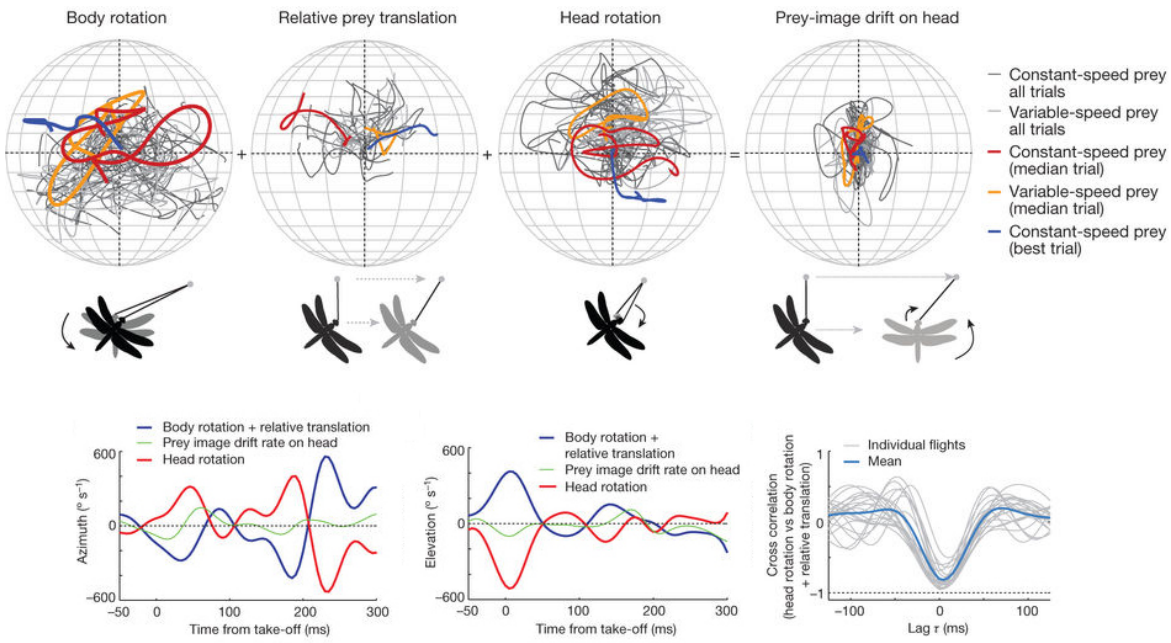

Figure 1-3: Decomposition of prey-image drift into its different sources. Reproduced from Figure 4 and 5, Mischiati et al. 2015. The prey-image drifts relative to the dragonfly eye due to (A) rotations of the dragonfly's body, (B) relative translation of the prey, or (C) rotations of the dragonfly's head. (D) The sum of these three contributing sources of prey-image drift is miniscule. (E-F) The effects of body rotation and relative prey translation are highly correlated with head rotations across both azimuth and elevation, but with opposite signs. (G) The compensatory head movements occur with a very short latency (~4 ms) relative to movements produced by body rotation and prey translation.

1.2 The organization of the insect visual system

The optimal set of sensory apparatus for any given animal is dependent on its behavioural niche. Insects inhabit an extremely diverse set of environments, each coming with their own sensory challenges and limitations. For this reason it is no surprise that the insect visual system contains many unique adaptations and variations, spanning from the compound eye to higher-order brain regions. Here we focus on the visual system of flying insects, and the key structures found in the visual system.

1.2.1 The design of compound eyes

There are at least 7 distinct classes of compound eyes found in invertebrates (Nilsson 1989). Different compound eye designs provide optimal performance in different behavioural niches, each coming with its own trade-offs in spatial resolution, sensitivity, size and complexity. The most common design is the apposition eye, the design adopted by most diurnal insects including dragonflies. Apposition compound eyes consist of a large array of replicated optical sensory units called ommatidia. Each ommatidium is a complex structure containing a corneal lens, a crystalline cone and a rhabdom.

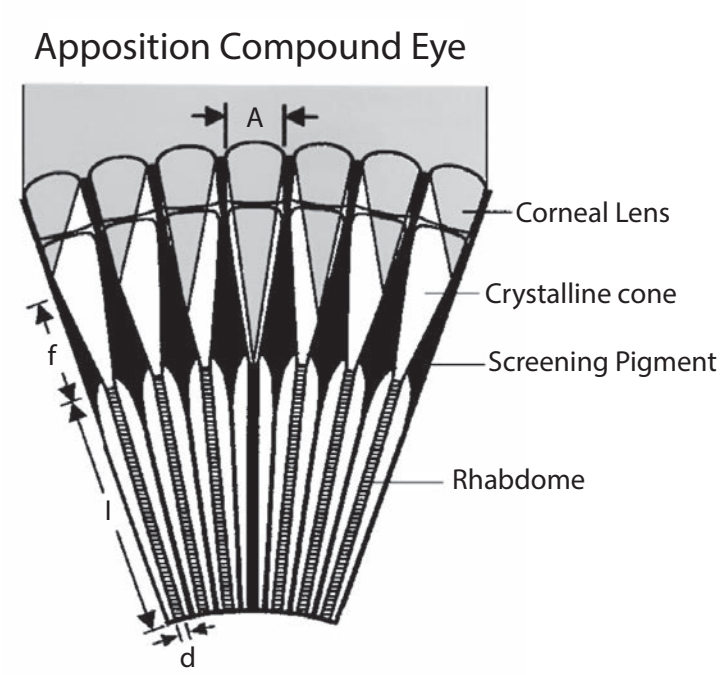

Figure 1-4: Schematic of the Apposition compound eye. Reproduced from Figure 1 of Warrant at al. 2004. The shaded area indicates the paths of parallel light rays entering the eye. A = diameter of the aperture of an individual ommatidium, f = focal length, l = rhabdom length, d = rhabdom diameter.

Incoming light is captured by the corneal facet lenses, and focussed onto a single rhabdom. A sheath of light-absorbing screening pigment cells line the borders of each ommatidium, such that each ommatidium is optically isolated from its neighbours. The Rhabdom is a rod-like structure composed of light sensitive elements containing several photoreceptor cells. The photoreceptor cells of each rhabdom form one visual pixel of the retinal image. Therefore the number of ommatidia, and the angular

separation between neighbouring ommatidia (interommatidial angle) determine the spatial resolution of the compound eye (Land 1997).

Compound eyes are rarely uniform structures. In most insects the facet diameter, interommatidial angles and spectral sensitivities vary greatly across the surface of the eyes (Land. 1989). These variations are not random – instead eyes form specialised regions optimised for specific behaviours. Some insects including dragonflies posses an ‘acute zone’, sometimes referred to as a fovea (Horridge 1978; Land and Eckert 1985; Wardill et al. 2017). This acute zone contains ommatidia with larger facet diameters that decrease diffraction, as well as decreased interommatidial angles that improve spatial resolution. Photoreceptors of the acute zone also have specialised phototransduction mechanisms that improve temporal resolution (Burton and Laughlin, 2003). Together these optical and biochemical specialisations improve the detection of small, fast moving objects such as prey or mates.

1.2.2 The structure and evolution of the invertebrate optic lobe

The ancestors of modern insects diverged from marine crustaceans approximately 510 million years ago, and were among the first animals to exploit terrestrial ecosystems (Misof et al. 2014). In both crustaceans and insects, visual information detected in the retina is processed within a series of neuropil called the optic lobe. The optic lobes of modern crustaceans and insects display several fundamental similarities, serving as evidence for a very early origin of the most basic optic lobe design (Strausfeld 2005). In the 500 million years since this diversion insect optic lobes have evolved many new phenotypes, some of which are highly conserved whilst others are unique to individual families.

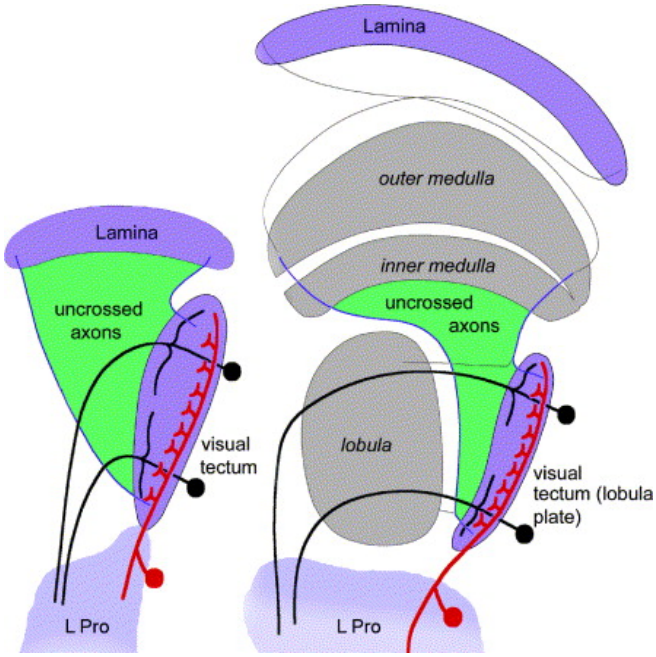

Figure 1-5: Homologous neuropil in the optic lobes of crustaceans and insects. Reproduced from Figure 4, Strausfeld 2005. The common optic lobe neuropil of crustaceans (left) and insects (right), the lamina and lobula plate. In some crustaceans, uncrossed axons directly link lamina outputs to a visual tectum. Modern insects such as flies have evolved two new intermediate optic lobe neuropil (the medulla and lobula).

The optic lobes of most modern insects are formed by 4 retinotopic neuropil, the lamina, medulla, lobula and lobula plate. The lamina is the major direct output target of retinal photoreceptors., though a subset of photoreceptors bypass the lamina and synapse in the medulla. Axons leaving the lamina preserve retinotopic organisation, but their orientation is inverted when entering the medulla such that the most dorsal lamina column terminates in the most ventral medulla column (and vice versa). This crossing of axons forms the first optic chiasm, an axon routing adaptation that minimises the volume and mass of the optic lobe. The medulla is the largest and most complex retinotopic structure in the insect optic lobe, formed by an inner and outer subunit with different developmental origins (Strausfeld 2005; Fischbach 1983). The inner medulla has at least two distinct output tracts, one of which crosses over in a similar fashion to lamina outputs, forming a second optic chiasm that terminates in the lobula. A second tract is uncrossed, and innervates the fourth and final retinotopic structure in the optic lobe, the lobula plate.

Together, the lobula and lobula plate form the lobula complex (LOX). While the organisation of the lamina and medulla are highly conserved across most insects, the LOX comes in many different designs. Most holometabolous insects (dipteran flies, moths, butterflies, beetles) share a common LOX design, the standard 'divided lobula', composed of a lobula and a motion sensitive posterior lobula plate (Ito et al. 2014). The exception to this rule is the hymenoptera (bees, wasps, ants), which have no lobula plate (Ribi 1981; Strausfeld 2005), instead processing motion in a sublobula structure fused to the anterior surface of the lobula (Cajal and Sanchez 1915; DeVoe et al. 1982). The LOX of older insect lineages such as the Orthoptera, Mantodea and Blattodea are highly segmented, with 4 or 5 subunits each (Kurylas et al. 2008; Rosner et al. 2017), but the physiological function of different subunits is poorly understood.

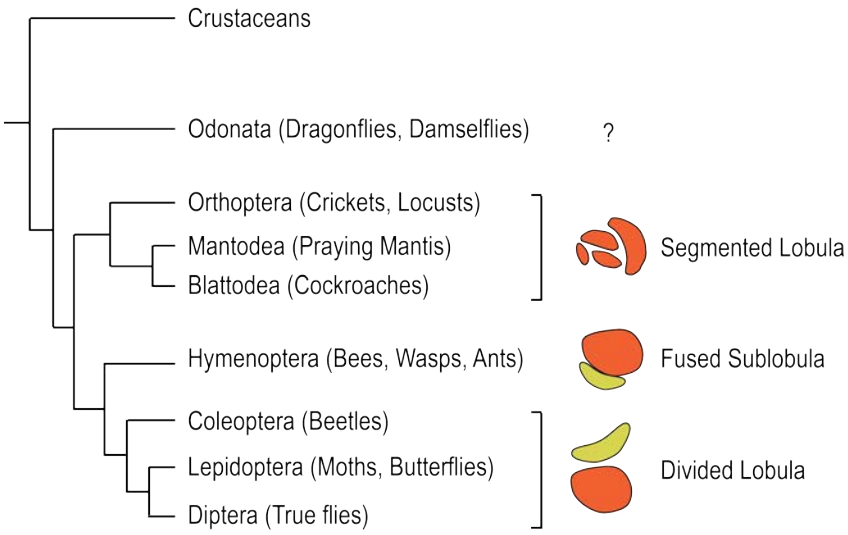

Figure 1-6: The insect lobula complex (LOX) has multiple common designs across insects.

1.2.3 The Dragonfly Optic Lobe

Our knowledge of the dragonfly optic lobe is less complete than that of most other insects, with significant discrepancies in current reports. Zawarzin (1914) provided the first detailed study on the optic lobes of dragonflies, performing methylene blue staining on Aeschna larvae.

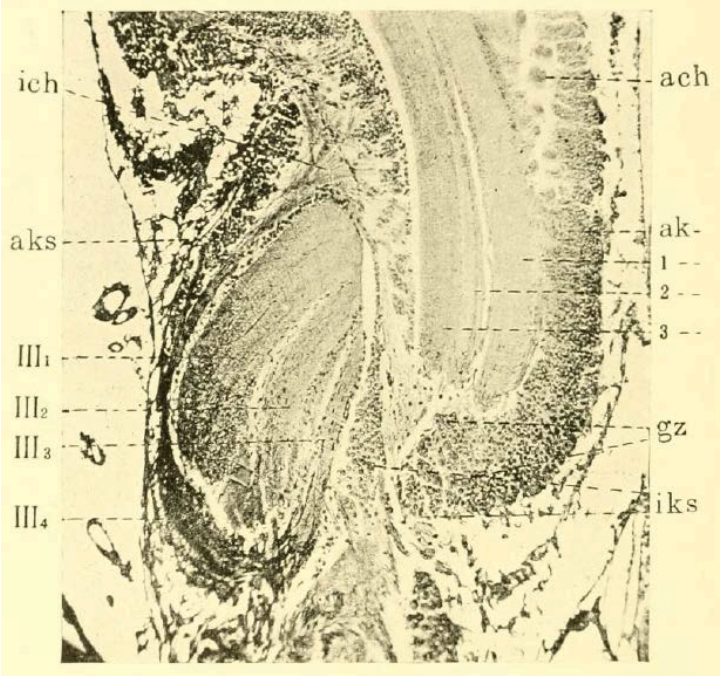

Figure 1-7: Methylene blue stained horizontal section through the optic lobe of Aeschna larvae. Reproduced from Figure 7, Zawarzin 1914. Ach = outer chiasm, ich = inner chiasm, 1-3 = three subunits of the medulla, III_{1-4} = four subunits of the lobula complex.

Zawarzin labels several optic lobe structures, and describes features that vary considerably from the optic lobes of other insects studied since. His work identifies the outer and inner optic chiasmata (ach, ich), and three optic ganglia, I (the Lamina), II (the medulla), and III (the lobula complex). The second optic ganglion (the medulla) was described as 3 distinct structures, labelled 1, 2 and 3. Structures 1 and 3 refer to the outer and inner subunits of the medulla, whilst the structure labelled 2 is an unusual thin region located in the vicinity of the serpentine layer of most insect medullas. Instead of a single serpentine layer of tangential axons that normally defines the boundary between the inner and outer medulla, the dragonfly has two serpentine layers which innervate the medulla on the distal and medial borders of this structure labelled '2'. The dragonfly LOX is segmented into 4 distinct subunits (III_{1-4}), with what appears to be a similar design to Orthoptera and Mantodea (Rosner et al. 2017).

Several less detailed descriptions of the dragonfly optic lobe have been presented in the more recent literature, with conflicting conclusions regarding the structure of the

lobula complex. Strausfeld (2005) studied the evolution of arthropod optic lobes, presenting comparative anatomical data from a diverse selection of insects and crustaceans. Here dragonflies are grouped with preying mantis and stoneflies, as insects that lack an anatomically distinct lobula plate. Strausfeld describes a common alternative structure present on the anterior surface of the lobula complex of all three insect groups, the sublobula. This structure is said to receive uncrossed axons from the medulla homologous to T4 cells of the fly, and plays a functionally equivalent role to the lobula plate of other insects. In contrast, a recent prominent systematic review of the neuroanatomy of insect brains has grouped the lobula complex of dragonflies with flies, beetles, butterflies and moths (Ito et al. 2014). These insects all share a common 'divided lobula' design, where the lobula complex consists of a lobula and posterior lobula plate. Given that the 3 best descriptions of the dragonfly lobula complex arrived at completely different conclusions, the true organisation of the dragonfly optic lobe, and particularly the lobula complex, remains unclear.

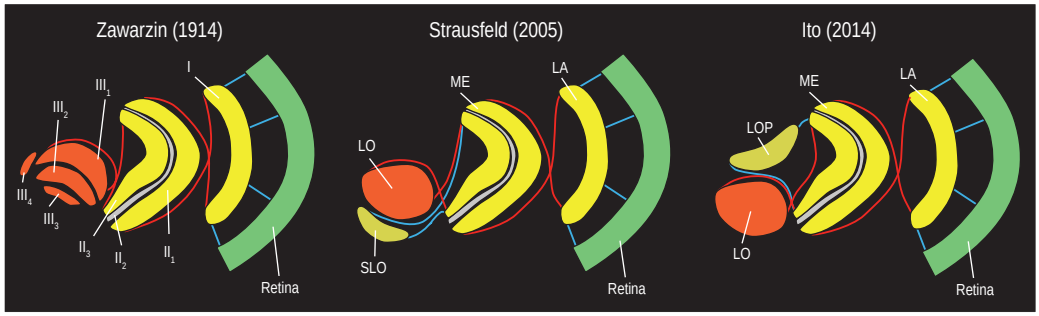

Figure 1-8: The optic lobe organisation of dragonflies, as described by 3 independent studies. All three studies report fundamentally different lobula complexes.

1.2.4 Key cell types in visual pathways

Photoreceptor cells in the insect retina transduce photons entering the compound eye into electrical potentials. These cells are organised in bundles of 8 cells sampling light captured within each ommatidium. Each of these 8 photoreceptors (R1-R8) expresses specific subtypes of photosensitive proteins called opsins, which account for their subtle differences in spectral sensitivities (Briscoe and Chittka 2001). The preferred spectra vary across insects, as well as across different eye regions in the same insect. In contrast to photoreceptor cells of vertebrates, insect photoreceptors are depolarised by increases in light intensity, and hyperpolarised by decreases in light intensity

(Kuwabara and Naka 1959; Clark and Demb 2016). These responses include a substantial transient component, quickly adapting to a steady state response following the presentation of a continuous stimulus. Photoreceptors extend output dendrites into either the lamina (R1-6) or directly to the medulla (R7-8).

The major downstream targets of R1-6 are the lamina monopolar cells (LMCs). Each column of the lamina contains 5 LMCs (L1-L5), although only L1-L3 receives direct input from photoreceptors (Meinertzhagen and O'Neil 1991; Rivera-Alba et al. 2011). The responses of LMCs to flashes of light represent an amplified and more transient representation of photoreceptor input (Laughlin and Hardie 1978; Laughlin 1987). When a photoreceptor depolarises, L1 is depolarised while L2 is hyperpolarised (and vice versa), with amplitudes approximately 6 times greater than photoreceptor input. These ON and OFF channels of visual information remain segregated during subsequent stages of visual processing (Joesch et al. 2010; Clark et al. 2011; Takemura et al. 2013;). Stimulation of neighbouring cartridges results in lateral inhibition (Dubs 1982). This inhibition subtracts background components of photoreceptor response, while amplification of the remaining contrast signal enhances the dynamic range and improves signal to noise ratio in the following visual pathways (Laughlin 1987).

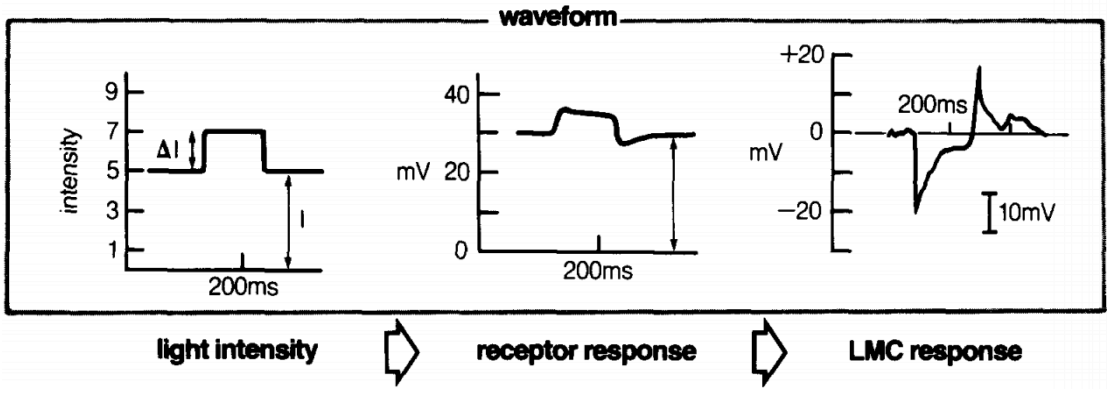

Figure 1-9: The response of Photoreceptors and LMCs in the fly, to a short pulse of light. Reproduced from figure 2, Laughlin. 1987.

The output projections of LMCs cross the first optic chiasm and terminate within the medulla. The medulla is extremely complex, containing more than 50 cell types per column, as well as many multi-columnar cell types (Gilbert 2013). In Drosophila the input dendrites of these neurons are distributed across 10 distinct synaptic layers

(Fischbach and Dittrich 1989). Mi1 and Tm3 cells in the medulla receive input from the ON sensitive L1, while Tm 1, Tm2 and Tm4 cells receive input from the OFF sensitive L2 (Takemura et al. 2013). These neurons project to T4 cells in the inner most layer of the medulla (ON), or T5 cells in the most proximal layer of the lobula (OFF). The medulla also contains neurons that receive inputs from both ON and OFF channels, called Rectifying Transient Cells (RTCs) (Osorio 1987; Wiederman and O'Carroll 2008). These neurons are equally excited by transient increases or decreases in light intensity, with responses of each channel quickly and independently adapting to a constant stimulus.

Just like the mammalian brain, insects processes different modalities of visual stimuli through parallel pathways (Borst and Helmstaedter 2015). The most obvious separation is made between wide-field (optic flow) or feature-based motion (Palka 1969; Geiger and Poggio 1975; Srinivasan and Bernard 1977, Rowell et al. 1977). These modalities are analyzed in separate neuropil that lie downstream of the medulla, which together form the lobula complex. The insect lobula complex contains at least two parallel neuropil, the lobula (sensitive to features) and lobula plate (sensitive to motion) (O'Carroll 1993; Hausen 1982). In flies, axons from medulla T4 neurons and lobula T5 neurons innervate the lobula plate. These cells are motion sensitive and direction selective, responding to drifting moving ON (T4) or OFF (T5) edges. The lobula plate has 4 distinct layers, each of which receives input exclusively from T4/T5 neurons with similar direction tuning (Maisak et al. 2013).

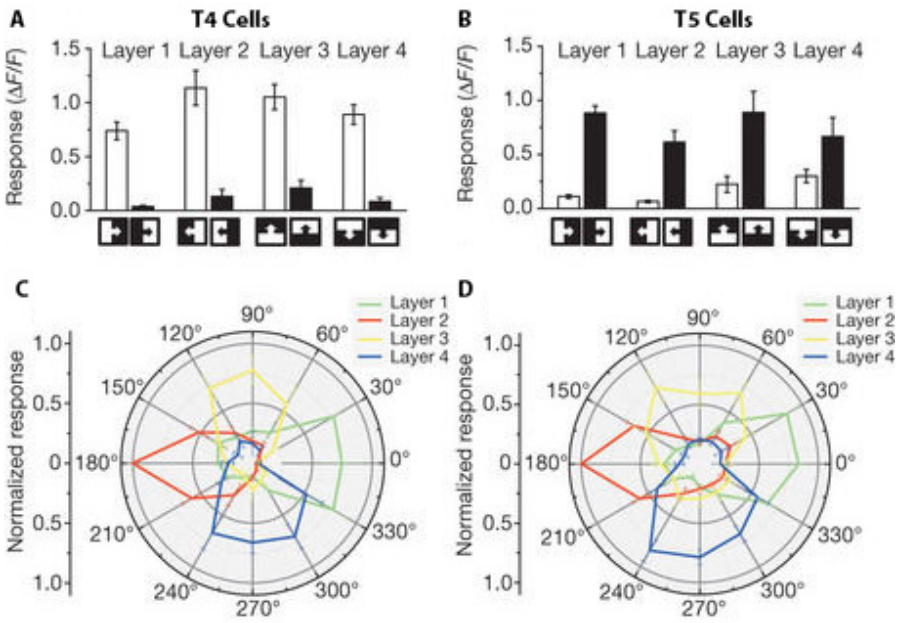

Figure 1-10: The physiology of T4 and T5 cells terminating in different layers of the lobula plate. Reproduced from figure 3, Maisak et al. 2013.

Hundreds of T4/T5 neurons viewing different locations in space form synaptic connections with Lobula Plate Tangential Cells (LPTCs) (Bausenwein et al. 1992). These neurons have characteristic broad dendritic trees and large axons that project into the protocerebrum (Hausen 1982). LPTCs are strongly direction-selective, and organised into a horizontal and vertical system, playing an important role in flight control (for review see Frye and Dickinson. 2001).

The lobula is primarily responsible for the detection of discrete features and objects. The physiology and tuning properties of lobula neurons are diverse, with cells tuned to large moving bars (O'Carroll 1993; Maddess and Yang 1997), looming objects (Rind and Simmons. 1992), and small moving targets (O'Carroll 1993; Nordström and O'Carroll 2006; Keles and Frye 2017) observed across multiple insect species. Detecting the motion and orientation of large bars may be useful for monitoring low spatial frequency components of natural scenes during flight. Looming stimuli generally indicate impending collisions, and so looming sensitive neurons have been suggested to control escape/avoidance behaviour (Santer et al. 2012).

1.3 Small target detecting neurons in insects

Many insect visual neurons have been proposed to play a role in the detection of small targets, however many do not represent a matched filter for small targets. For example, Figure-Detection neurons in the moth provide robust responses to small features, but responses are abolished when co-stimulated with a drifting grating (Collett 1971). However a subset of identified neurons in the lobula of dragonflies (O'Carroll 1993), hoverflies (Nordström and O'Carroll 2006), and *Drosophila* (Keles and Frye 2017) are small-target selective. In the dragonfly and hoverfly these neurons are known as small target motion detectors (STMDs), and display extremely diverse physiological and neuroanatomical properties. As a family, STMD neurons have varying receptive field sizes, receptive field location and selectivity of direction. 'Small-field' STMDs have receptive fields spanning just a few degrees of visual space, whilst other STMD classes exhibit much larger and often less homogenous receptive field structures (Barnett et al. 2007; Geurten et al. 2007; Bolzon et al. 2009; Dunbier et al. 2012). These neurons likely sit at different hierarchies in the same visual pathway, potentially combining to generate complex physiological phenomena. LC11 neurons in drosophila display similar physiological responses to STMD neurons, but with much more stereotypical receptive field organization, each spanning approximately 20° of visual space. Large-field cells equivalent to the well-studied large-field STMD neurons of the hoverfly and dragonfly may be relocated to midbrain structures, a hypothesis supported by the recent identification of target selective optic-glomeruli interneurons (Kim et al. 2015).

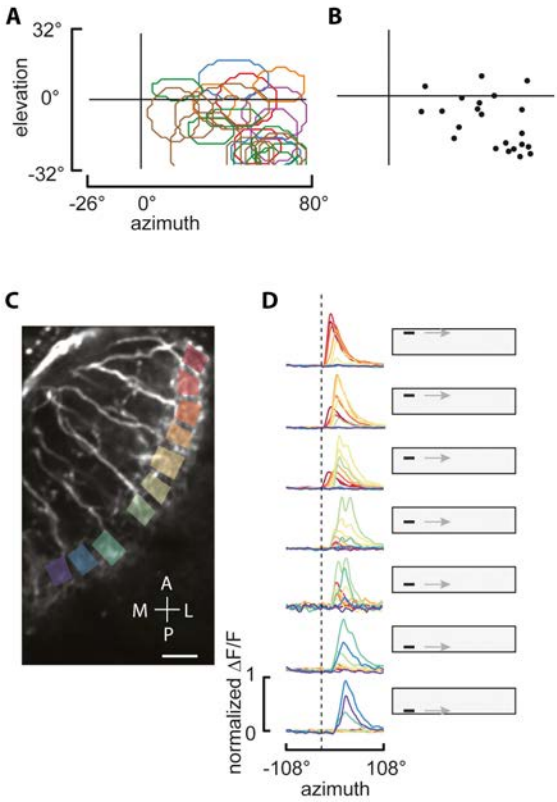

Figure 1-11. The receptive fields and input morphology of LC11 neurons in the drosophila lobula. Reproduced from Figure 2, Keles and Frye 2017. A) The receptive fields of a population of small target selective LC11 neurons. B) The centroids of each receptive field plotted in A. C) The input dendrites of LC11 neurons are retinotopically organized within the lobula, with 10 individual units highlighted with different colors. D) Receptive field elevation correlates with the retinotopic anatomical organization.

1.3.1 Small Target Motion Detectors in dragonflies

In nature, a population of STMD neurons must detect and track the motion of prey amongst a complex cluttered background. The visual input of STMD neurons is ultimately limited by the spatial sampling resolution of the compound eye, and therefore optical blur makes this discrimination a significant sensory challenge (Nordström et al. 2006; O'Carroll and Wiederman 2014). Additionally, as the size of features diminishes, so does the visual systems capacity to improve signal strength by pooling responses across an array of detectors. Despite these challenges, STMD neurons produce robust responses to targets presented against a complex moving background, and sometimes even when the velocity of the target and background are perfectly matched (Nordström et al. 2006).

1.3.2 Small-field Small Target Motion Detectors

As their name suggest, Small-field Small Target Motion Detectors (SF-STMDs) are neurons sensitive to moving targets presented within a narrow region of the visual field (generally 5-20°). SF-STMDs have been found in the dragonfly (O'Carroll, 1993) and the hoverfly (Barnett et al. 2007), and may be homologous to LC11 cells of

Drosophila (Keles and Frye 2017).

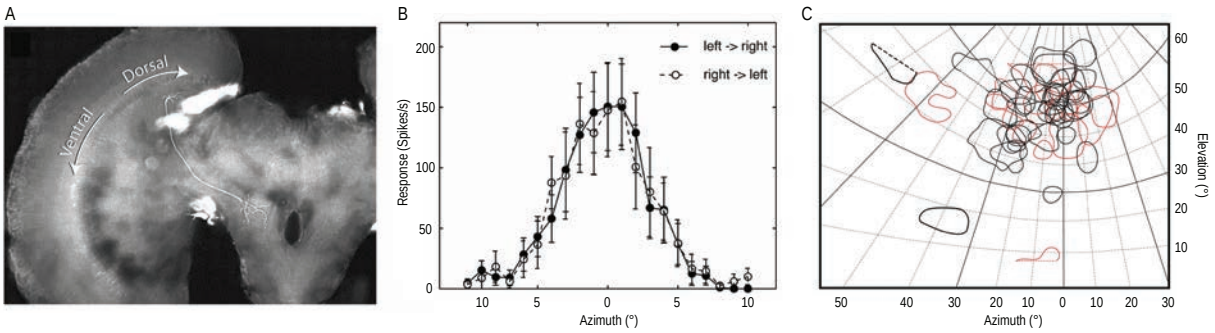

Figure 1-12: The anatomy and receptive fields of SF-STMD neurons in the hoverfly. Reproduced from Figures 2, 3 and 6, Barnett et al. 2007. A) The morphology of a single SF-STMD neuron, intracellularly labeled by Lucifer yellow injection. B) The mean receptive field from a population of SF-STMDs, mapped by drifting targets. C) The retinotopic organization of SF-STMD receptive fields.

These SF-STMD neurons receive inputs in the outermost layers of the lobula, and commonly project into the lateral midbrain. Beyond their basic tuning properties and receptive field organization, little is known about the functions or physiology of SF-STMDs. This is largely due to the thin diameter of their axons, which limits our capacity to perform long healthy intracellular recordings.

1.3.3 Centrifugal Small Target Motion Detector 1

The Centrifugal Small Target Motion Detector 1 (CSTMD1) is a large interneuron that has been characterized in the lobula of dragonflies and hoverflies (Nordström and O'Carroll 2006; Geurten et al. 2007). Unlike many STMD neurons, CSTMD1 is an efferent neuron. CSTMD1 receives input in the anterior optic tubercle, a lateral midbrain structure, before projecting target-selective information to the outer layers of the lobula. The receptive field is large, receiving either excitatory or inhibitory input across the entire fronto-dorsal visual field, presumably by integrating the inputs of a large population of SF-STMD neurons. Because of this higher-order integrating property CSTMD1 is a model neuron for studying the STMD pathway as a whole. In addition, CSTMD1's axon is unusually large, and has an orientation that facilitates frequent lengthy intracellular recordings in subsequent animals (Nordström et al. 2011; Dunbier et al. 2012; Wiederman et al. 2013).

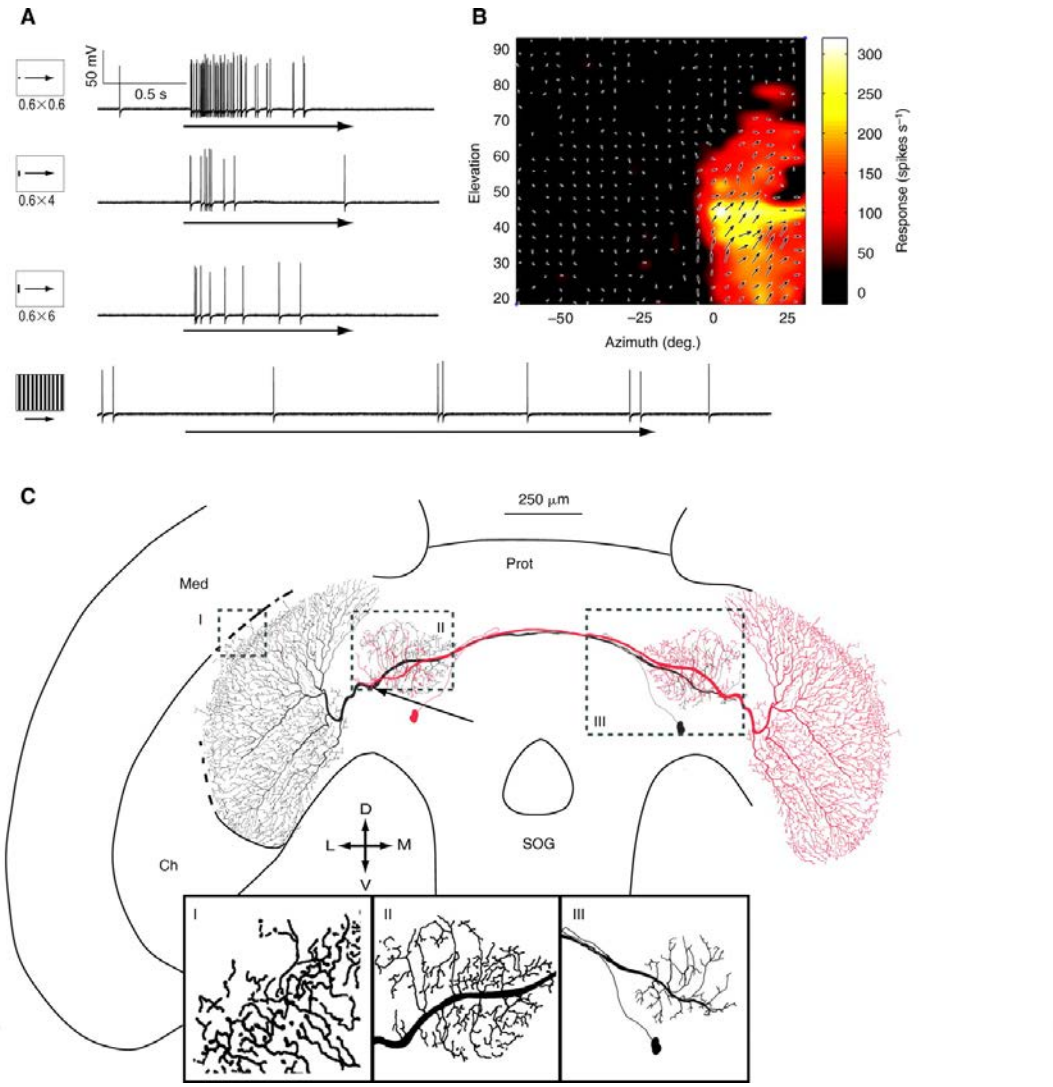

Figure 1-13: The physiology and morphology of CSTMD1. Reproduced from Figure 1, Geurten et al. 2007. A) CSTMD1 responds robustly to small drifting targets, however responses are severely reduced as the target size increases. Gratings produce no response above spontaneous levels. B) The receptive field of CSTMD1, as mapped by a series of small drifting targets. Arrows represent local direction tuning. C) The morphology of CSTMD1. The two mirror opponent cells projecting to each lobula are shown.

CSTMD1's receptive field includes a sharp distinction between excitatory (ipsilateral) and inhibitory (contralateral) inputs, situated along the animal's frontal midline, and is selective for small targets with an optimum target size of 1-3° (Geurten et al. 2007). Targets presented within the excitatory receptive field produce robust responses, with maximal responses observed in a frontal 'hotspot' at approximately 50° elevation, correlating with the animal's dorsal acute zone. CSTMD1 has high spontaneous spike

activity (10-20 spikes/s), with targets presented within CSTMD1's inhibitory receptive field abolishing all spiking activity (Wiederman and O'Carroll 2013). CSTMD1's large (80mV) biphasic action potentials, unique receptive field and robust responses to small features permit identification of CSTMD1 in subsequent recordings from different animals, as confirmed by intracellular labeling (Geurten et al. 2007).

1.3.4 Target Selective Descending Neurons

To capture prey, a visual stimulus must result in the appropriate motor response in flight muscles. 8 pairs of Target Selective Descending Neurons (TSDNs) receive inputs in the protocerebrum, and project to wing motor centers in the ventral nerve cord (Olberg 1986). These cells respond to small drifting targets, with variable levels of small-target selectivity (Frye and Olberg 1995). TSDNs have been proposed to be a downstream target of STMD pathways, although this is yet to be confirmed (Nordström 2012). The receptive fields of TSDNs are large, heterogeneous and strongly direction selective (Olberg 1986; Frye and Olberg 1995). Gonzales-Bellido et al (2013) noted that the population direction vector of these 8 pairs of neurons accurately matched the direction of a moving target. This led the authors to propose that a population code across TSDNs may form a reactive control system sensitive to prey drift. This model is supported by evidence that links TSDN activity with the contraction of wing muscles (Olberg 1983; Olberg 2012). However while a simple neuronal 'autopilot' model is appealing for motor control, the latencies and kinematics of dragonfly behavior argues against a reactive control mechanism (Mischiati et al. 2015).

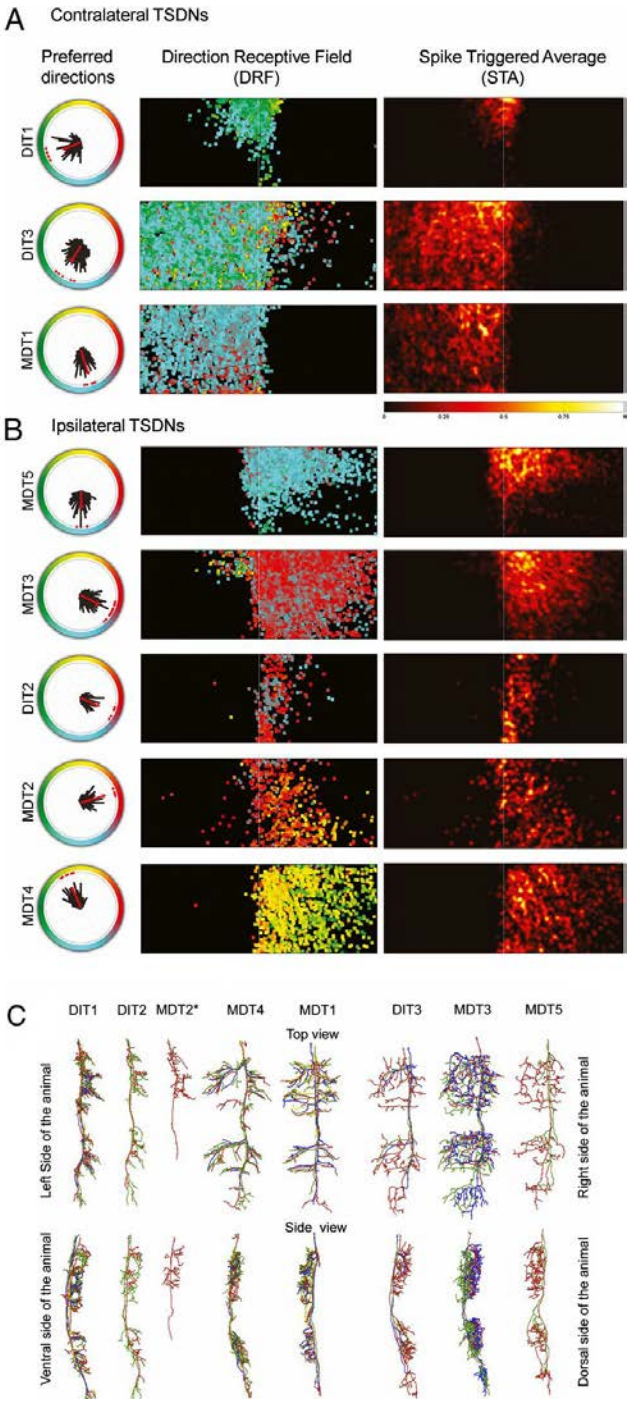

Figure 1-14: The receptive fields and morphology of the 8 pairs of TSDNs in the dragonfly ventral nerve chord. Reproduced from figures 2 and 4, Gonzalez-Bellido et al. 2013.

1.4 Fundamental mechanisms underlying motion vision

In vision science increments in light intensity are commonly described as an ON signal, and decrements in light intensity as OFF. We now know that ON and OFF signals are processed in separate pathways in the insect brain (Joesch et al. 2010), and form fundamental components of motion detection circuits.

1.4.1 The optomotor response and Elementary Motion Detectors

When a freely moving insect such as a fly is stimulated with a grating pattern that moves in one direction, the fly will attempt to make a reactionary turn in the opposite direction to cancel motion on the retina. This effect is known as the optomotor response, first studied in the 1950s and was used extensively by Hassenstein and Reichardt to develop what still remains a prominent model for motion detection, the Hassenstein-Reichardt detector, also known as the Elementary Motion Detector (EMD) (Reichardt 1961; Reichardt 1987; Borst et al. 2010). An EMD is composed of two subunits located in nearest neighbour ommatidia. Each subunit detects local changes in luminance (ON or OFF), and produces an output signal. Each component of a moving pattern or object will stimulate neighbouring positions on the retina at different times. Motion is detected by correlating the undelayed output signal of one subunit with the delayed output signal of its nearest neighbour, and vice versa. The outputs of each subunit can then be subtracted from each other, computing a motion signal that is direction selective. In this model, temporal frequency tuning is dependent on the time delay constant (τ, TD) and the spatial frequency tuning is dependent on the distance between neighbouring subunits (ϕ).

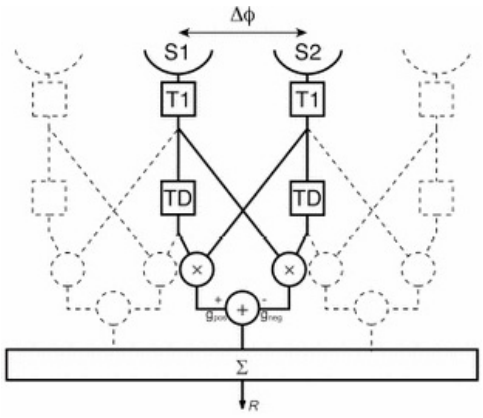

Figure 1-15: The Hassenstein-Reichardt Elementary Motion Detector. Reproduced from Figure 3, Dunbier et al. 2011.

Although behavioural and physiological evidence exists for insects using a model similar to the Hassenstien-Reichardt EMD, its biological basis is still the subject of intense study. It has been proposed that medulla neurons Mi1 and TM3 represent the two arms of the ON elementary motion detector, and that Tm1 and TM2 represent the OFF arms (Takemura et al. 2013; Shinomiya et al. 2014; Borst and Helmstaedter 2015). When presented with a Gaussian noise stimulus, Mi1 responses lag Tm3 responses by 18 ms, and Tm1 lags Tm2 by 12 ms (Behnia et al. 2014). These short but significant discrepancies in latency between the two arms of each detector may represent the delay mechanism of the EMD, although this delay may be too short to account for T4's temporal frequency optimum of 1Hz (Maisak et al. 2013). Takemura (2013) also observed a small spatial offset in the receptive fields of Mi1 and Tm3 that matched the direction preference of T4 in approximately 70% of cases, although recent studies could not replicate this finding (Takemura et al. 2017). T4 cells of the medulla and T5 cells of the lobula combine the inputs from the ON and OFF pathway respectively, and contain the first direction selective signals in the insect optic lobe (Fisher et al. 2015). Subpopulations of T4 and T5 cells are tuned to each of the four cardinal directions: upward, downward, left and right (Maisak et al. 2013), and terminate in different layers of the lobula plate.

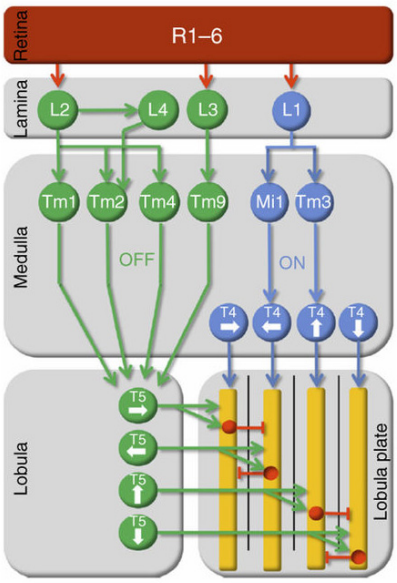

Figure 1-16: A proposed circuit for the detection of motion in *Drosophila.* Reproduced from Borst and Helmstaedter. 2015.

1.4.2 Elementary Small Target Motion Detectors

Some STMD neurons can detect the motion of small targets in the absence of relative motion cues (Nordström and O'Carroll 2006). This means that the spatiotemporal

signature of a target alone is sufficient for target detection. A drifting black target will produce an OFF signal (leading edge), and after a short delay a corresponding ON (trailing edge), at every location along its path. The elementary small target motion detector (ESTMD) model proposes that correlating local ON signals with delayed OFF signals within the same visual column could produce a matched filter for moving objects (Wiederman and O'Carroll 2008). This is in contrast to EMD models, where correlations are only made between signals of the same sign (ON with ON, OFF with OFF), across neighbouring units. In the ESTMD model height and width tuning is generated by separate mechanisms; the duration of the temporal delay filter produces 'width' tuning in the axis of motion, and strong surround antagonism between neighbouring ESTMD units produces 'height' tuning in the axis orthogonal to a targets motion. Although the connectomics of a hypothetical ESTMD circuit have not been investigated in detail, several predictions of the ESTMD model are supported by physiological properties of STMD neurons (Wiederman and O'Carroll 2011; Wiederman et al. 2013b).

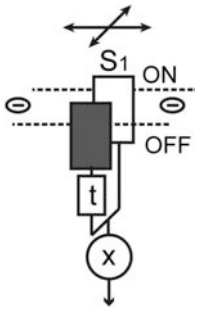

Figure 1-17: A single elementary small target motion detector (ESTMD) unit. Reproduced from figure 1, Wiederman et al. 2013.

1.4.3 Contrast sensitivity

The term contrast sensitivity describes the ability of a visual system to discriminate an object from its surround as the difference in their intensities is reduced. Contrast sensitivity functions are the vision scientists equivalent of a dose-response curve, and have been used extensively to examine optical properties of eyes and their underlying neural circuits. There are two common methods for measuring contrast, each having applications for different situations. Michelson contrast is widely used for defining the contrast of a pattern such as a sinusoidal grating, where:

$$c_m = \frac{I_{max} - I_{min}}{I_{max} + I_{min}}$$

I_{max} and I_{min} represent the highest and lowest intensity respectively. Thus, Michelson contrast reflects the amplitude of intensity changes, relative to the overall stimulus intensity.

Weber contrast is more commonly used for defining the contrast of a feature presented on a large uniform background, where the difference between overall luminance and background luminance is negligible, where:

$$c_w = \frac{I_{feature} - I_{background}}{I_{background}}$$

Ranging between 1 for a white target on a black background, and -1 for a black target on a white background, Weber contrast quantifies the discriminability of a feature relative to the intensity of the background.

Most experiments that study contrast sensitivity use moving grating patterns. For example, psychophysical experiments have shown that in optimal lighting conditions humans are sensitive to gratings with contrasts as low as 0.5% (De Valois et al. 1974). The visual systems of invertebrates such as hoverflies, blowflies, bees and moths are less sensitive, detecting gratings with thresholds between 1-3% contrast (Dvorak et al. 1980; O'Carroll et al. 1996; Bidwell and Goodman 1993). A common feature of visual systems is that contrast sensitivity increases as the size of a stimulus is increased. When a large grating pattern moves, many elementary motion detectors viewing different parts of the pattern are stimulated (Dvorak et al. 1980). Downstream pathways can integrate these motion detector responses across space, which results in larger and more detectable signals. Conversely, a small feature may only stimulate a single motion detector at any given time. When spatial integration is not available, contrast sensitivity, and as a result signal detectability, is expected to decrease.

For this reason, we would expect contrast sensitivity values for small target detection to be far below that of wide-field motion sensing. However, recent work has presented data that questions this idea. Invertebrate photoreceptors and target-detecting neurons both have target-detectability thresholds of 2-3% contrast, with increases in response as target contrast increases until saturation. Although detectability thresholds are almost identical at different stages of visual processing, contrast-gain for suprathreshold targets is significantly greater for target detecting

neurons than for photoreceptors (O'Carroll and Wiederman 2014). In otherwise optimal conditions the response of a target-detecting neuron can saturate for targets as low as 8% contrast, a stimulus which produces photoreceptor responses smaller than 1mV, ~1/20th of its dynamic range. This means that responses of STMD neurons remain highly robust, even as a target approaches the absolute detection limits of photoreceptors. fMRI studies in humans have demonstrated that the slope of the contrast sensitivity function is highest in early visual processing areas, and significantly decreased in higher-order object detecting areas (Avidan et al. 2002). This contrast invariance, also known as contrast normalisation, suggests that while early retinotopic layers utilise their full dynamic range to signal the intensity of an object, later areas are more 'switch-like', signalling an objects presence rather than its intensity.

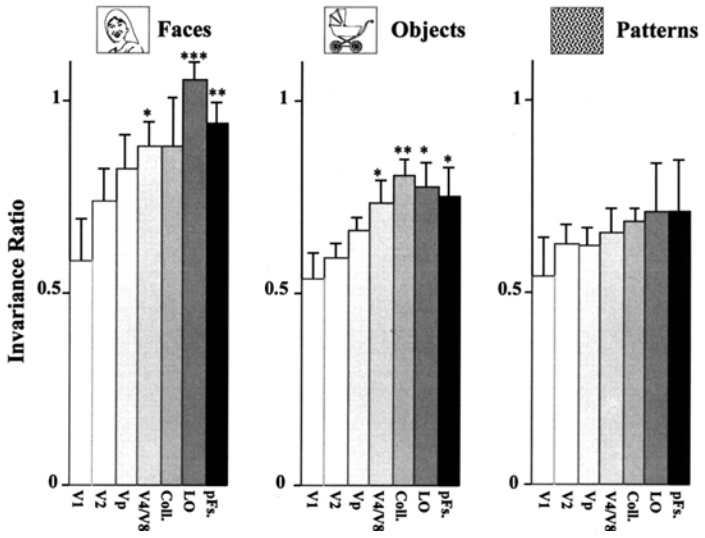

Figure 1-18: Contrast invariance increases in the human brain between early retinotopic visual areas and higher-order object sensitive areas. Reproduced from Figure 4, Avidan et al. 2002.

1.4.4 Direction selectivity

Detecting the motion of visual objects and patterns is a fundamental task of visual systems. The separation of visual information into its directional components occurs in the retina of mammals (Demb 2007), and the medulla of invertebrates (Fisher et al. 2015). Most descriptions of direction selectivity in vision science relate to the intrinsic properties of a Hassenstein-Reichardt or Barlow-Levick motion detector (Reichardt 1961; Barlow and Levick 1965). However these correlators lack the size

selectivity that characterises STMD neurons. In its most basic form the ESTMD model is essentially a local flicker detector, and does not induce direction selectivity (Wiederman and O'Carroll. 2008). However, many STMD neurons do show varying degrees of direction selectivity (O'Carroll 1993; Nordström and O'Carroll 2006; Barnett et al. 2007). Direction selectivity can be added to the ESTMD model by combining it with a HR EMD (Wiederman and O'Carroll 2013b). The outputs of an EMD could serve as inputs for an ESTMD (EMD-ESTMD), or the outputs of two neighbouring ESTMDs could serve as inputs for an EMD (ESTMD-EMD). Both options inherit the size selectivity of an ESTMD, and the direction selectivity of an EMD (Wiederman and O'Carroll 2013b).

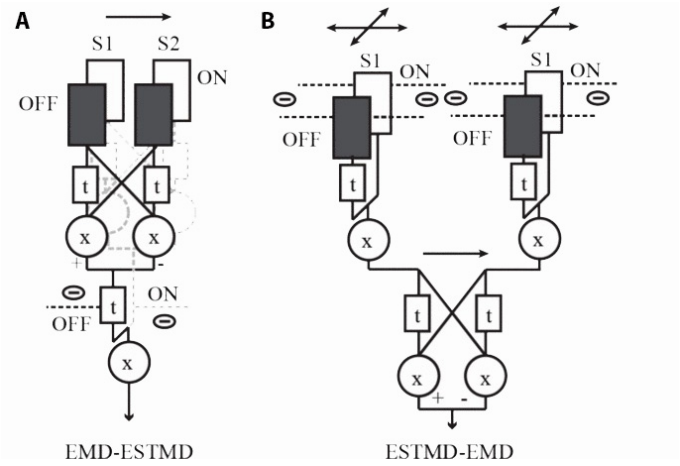

Figure 1-19: Cascaded second-order motion detectors produce direction-selective and small target-selective motion signals. Reproduced from Figure 1, Wiederman and O'Carroll, 2013b. A) The outputs of a 2 detector HR EMD could serve as the inputs to an ESTMD. B) ESTMDs viewing neighbouring regions could serve as the inputs to a single EMD.

1.5 Modulation of neural circuits by prediction and attention.

Sensory systems have evolved clever strategies that minimise the processing resources required for behaviour and maximising performance. Understanding these strategies is a key objective of both theoretical and experimental neuroscientists.

1.5.1 Predictive coding strategies

Prediction plays a fundamental role in sensory processing, and has become a hot topic in neuroscience research (Summerfield and Egner 2009). When presented with a visual scene, one might expect that a brain should form continuous high fidelity bottom-up representations of the incoming information. However, large portions of natural scenes are highly correlated over time, and therefore this strategy results in the brain signaling a large amount of redundant information. Neuronal signaling is energetically expensive (Laughlin et al. 1998), which provides a strong driving force for brains to reduce redundancy. An alternative strategy is for the brain to assume that the current sensory environment should remain unchanged (i.e. a tree in the immediate past will remain a tree in the immediate future), and thus the only information that must be encoded is deviations from this assumption. This is the underlying concept that is used in predictive coding models (Rao and Ballard 1999).

If this strategy were to be implemented in a sensory pathway, responses of a sensory neuron should reflect its novelty. In other words, stimuli that match expectations should elicit weaker neuronal responses than stimuli that deviate from predictions (Spratling 2008; de-Wit et al. 2010). There is a growing body of evidence that support this hypothesis. For example, a recent study demonstrated that responses from a subset of Retinal Ganglion cells were consistent with a role in novelty detection (Schwartz et al. 2007). When presented with a series of periodic flashes of light, responses quickly adapted. However, the random omission of a single flash resulted in a robust response. This 'Omitted Stimulus Response' signals a deviation from the expected stimulus.

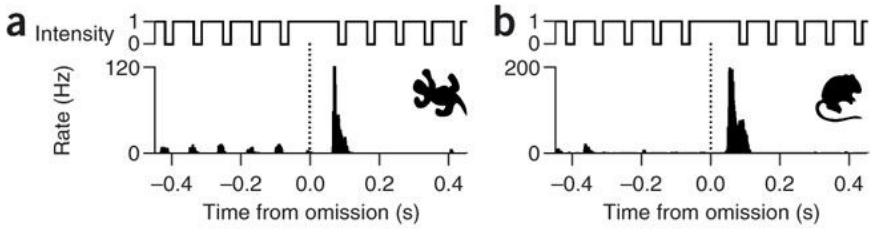

Figure 1-20: The Omitted Stimulus Response in retinal ganglion cells of the salamander and mouse. Reproduced from figure 1, Schwarz et al. 2007.

However other studies have suggested that under some circumstances the silencing effect of predictive coding can be reversed (Doherty et al. 2005; Rauss et al. 2011). Using fMRI on human observers, Kok et al (2011) suggested that the presence or absence of spatial attention was the deciding factor in whether a predicted stimulus would be enhanced or silenced. Attention generally increases the magnitude of responses (Reynolds et al. 2000). However attending to a space also reduces perceptual uncertainty (Rao 2005; Friston 2009), which leads to more precise predictions of upcoming stimuli in that space. It has been proposed that when prediction and attention meet, instead of working in opposition prediction and attention work synergistically to enhance task relevant inputs (Kok et al. 2011).

1.5.2 Attentional modulation

Natural environments are complex, containing an abundance of sensory information. Brains have limited resources, and lack the bandwidth to process all available information. In the face of this problem, brains evolved attention mechanisms that best allocate their limited resources. Attention prioritises the processing of task-relevant stimuli, at the cost of ignoring equally salient but less relevant background stimuli. Psychologists have studied attention in detail for more than 60 years (Shepard 1957), but identifying the neuronal correlates of attention remains one of greatest current questions in neuroscience.

Studies of visual attention generally use cues that direct a subject's attention to a particular region of space. This can be done in human observers during psychophysical experimentation, or during electrophysiological recording from live trained animals, commonly non-human primates. At the level of human perception, cuing attention at a certain position results in improvements in contrast sensitivity (Carrasco et al. 2000), spatial resolution (Carrasco et al. 2002) and processing speed (Carrasco and McElree 2001). Reynolds et al (2000) presented a similar stimulus paradigm to Macaque monkeys while recording from neurons in V4. When attention was cued to locations that lie within the receptive field of recorded neurons, their responses to gratings was increased. These effects had the strongest effects at low contrasts, suggesting that attention boosts contrast gain.

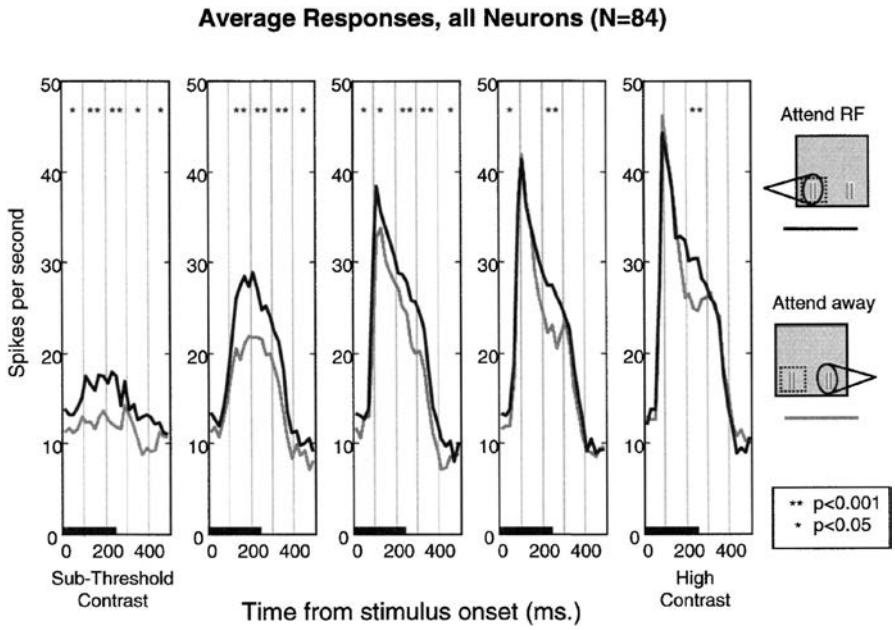

Figure 1-21: Cued spatial attention that overlaps with the receptive field of V4 neurons improves contrast sensitivity in the macaque. Reproduced from Figure 4, Reynolds et al. 2000.

The mechanisms that generate such effects within specific neuronal circuits are poorly understood. One promising mechanism that has been explored in vertebrates is the remapping of receptive fields. The receptive fields of neurons in several higher-order visual areas in primates are not static – shifting their position in space during behaviour (Sommer and Wurtz 2006). A common trigger for the shift of receptive fields is eye saccades, where the position of objects in a scene rapidly shifts on the retina (Sommer and Wurtz 2008). Zirnsak et al (2014) showed that receptive fields in the frontal eye fields (FEF) of rhesus monkeys shift in space following a saccade, in order to remain static relative to the current fixation point. However, immediately before a saccade occurs, receptive fields of neurons viewing different areas of a scene compress onto the saccades planned location.

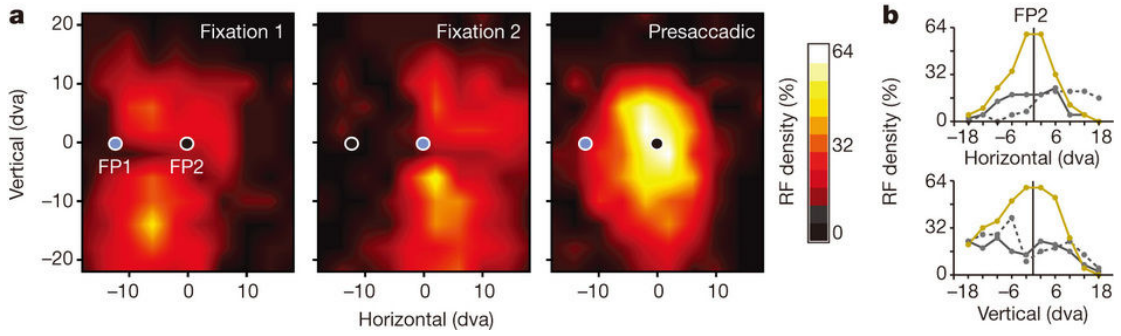

Figure 1-22: The shifting density of FEF neuron receptive fields prior to saccades. Reproduced from Figure 3, Zirnsak et al. 2014. A) Receptive fields of FEF neurons maintain their position in space relative to fixation points (FP1 and FP2) before and after a saccade. However, immediately before a saccade (Presaccadic) receptive fields compress, producing a large increase in receptive field density centered on the future saccade location, and a decrease in receptive field density elsewhere. B) Horizontal sections through the density plots in (A) reveal a large difference in the spatial distribution of receptive fields.

During this shift, the number of neurons with receptive fields covering the planned position increases approximately 3-fold. This re-allocation of processing recourses increases the accuracy of perception at the new saccade position, at the sacrifice of sensitivity in the periphery. Similar mechanisms in different visual processing areas could potentially account for many of the attentional effects reported in human observers (Pestilli and Carrasco 2005).

1.6 Higher-order physiological properties of Dragonfly STMD neurons.

1.6.1 Neuronal Facilitation

All neuronal signaling occurs with temporal latencies, due to biochemical processes such as phototransduction and synaptic transmission (Thorpe et al. 1996; Bolzon et al. 2009). Upon the presentation of a small moving target, responses in STMD neurons have an absolute latency of approximately 40 ms. In CSTMD1, this absolute latency is followed by a prolonged response build-up that occurs over several hundred milliseconds (Nordström et al. 2011).

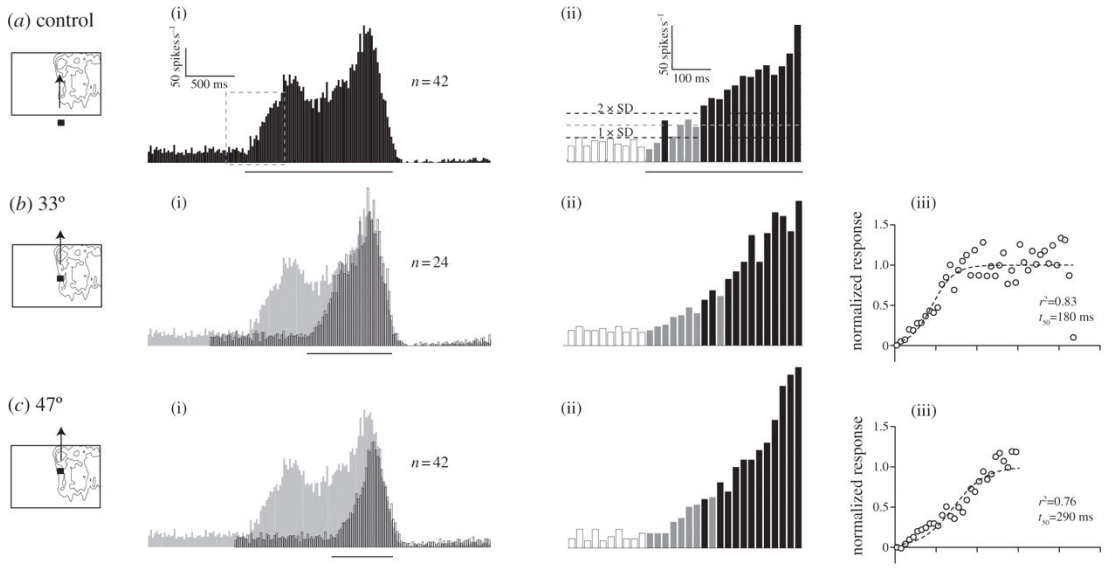

Figure 1-23: Facilitation by targets moving on continuous trajectories through the receptive field of CSTMD1. Reproduced from Figure 1, Nordström et al. 2011. i) peri-stimulus time histograms showing responses to vertically drifting targets of varying length (A-C). ii) Response following the onset of target motion, where white bars represent pre-stimulus spontaneous activity, grey bars represents peri-stimulus activity and black bars represent time points where activity is significantly greater than spontaneous. iii) Normalized response (short path/long path) fit with a logistic function.

The biophysical processes that produce absolute latencies do not explain the prolonged response build-up that follows. We know that CSTMD1 has rapid response kinetics, as evidenced by the rapid response offset upon the removal of a moving target (Nördstrom et al. 2011). Hence there are only two possible explanations for this prolonged response build-up: a presynaptic motion detector with an abnormally long temporal delay filter, or a facilitation mechanism where repetitive stimulation enhances responses. Dunbier et al (2011) showed that CSTMD1 is tuned to target velocities inconsistent with an unusually long temporal delay filter, strongly suggesting that a facilitation mechanism enhances responses in CSTMD1.

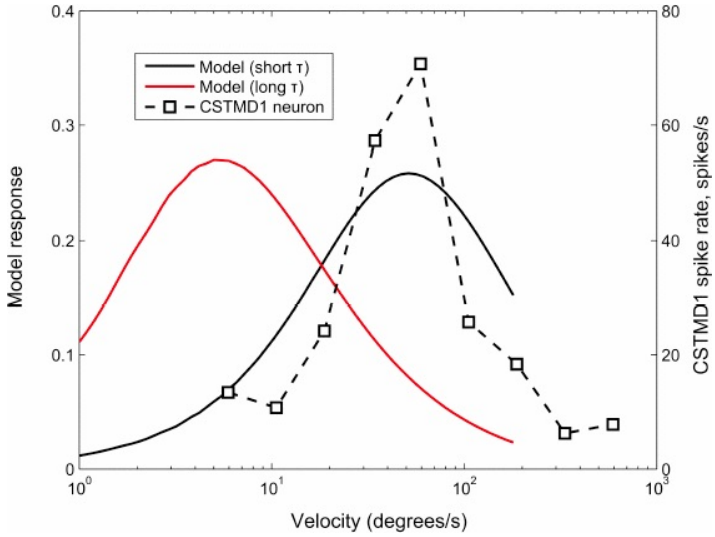

Figure 1-24: The velocity tuning of CSTMD1 is inconsistent with a long delay filter. Reproduced from Figure 7, Dunbier et al. 2011.

Further experiments demonstrated that facilitation is a local phenomenon. Dunbier et al (2012) presented CSTMD1 with 1s of target motion, either as a continuous path or segmented into a series of shorter paths presented at different horizontal positions. The strength of responses decreased dramatically when an otherwise identical target is discontinuous in space. This means that the facilitation of responses does not build globally over time due to continuous stimulation, but is instead generated in a defined position within the receptive field. Each time a target trajectory is interrupted, the state of facilitation must be re-built at its new location.

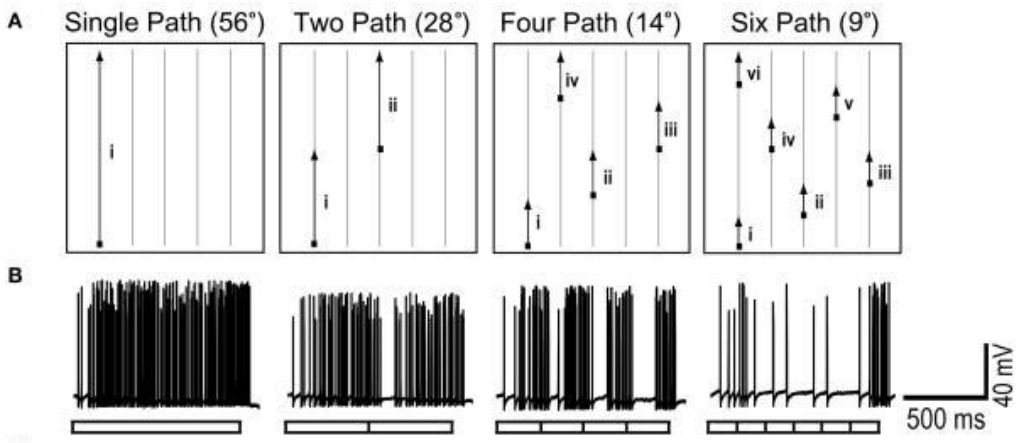

Figure 1-25: Facilitation requires motion on continuous trajectories. Reproduced from figure 1, Dunbier et al. 2012. A) All trials consisted of 1s of target motion, consisting of a target drifting vertically across a region of interest. Targets could drift the same distance on a single path, or multiple horizontally separated shorter paths. B) Example responses to each condition, revealing that robust responses require target motion to be continuous in space.

For these reasons it has been proposed that the prolonged response build-up may be due to STMD pathways utilizing a 2nd order motion detector network, as described by Zanker (1994). Such a network involves an initial layer mediating target detection on a small spatial scale, such as the elementary small target motion detection (ESTMD) scheme proposed by Wiederman et al. (2008). Outputs of this initial layer converge on a second layer of motion detectors that operate on a larger spatial and temporal scale. The key advantage of a 2nd order motion detector network is that signal strength is amplified when objects are continuous in space and time, while discontinuous background noise and false positives are ignored (Nordström et al. 2011).

1.6.2 Selective Attention

Given that dragonflies often hunt in swarms (Russell et al. 1998), STMD neurons in behaving animals would often be faced with more than one potential target. Prey that in a single target scenario represent a promising meal now represent a distraction from the dragonfly's goal. In this situation, the dragonfly brain must implement a selective attention mechanism for successful prey capture. This situation was simulated experimentally by presenting CSTMD1 with two identical targets simultaneously drifting through its receptive field (Wiederman and O'Carroll 2013). Given the inhomogeneity across CSTMD1's large receptive field, targets presented in different locations produce a unique, 'signature' response over time. When two targets were presented simultaneously, the authors were able to use this signature to determine which target was responsible for the neurons response. In each trial CSTMD1 responded as if only one target was presented, completely ignoring the existence of a distractor. The target that was selected differed across trials, with no clear pattern allowing the prediction of which target would 'win' in any given trial. This work highlighted STMD neurons as a robust model for studying selective attention at the single neuron scale, allowing direct recordings from identified neurons across multiple animals.

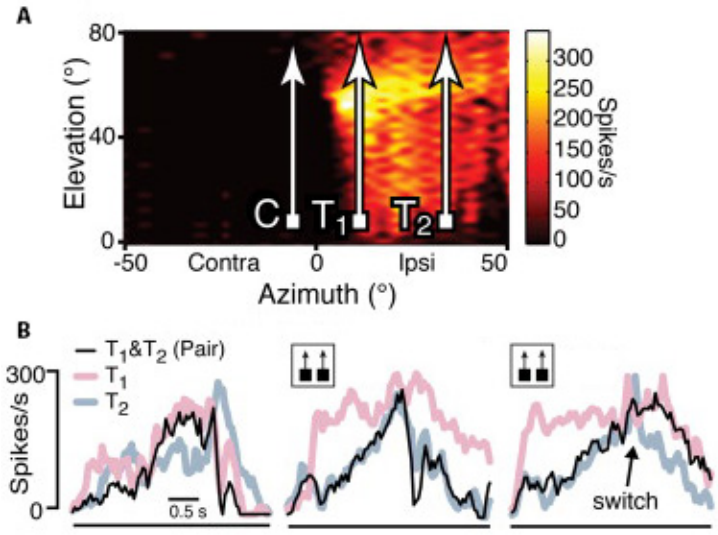

Figure 1-26: Selective attention in CSTMD1. Reproduced from figure 1 and 2, Wiederman and O'Carroll. 2013. A) The large and inhomogeneous receptive field of CSTMD1, overlaid with the two stimulus paths. B) Simultaneous presentation of both targets results in a response indistinguishable from that of T1 or T2 alone. In rare occurrences, the selected target can switch mid trial.

Given that dragonflies attend to targets of interest, facilitation could potentially be a result of the build-up of spatial attention (Hoffman 1986). Spatial attention is known to modulate receptive field structure in mammalian systems. Connor et al (1996) demonstrated that when a macaque devotes spatial attention to a location the receptive fields of feature detecting neurons close to the attended space became skewed such that features closer to the attended space produce enhanced responses. Similarly, spatial attention elicited by the motion of a continuous trajectory target has been shown to decrease response latency in feature detecting cells in the cat (Jancke et al. 2004). Facilitation in STMD neurons may represent a similar system, where a continuous target trajectory catches the dragonflies attention, resulting in enhanced responses for targets in the attended position and suppressed responses for targets elsewhere. However, until now, no work has attempted to link facilitation and selective attention in STMD neurons.

1.7 Small target detection and trajectory encoding in human observers

While the visual circuits underlying target detection in a human are certainly not homologous to the dragonfly STMD system, evolution often converges on similar solutions for similar sensory challenges. Thus, understanding the capabilities and limitations of a human observer or a class vertebrate neurons can help place our findings into broader scientific relevance, and even inspire new research questions.

1.7.1 Target tracking in psychophysics

Psychophysical studies in trained human observers allow researchers to investigate how properties of a visual stimulus effect our perception. Several of these studies have investigated the cues that affect our ability to perceive the motion of small targets, and in some cases report results that accurately reflect physiological properties of STMD neurons. Newton's first law of motion states that a physical object moving at a uniform velocity in one direction will preserve in its state of uniform motion unless acted upon by an external force. Visual systems have evolved to process objects in the physical world, and therefore one may expect that objects inertia should be informative for interpreting upcoming sensory input. Classical psychophysical experiments have studied the concept of 'motion inertia' in human perception. If a dot is presented at two neighboring points in quick succession, the dot will appear to move from the first point to the second (Korte 1915). If two pairs of dots are presented in quick succession, one pair oriented north-south and the other east-west (such that if presented together they would form the corners of a diamond), observers' report two mutually exclusive percepts with equal frequency (Gengerelli 1948). However, an observer's perception can be biased to form only one percept by embedding the same stimulus within two long parallel rows, consisting of dots that are flashed sequentially (Ramachandran and Anstis 1983). This tells us that prior motion generates 'momentum' which can strongly influence the perception of stimuli into the future, even when those stimuli are ambiguous when presented alone.

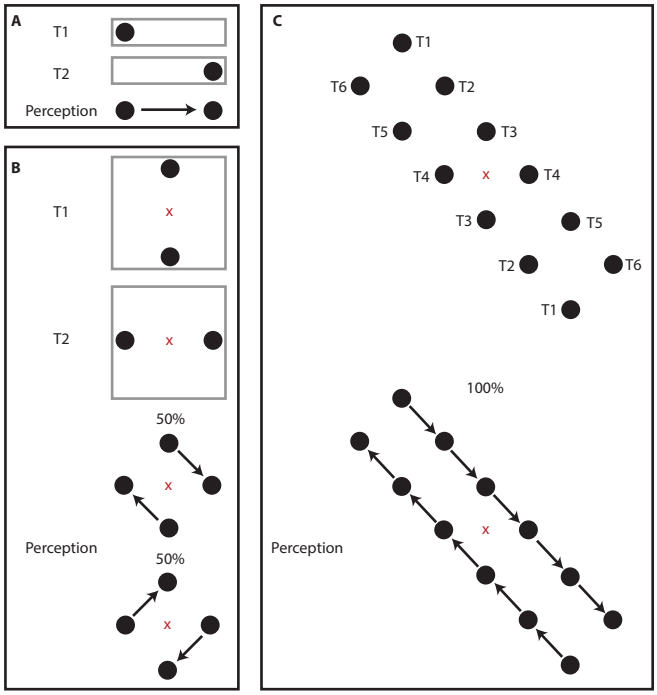

Figure 1-27: Apparent motion is affected by motion inertia. Reproduced from Figure 1, Ramachandran and Anstis. 1983). A) Apparent motion is produced by flashing two dots at neighboring locations sequentially (Tx = time-point x). B) A diamond matrix of four dots surrounding a central fixation point (red x), where north and south dots alternate in presentation with the east and west pair. C) Identical stimuli to B, but embedded within two long parallel rows of dots flashed sequentially.

Watamaniuk et al (1995) built on this work by presenting 'target' dots moving on trajectories of different length against a background pattern consisting of many identical dots moving on short random paths. On a frame-by-frame basis the 'target' dot and background dots were indistinguishable, therefore successful detection is only possible if the brain tracks an objects trajectory across multiple frames. The ability of an observer to detect a target trajectory rapidly improved as the trajectory duration increased, saturating after approximately 400 ms. This suggests that the visual system performs some form of spatiotemporal integration of target motion, extracting a single detectable signal from a series of sub-threshold segments.

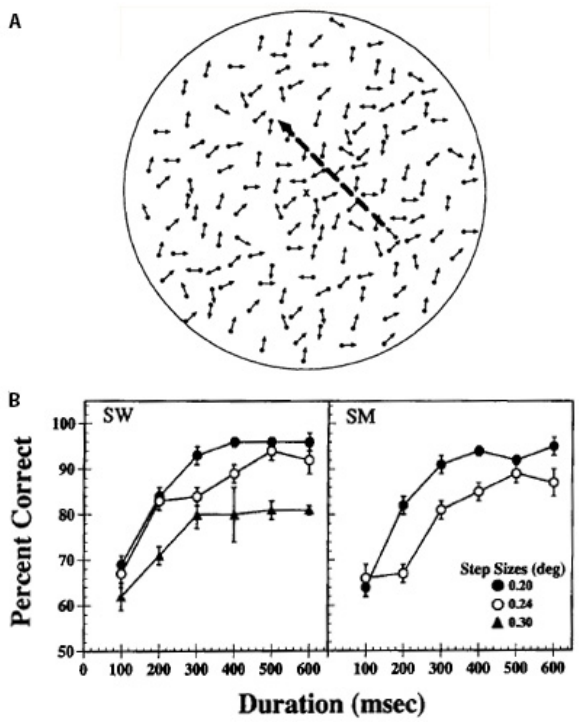

Figure 1-28: The detection of target trajectories amongst a background of random moving dots. Reproduced from figure 1 and 2, Watamaniuk et al. 1995. A) The stimulus paradigm, where background dots move on short paths in random directions. A target trajectory is presented amongst the background, composed of a dot moving on multiple short, coherent paths of varying duration. B) Observer performance increases as the duration of a target trajectory increases, or the step size between each target path segment decreases.

Watamaniuk et al (1995) continued by demonstrating that this spatiotemporal integration requires trajectories to be coherent in space and time. If the individual components of a trajectory are presented in the incorrect order, observers' ability to detect a trajectory is significantly reduced. Similarly, if a continuous trajectory has regular interruptions the facilitative build up of detectability over time is also reduced.

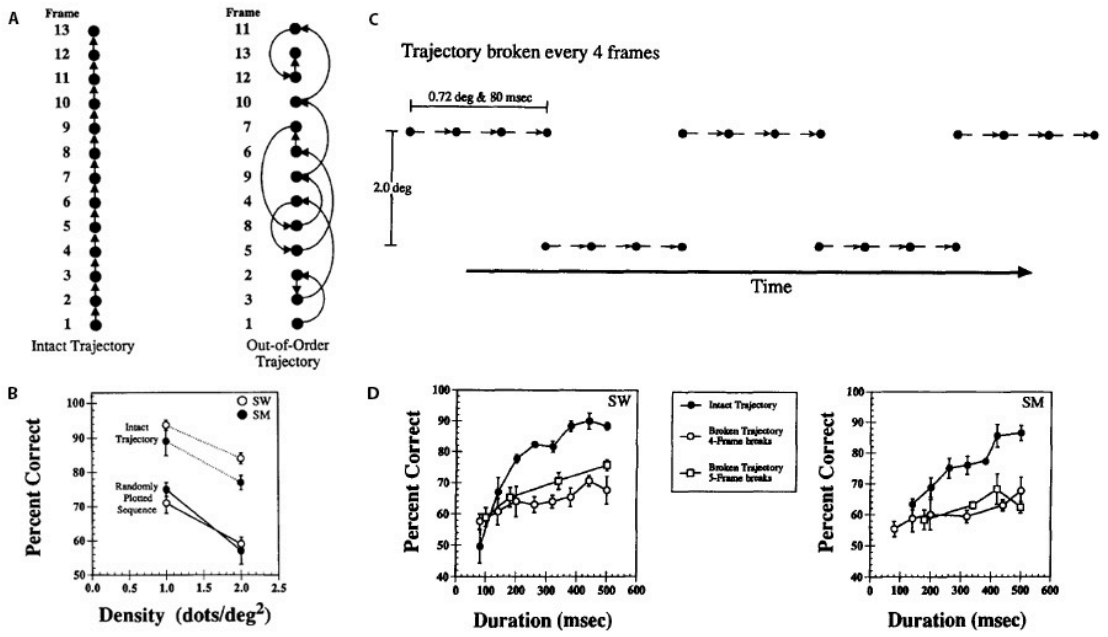

Figure 1-29: The detection of continuous and discontinuous target trajectories by human observers. Reproduced from figures 5 and 7, Watamaniuk et al. 1995. A) 13 frames of a target trajectory were presented, either in the correct sequence or out of order. B) The performance of observers was significantly better when a trajectory was presented in the correct sequence. C) Observers were presented with trajectories that are not random, but broken at regular intervals. D) These brakes in trajectory prevents the build-up of facilitation in response to a continuous trajectory.

400 ms is significantly slower than the integration time for single motion detectors. This suggests that the slow increase in detectability is due to interactions between neighboring motion detectors along the motion path. Grzywacz et al (1995) proposed that the currently stimulated motion detector could send facilitatory signals to the next motion detector with similar direction tuning, such that repetitive stimulation in time and space produces a slowly building cascade of improving sensitivity. This directionally tuned facilitation of response by target trajectory spreads in time and space, allowing the robust detection of targets that are temporally occluded by foreground objects (Watamaniuk and McKee 1995; Watamaniuk 2005; Krekelberg and Lappe 1999).

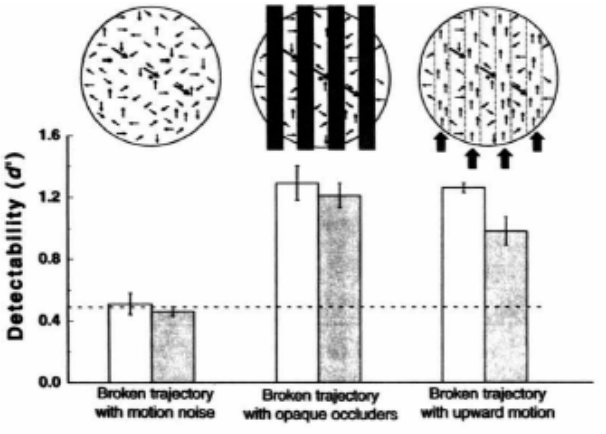

Figure 1-30: The detection of a moving object during occlusion. Reproduced from figure 1, Watamaniuk and McKee. 1995.

The ability to detect objects that are temporarily occluded requires some form of feed-forward prediction of objects future movements. In order to improve success rates in complex tasks the human visual system extends these predictive mechanisms across many parameters of an objects motion. Unlike insects, humans are able to perform eye movements distinct from the movements of the head. These eye movements are often deployed in a predictive manner, in the form of saccades or smooth pursuit. During saccadic eye movements, the retinal movement skips the subjects' gaze ahead of a target in space based on a prediction of target position learned through prior experiences (Diaz et al. 2013). During smooth pursuit, when a moving target is temporarily occluded a subject maintains tracking at target-matched velocities when there is an expectation of the targets motion continuing (Bennet and Barnes 2003). These predictive movements are able to take into account complex target properties including velocity, trajectory, gravitational acceleration and even the elastic properties of a bouncing ball (Lackner and DiZeo 2000; Diaz et al. 2013). The accuracy of these predictive eye movements has been correlated with performance of individuals in visually demanding situations, such as hitting a cricket ball (Mann et al. 2013).

1.7.2 Neuronal mechanisms of trajectory encoding and motion extrapolation

The neuronal mechanisms that underlie the brains capacity for encoding and extrapolating a targets trajectory over space have been studied, most commonly in the context of the latencies in visual processing. One inescapable issue with sensing your surroundings is that every stage of biological signaling takes time. This means that a

response in a neuronal system will always occur with a time delay relative to the stimuli that elicited it. These temporal delays should result in a moving object being perceived behind its actual location. Human photoreceptors have a temporal response lag of between 30-100 ms, depending on the intensity and wavelength of light (Stockman et al. 1991). However, consider a professional tennis player who regularly returns a ball moving in excess of 250 kph. In the short time taken for a photoreceptor to detect the ball, the ball has moved somewhere between 2.1 and 7 meters. What neuronal processes can account for a human's ability to accurately detect and interact with the real position of moving objects?

When a human observer is faced with a flashed stimulus presented perfectly aligned in space with a moving object, the flashed stimulus is perceived as trailing behind the moving stimulus. This effect has been labeled the flash-lag effect (MacKay. 1961) and has been studied in multiple forms since (for review see Nijhawan 2002). This illusion tells us that objects moving on predictable trajectories are processed differently to stationary, unpredictable objects. The best physiological explanation of this effect comes from studies in the mammalian and amphibian retina. Berry et al (1999) reconstructed the neural image from recordings of a population of Retinal Ganglion Cells (RGCs) in the salamander and rabbit retina following the presentation of drifting and flashed bars.

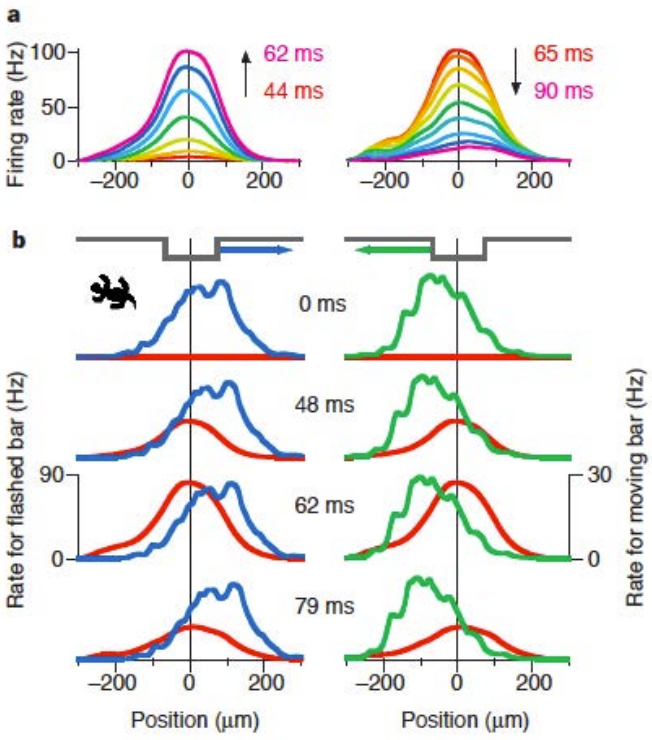

Figure 1-31: The population response of retinal ganglion cells to flashed and moving bars. Reproduced from figure 2, Berry et al. 1999. A) A flashed bar elicits responses that reach peak amplitude at approximately 62 ms, and are strongest at positions that correlate with the center of the bar. B) The population response at four time points following a flashed bar (red) and drifting (blue/green) bar at the same position.

Following the presentation of a stationary flashed bar, the neural image produced by a population of RGCs is centered on the bars current position. However, when presented with a bar that drifts on a continuous path, the neural image is centered at the bars leading edge. This effect is produced by a combination of strong neural adaptation to repetitive stimulation, and the strong overlap in RGC receptive field organization. RGC receptive fields are large when mapped by a series of stationary stimuli, when mapped by a drifting object the same receptive field becomes skewed in the opposite direction to motion. This skewing is a result of neuronal adaptation that builds during stimulation. When an object drifts across an array RGCs with overlapping receptive fields, cells with receptive fields centered ahead of the object produce strong non-adapted responses, whilst the responses of cells with receptive

fields centered behind the object have adapted away. This effect is responsible for the short forward offset in the retinal image of drifting objects.

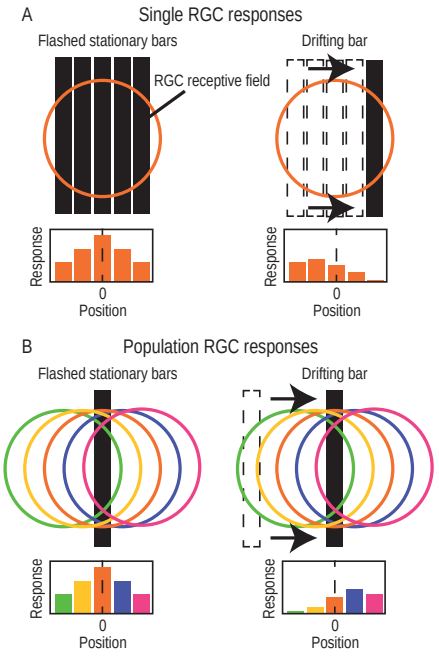

Figure 1-32: The Berry (1999) model for motion extrapolation in the salamander and rabbit retina. A) The receptive field of a single RGC differs when mapped with a series of stationary flashed bars compared to a single drifted bar. This difference is a result of strong adaptation, skewing the receptive field to favor objects entering the receptive field over objects exiting it. B) The resulting population responses at different positions in the retina, following flashed or drifted bars. Cells with receptive fields centered behind the object are strongly adapted, whilst cells with receptive fields centered ahead still respond strongly, resulting in a pattern of neuronal activity that spreads ahead of an objects current position.

Motion extrapolation is the process of using an objects prior trajectory to predict its future position (Nijhawan 1994). These retinal processing mechanisms have formed the basis for many models of motion extrapolation (Leonardo and Meister 2013; Johnston and Lagnado 2015; Borghuis and Leonardo 2015). However, the ability of a human observer to detect objects that have been masked by an occlusion requires the modulation of sensitivity in a position that has not yet been stimulated (Watamaniuk and McKee 1995). In addition, predictable object motion enhances the strength and detectability of motion signals in human observers (Watamaniuk et al. 1995). Models of retinal processing cannot explain either of these phenomena, therefore additional

processing in the brain must be involved. The most detailed studies of trajectory encoding within the brain come from non-human primates. A subset of neurons in the posterior parietal (PP) cortex of rhesus monkeys responds to drifting objects. Assad and Maunsell (1995) presented targets that either drifted on a continuous trajectory, or drifted whilst hidden behind an occluder. As was expected, PP neurons responded robustly when presented with the continuous condition. However, responses during the occlusion condition were also elevated, despite the lack of any visual motion. This tells us that some regions of the human brain encode inferred visual motion, providing a neuronal representation of expectation even in the absence of a physical stimulus.

1.8 Thesis aims and scope

In the introduction above I have covered a broad range of topics. These include descriptions of prey pursuit and capture behavior, the structure and function of the insect visual system, the identity and physiological properties of neurons involved in target detection, and finally a description of some higher-order properties of vertebrate systems that aid target detection. My PhD will focus on improving our state of knowledge surrounding the neuronal basis of target detection in dragonflies, a simple but highly effective predator. I have focused my study on meeting three key objectives;

1) To provide an up-to-date and detailed description of the organization of dragonfly optic lobe, with specific emphasis on the lobula complex.
2) To investigate the effects of facilitation by continuous target trajectories on the responses of CSTMD1.
3) To investigate the presence of facilitation in pre-synaptic SF-STMD units.
4) To investigate the relationship between neuronal facilitation and selective attention in CSTMD1.

The following chapters will describe work I performed during this project in order to addressing these objectives.

1.9 References

1. Assad, J. A., and Maunsell, J. H. (1995). Neuronal correlates of inferred motion in primate posterior parietal cortex. *Nature* 373 518-521.

2. Azevedo, F. A., Carvalho, L. R., Grinberg, L. T., Farfel, J. M., Ferretti, R. E., Leite, R. E., Jacob Filho, W., Lent, R., and Herculano-Houzel, S. (2009). Equal numbers of neuronal and nonneuronal cells make the human brain an isometrically scaled-up primate brain. *Journal of Comparative Neurology* 513 532-541.

3. Barlow, H. B., and Levick, W. R. (1965). The mechanism of directionally selective units in the rabbit's retina. *Journal of Physiology* 178, 477-504.

4. Barnett, P.D., Nordström, K., and O'Carroll, D.C. (2007). Retinotopic Organization of Small-Field- Target-Detecting Neurons in the Insect Visual System. *Current Biology* 17, 569-578

5. Bausenwein, B., Dittrich, A. P. M., and Fischbach, K, F. (1992). The optic lobe of *Drosophila melanogaster* II. Sorting of retinotopic pathways in the medulla. *Cell and Tissue Research* 267, 17-28.

6. Behnia, R., Clark, D. A., Carter, A. G., Clandinin, T. R., and Desplan, C. (2014). Processing properties of ON and OFF pathways for *Drosophila* motion detection. *Nature* 512, 427-430.

7. Bennet, S.J., and Barnes G.R. (2003). Human Ocular Pursuit During the Transient Disappearance of a Visual Target. *J Neurophysiol* 90, 2504-2520.

8. Berry, M. J., Brivanlou, I, H., Jordan, T, A., and Meister, M. (1999). Anticipation of moving stimuli by the retina. *Nature* 398, 334-338.

9. Boeddeker, N., Kern, R., and Egelhaaf, M. (2003). Chasing a dummy target: smooth pursuit and velocity control in male blowflies. *Proceedings of the Royal Society of London. Series B, Biological Sciences* 270, 393-399.

10. Bolzon, D. M., Nordström, K., and O'Carroll, D.C. (2009). Local and Large-Range Inhibition in Feature Detection. *Journal of Neuroscience* 29 14143-14510.

11. Borghuis, B. G., and Leonardo, A. (2015). The Role of Motion Extrapolation in Amphibian Prey Capture. *Journal of Neuroscience* 35, 15430-15441.

12. Borst, A., and Helmstaedter, M. (2015). Common circuit design in fly and mammalian motion vision. *Nature Neuroscience* 18, 1067-1076.

13. Borst, A., Haag, J., and Reiff, D. F. (2010). Fly Motion Vision. *Annual Review Neuroscience* 33, 49-70.

14. Briscoe, A., and Chittka, L. (2001). The evolution of color vision in insects. *Annual Review of Entomology* 46, 471-510.

15. Burton, B. G., and Laughlin, S. B. (2003). Neural images of pursuit targets in the photoreceptor arrays of male and female houseflies *Musca domestica*. *Journal of Experimental Biology* 206, 3963-3977.

16. Carrasco, M., Penpeci-Talgar, C., and Eckstein, M. P. (2000). Spatial covert attention increases contrast sensitivity across the CSF: support for signal enhancement. *Vision Research* 40, 1203-1215.

17. Carrasco, M., Williams, P. E., and Yeshurun, Y. (2002). Covert attention increases spatial resolution with or without masks: Support for signal enhancement. *Journal of Vision* 2, 467-479.

18. Carrasco, M., and McElree, B. (2001). Covert attention accelerates the rate of visual information processing. *Proceedings of the National Academy of Sciences* 98, 5363-5367.

19. Cajal, S. R., and Sanchez D (1915) Contribucion al conocimiento de los centros nerviosos de los insectes. Trab Lab Invest

20. Clark, D. A., Bursztyn, L., Horowitz, M. A., Schnitzer, M. J., and Clandinin, T. R. (2011). Defining the computational structure of the motion detector in *Drosophila*. *Neuron* 70, 1165-1177.

21. Clark, D. A., and Demb, J. B. (2016). Parallel Computations in Insect and Mammalian Visual Motion Processing. *Current Biology* 26, R1062-R1072.

22. Collett, T. S., and Land, M. F. (1978). How hoverflies compute interception courses. *Journal of Comparative Physiology A* 125, 191-204.

23. Collett, T. S. (1971). Visual neurons for tracking moving targets. *Nature* 232, 127-130.

24. Combes, A. A., Salcedo, M. K., Pandit, M. M., and Iwasaki, J. M. (2013). Capture Success and Efficiency of Dragonflies Pursuing Different Types of Prey. *Integrative and Comparative Biology* 53, 787-798.

25. Connor, C. E., Gallan, J. L., Preddie, D. C., and Van Essen, D. C. (1996). Responses in Area V4 Depend on the Spatial Relationship Between Stimulus and Attention. *Journal of Neurophysiology 75*, 1306-1308

26. Demb, J. B. (2007). Cellular Mechanisms for Direction Selectivity in the Retina. *Neuron* 55, 179-186.

27. DeVoe, R. D., Kaiser, W., Ohm, J., and Stone, L. S. (1982). Horizontal movement detectors of honeybees: Directionally-selective visual neurons in the lobula and brain. *Journal of Comparative Physiology* 147, 155-170.

28. de-Wit, L., Machilsen, B., and Putzeys, T. (2010). Predictive Coding and the Neural Response to Predictable Stimuli. *The Journal of Neuroscience* 30, 8702-8703.

29. Diaz, G. D., Cooper, J., Rothkopf, C., and Hayhoe, M., (2013). Saccades to future ball location reveal memory-based prediction in a virtual-reality interception task. *Journal of Vision 13*, 20.

30. Diaz, G. D., Phillips, F., Fajen, B. R. (2009). Intercepting moving targets: a little foresight helps a lot. *Experimental Brain Research* 195, 345-360.

31. Doherty, J. R., Rao, A., Mesulam, M. M., and Nobre, A. C. (2005). Synergistic Effects of Combined Temporal and Spatial Expectations on Visual Attention. *The Journal of Neuroscience* 25, 8259-8266

32. Dubs, A. (1982). The spatial integration of signals in the retina and lamina of the fly compound eye under different conditions of luminance. *Journal of Comparative Physiology* 146, 321-343

33. Dunbier, J. R., Wiederman, S. D., Shoemaker, P. A., and O'Carroll, D. C. (2012). Facilitation of dragonfly target-detecting neurons by slow moving features on continuous paths. *Frontiers in neural circuits, 6.*

34. Dunbier, J. R., Wiederman, S. D., Shoemaker, P. A., and O'Carroll, D. C. (2011). Modelling the temporal response properties of an insect small target motion detector. *Intelligent Sensors, Sensor Networks and Information Processing* 125-130.

35. Dvorak, D. R., Srinivasan, M. V., and French, A. S. (1980). The contrast sensitivity of fly movement-detecting neurons. *Vision Research* 20, 397-407.

36. Fischbach, K. F., and Dittrich, A. P. M. (1989). The optic lobe of *Drosophila melanogaster*. I: A. Golgi analysis of wild-type structure. *Cell and Tissue Reserch* 258, 441–475.

37. Fischbach, K. F. (1983). Neural cell types surviving congenital sensory deprivation in the optic lobes of *Drosophila melanogaster*. *Developmental Biology* 95, 1-18.

38. Fisher, Y. E., Silies, M., and Clandinin, T. R. (2015). Orientation Selectivity Sharpens Motion Detection in *Drosophila*. *Neuron* 88 390-402.

39. Friston, K. J. (2009). The free-energy principle: a rough guide to the brain? *Trends in Cognitive Sciences* 13, 293-301.

40. Frye, M. A., and Dickinson, M. H. (2001). Fly Flight: A Model for the Neural Control of Complex Behaviour. *Neuron* 32, 385-388.

41. Frye, M. A., and Olberg, R. M. (1995). Visual receptive field properties of feature detecting neurons in the dragonfly. *Journal of Comparative Physiology A* 177, 569-576.

42. Geiger, G., and Poggio, T. (1975). The orientation of flies towards visual patturns: on the search for the underlying functional interactions. *Biological Cybernetics* 619, 39-54.

43. Gengerelli, J. A. (1948). Apparent movement in relation to homogenous and heterogenous stimulation of the cerebral hemispheres. *Journal of Experimental Psychology* 38, 592-599.

44. Geurten, B. R. H., Nordström, K., Sprayberry, J. D. H., Bolzon, D. M., and O'Carroll, D. C. (2007). Neural mechanisms underlying target detection in a dragonfly centrifugal neuron. *Journal of Experimental Biology A*, 210 3277-3284.

45. Gilbert, C. (2013). Brain Connectivity: Revealing the Fly Visual Motion Circuit. *Current Biology* 23, R851-R853.

46. Gonzalez-Bellido, P. T., Fabian, S. T., and Nordström, K. (2016). Target detection in insects: optical, neural and behavioural optimizations. *Current Opinion in Neurobiology* 41, 122-128.

47. Gonzalez-Bellido, P. T., Peng, H., Yang, J., Georgopoulos, A. P., and Olberg, R. M. (2013). Eight pairs of descending neurons in the dragonfly give wing motor centers accurate population vector of prey direction. *Proceedings of the Nationall Acadamy of Sciences USA* 110, 676-701.

48. Grzywacz, N. M., Watamaniuk, S. N. J., McKee, S. P. (1995) Temporal coherence theory for the detection and measurement of visual motion. *Vision Research* 35, 3183-3203

49. Hausen, K. (1982). Motion Sensitive Interneurons in the Optopmotor System of the Fly. I. The Horizontal Cells: Structure and Signals. *Biological Cybernetics* 45, 143-156.

50. Hoffman, J. (1986). Spatial attention in vision. *Psychological Research* 47, 221-229.

51. Horridge, G. A. (1978). The separation of visual axes in apposition compound eyes. *Philosophical Transactions of the Royal Society of London. Series B, Biological Sciences*, 1-59.

52. Ito, K., Shinomiya, K., Ito, M., Armstrong, J. D., Boyan, G., Hartenstein, V., Harzsch, S., Heisenberg, M., Homberg, U., Jenett, A., Keshishian, H., Restifo, L. L., Rössler, W., Simpson, J. H., Strauss, R., Vosshall, L. B., et al. (2014). Insect Brain Name Working Group. A systematic nomenclature for the insect brain. *Neuron* 19, 755-65

53. Jancke, D., Erlhagen, W., Schöner, G., and Dinse, H. R. (2004). Shorter latencies for motion trajectories than for flashes in population responses of cat primary visual cortex. *Journal of Physiology* 556, 971-982.

54. Joesch, M., Schnell, B., Varija Raghu, S., Reiff, D. F., and Borst, A. (2010). ON and OFF pathways in *Drosophila* motion vision. *Nature* 468, 300-304.

55. Johnston, J., and Lagnado, L. (2015). General features of the retinal connectome determine the computation of motion anticipation. *eLife* 4, e06250

56. Keles, M. F., and Frye, M. A. (2017). Object-Detecting Neurons in Drosophila. *Current Biology* 27, 680-687.

57. Kim, A. J., Fitzgerald, J. K., and Maimon, G. (2015). Cellular evidence for efference copy in *Drosophila* visuomotor processing. *Nature Neuroscience* 18, 1247-1255.

58. Kirschfeld, K., and Wenk, P. (1976). The dorsal compound eye of simuliid flies: an eye specialized for the detection of small, rapidly moving objects. *Zeitschrift für Naturforschung. Section C: Biosciences*, 31 764-765.

59. Kok, P., Rahnev, D., Jehee, J. F. M., Lau, H. C., de Lange, F. P. (2011) Attention reverses the effect of prediction in silencing sensory signals. *Cerebral Cortex* 22, 2197-2206.

60. Korte, A. (1915). Kinematoskopische Untersuchengen. *Zeitschrift Fur Psychologie* 72, 193-296.

61. Krekelberg, B., Lappe, M. (1999). Temporal recruitment along the trajectory of moving objects and the perception of position. *Vision Research* 39, 2669-2679.

62. Kurylas, A. E., Rohlfing, T., Krofczik, S., Jenett, A., and Homberg, U. (2008). Standardized atlas of the brain of the desert locust, *Schistocerca gregaria*. *Cell and Tissue Research* 333, 125-145.

63. Kuwabara, M., and Naka, K. (1959). Response of a single retinula cell to polarized light. *Nature* 184, 455

64. Lackner, J. R., and DiZeo, P. (2000). Human orientation and movement control in

weightless and artificial gravity environments. *Experimental Brain Research* 130, 2-26.

65. Land, M. F. (1989). Variations in the Structure and Design of Compound Eyes. In Facets of Vision 90-111. Springer Berlin Heidelberg.

66. Land, M. F., and Collett, T. S. (1974). Chasing behavior of houseflies (*Fannia canicularis*). *Journal of Comparative Physiology* 89, 331-357.

67. Land, M. F. (1997). Visual Acuity in Insects. *Annual Review of Entomology 42*, 147-77.

68. Laughlin, S. B., de Ruyter van Steveninck, R. R., and Anderson, J. C. (1998). The metabolic cost of neural information. *Nature Neuroscience 1*(1) 36-41

69. Laughlin, S. B. (1987). Form and function in retinal processing. *Trends in Neuroscience* 10, 478-483.

70. Laughlin, S. B., and Hardie, R. C. (1978). Common strategies for light adaptation in the peripheral visual systems of fly and dragonfly. *Journal of Comparative Physiology* 128, 319-340.

71. Leonardo, A., and Meister, M. (2013). Nonlinear Dynamics Support a Linear Population Code in a Retinal Target-Tracking Circuit. *Journal of Neuroscience* 33, 16971-16987

72. MacKay, D. M. (1961). Interactive processes in visual perception. W.A. Rosenblith (Ed.), Sensory Communication, MIT Press, 339-355

73. Maddess, T., and Yang, E. (1997). Orientation-sensitive Neurons in the Brain of the Honey Bee (*Apis mellifera*). *Journal of Insect Physiology* 43, 329-336.

74. Maisak, M. S., Haag, J. H., Ammer, G., Serbe, E., Meier, M., Leonhardt, A., Schilling, T., Bahl, A., Rubin, G. M., Nern, A., Dickson, B. J., Reiff, D. F., Hopp, E., and Borst, A. (2013). A directional tuning map of *Drosophila* elementary motion detectors. *Nature* 500, 212-216.

75. Mann, D. L., Spratford, W., Abernethy, B. (2013) The Head Tracks and Gaze

Predicts: How the World's Best Batters Hit a Ball. *PLoS ONE* 8, e58289.

76. Meinertzhagen, I. A., and O'Neil, S. D. Synaptic organization of columnar elements in the lamina of the wild type in Drosophila melanogaster. (1991). *Journal of Comparative Neurology* 305, 232-263.

77. Mischiati, M., Lin, H., Herold, P., Imler, E., Olber, R., and Leonardo, A. (2014). Internal models direct dragonfly interception steering. *Nature* 517, 333-338.

78. Misof B. et al. (2014). Phylogenomics resolves the timing and pattern of insect evolution. *Science* 346, 763-767.

79. Nilsson, D. E. (1989). Optics and evolution of the compound eye. In Facets of Vision 30-73. Springer Berlin Heidelberg.

80. Nijhawan, R. (1994). Motion extrapolation in catching. *Nature* 370, 256-257.

81. Nijhawan, R. (2002). Neural delays, visual motion and the flash-lag effect. *Trends in Cognitive Sciences* 6, 387-393.

82. Nordström, K and O'Carroll, D. C. (2006). Small object detection neurons in female hoverflies. *Proceedings of the Royal Society of London B, Biological Sciences* 273, 1211-1216.

83. Nordström, K., Bolzon, D. M., and O'Carroll, D. C. (2011). Spatial facilitation by a high-performance dragonfly target-detecting neuron. *Biology Letters. 7,* 588-592.

84. Nordström, K. (2012). Neural specializations for small target detection in insects. *Current Opinion in Neurobiology* 22, 272-278.

85. O'Carroll, D. C. (1993). Feature-detecting neurons in dragonflies. N*ature* 362, 541-543.

86. O'Carroll, D. C. and Wiederman, S. D., (2014). Contrast sensitivity and the detection of moving patterns and features. *Philosophical Transactions of the Royal Society B: Biological Sciences* 369, 20130043

87. Olberg, R. M. (1983). Identified interneurons steer flight in the dragonfly. *Society for Neuroscience* 9, 326.

88. Olberg, R. M., (1986). Identified target-selective visual interneurons descending from the dragonfly brain. *Journal of Comparative Physiology A* 159, 827-840.

89. Olberg, R. M., Seaman, R. C., Coats, M. I. and Henry, A. F. (2007) Eye movements and target fixation during dragonfly prey-interception flights. *Journal of Comparative Physiology A* 193, 685-693.

90. Olberg, R. M., (2012) Visual control of prey-capture flight in dragonflies. *Current Opinion in Neurobiology* 22, 267-271.

91. Olberg, R. M., Worthington. A. H., and Venator, K. R., (2000). Prey pursuit and interception in dragonflies. *Journal of Comparative Physiology A* 186, 155-162.

92. Osorio, D. (1987). The temporal properties of non-linear, transient cells in the locust medulla. *Journal of Comparative Physiology A* 161, 431-440.

93. Pakkenberg B, Pelvig D, Marner L, Bundgaard MJ, Gundersen HJ, Nyengaard JR, Regeur L. (2003). Aging and the human neocortex. *Experimental Gerontology* 38, 95-99.

94. Palka, J. (1969). Discrimination between movements of eye and object by visual interneurons of crickets. *Journal of Experimental Biology* 50, 723-732.

95. Pestilli, F., and Carrasco, M. (2005). Attention enhances contrast sensitivity at cued and impairs it at uncued locations. *Vision Research* 45, 1867-1875.

96. Ramachandran, V. S., and Anstis, S. M. (1983). Extrapolation of motion path in human visual perception. *Vision Research* 23, 83-85.

97. Rao, R. P. N. and Ballard, D. H. (1999). Predictive coding in the visual cortex: a functional interpretation of some extra-classical receptive-field effects. *Nature Neuroscience* 2, 79-87.

98. Rao, R. P. N. (2005). Bayesian inference and the attentional modulation of the visual cortex. *Cognitive neuroscience and neuropsychology* 16, 1843-1848.

99. Rauss, K., Schwartz, S., Pourtois, G. (2011). Top-down effects on early visual processing in humans: a predictive coding framework. *Neuroscience and*

Biobehavioral Reviews 35, 1237-1253.

100. Reichardt W. 1961. Autocorrelation, a principle for the evaluation of sensory information by the central nervous system. In Sensory Communication, ed. WA Rosenblith, pp. 303–17. New York/London: MIT Press/Wiley.

101. Reichardt W. 1987. Evaluation of optical motion information by movement detectors. *Journal of Comparative Physiology A* 161, 533–47

102. Reynolds, J. H., Pasternak, T., and Desimone, R. (2000). Attention Increases Sensitivity of V4 Neurons. *Neuron* 26, 703-714.

103. Ribi, W. A., and Scheel, M. (1981). The second and third optic ganglia of the worker bee. *Cell and Tissue Research* 221, 17-43.

104. Rind, F. C., and Simmons, P. J. (1992). Orthopteran DCMD neuron: a reevaluation of responses to moving objects. 1. Selective responses to approaching objects. *Journal of Neurophysiology* 68, 1654-1666.

105. Rivera-Alba, M., Vitaladevuni, S. N., Mischenko, Y., Lu, Z., Takemura, S-Y., Scheffer, L., Meinertzhagen, I. A., Chklovskii, D. B., and de Polavieja, G. G. (2011). Wiring economy and volume exclusion determine neuronal placement in the *Drosophila* brain. *Current Biology* 21, 2000-2005.

106. Rosner, R., von Haldeln, J., Salden, T., and Homberg, U. (2017). Anatomy of the lobula complex in the brain of the praying mantis compared to the lobula complexes of the locust and cockroach. *Journal of Comparative Neurology* 525, 2343-2357.

107. Rowell, C. H. F., O'Shea, M., and Williams, J. L. (1977). The neuronal basis of a sensory analyser, the acridid movement detector system. IV. The preference for small field stimuli. *Journal of Experimental Biology*, 68 157-185.

108. Russell, R. W., May, M. L., Soltesz, K. L., Fitzpatrick, J. W., (1998). Massive Swarm Migrations of Dragonflies (Odonata) in Eastern North America. *The American Midland Naturalist* 140, 325-342.

109. Santer, R. D., Rind, C. F., and Simmons, P. J. (2012). Predator versus Prey: Locust Looming-Detector Neuron and Behavioural Responses to Stimuli Representing Attacking Bird Predators. *PLOS ONE* 7, e50146.

110. Schwartz, G., Harris, R., Shrom, D., and Berry, M. J. (2007). Detection and prediction of periodic patterns by the retina. *Nature Neuroscience* 10, 552-554.

111. Shepard, R. N. (1957). Stimulus and response generalization: a stochastic model relating generalization to distance in psychological space. *Psychometrika* 22, 325-45.

112. Shinomiya, K., Karuppudurai, T., Lin, T., Lu, Z., Lee, C., and Meinertzhagen, I. A. (2014). Candidate Neural Substrates for Off-Edge Motion Detection in *Drosophila*. *Current Biology* 24, 1062-1070.

113. Sommer, M. A., and Wurtz, R. H. (2008). Brain circuits for the internal monitoring of movements. *Annual Review of Neuroscience* 31, 317-338.

114. Sommer, M. A., and Wurtz, R. H. (2006). Influence of the thalamus on spatial visual processing in frontal cortex. *Nature* 444, 374-377.

115. Spratling, M. W. (2008). Reconciling predictive coding and biased competition models of cortical function. *Frontiers in computational neuroscience* 2, 4.

116. Srinivasan, M. V., and Bernard, G. D. (1977). The pursuit response of the housefly and its interaction with the optomotor response. *Journal of Comparative Physiology* 115, 101-117.

117. Strausfeld, N. J. (2005). The evolution of crustacean and insect optic lobes and the origins of chiasmata. *Arthropod Structure and Development* 34, 235-256.

118. Stockman, A., MacLeod, D. I. A., and DePriest, D. D. (1991). The temporal properties of the human short-wave photoreceptors and their associated pathways. *Vision Research* 31, 189-208.

119. Summerfield, C., and Egner, T. (2009). Expectation (and attention) in visual cognition. *Trends in cognitive Sciences 13*, 403-409

120. Takemura, S-Y., Bharioke, A., Lu, Z., Nern, A., Vitaladevuni, S., Rivlin, P. K., Katz, W. T., Olbris, D. J. Plaza, S. M., Winston, P., et al. (2013). A visual motion detection circuit suggested by *Drosophila* connectomics. *Nature* 500, 175-181.

121. Takemura, S-Y., Nern, A., Chklovsii, D. B., Scheffer, L. K., Rubin, G. M., and Meinertzhagen, I. A. (2017). The comprehensive connectome of a neural substrate for 'ON' motion detection in *Drosophila*. *eLife* 6, e24394.

122. Thorpe, S., Fize, D., and Marlot, C. (1996). Speed of processing in the human visual system. *Nature* 381, 520-522.

123. Wardill, T. J., Fabian, S. T., Pettigrew, A. C., Stavenga, D. G., Nordström, K., and Gonzalez-Bellido, P. T. (2017). A Novel Interception Strategy in a Miniature Robber Fly with Extreme Visual Acuity. *Current Biology* 27, 854-859.

124. Warrant, E. Vision in the dimmest habitats on Earth. (2004). *Journal of Comparative Physiology A* 190, 765-789.

125. Watamaniuk, S. N. J., McKee, S. P., Grzywacz, N. M. (1995). Detecting a trajectory embedded in a random-direction motion noise. *Vision Research* 35, 65-77

126. Watamaniuk, S. N. J and McKee, S. P. (1995) Seeing motion behind occluders. *Nature* 377, 929-730.

127. Watamaniuk, S. N. J. (2005). The predictive power of trajectory motion. *Vision research* 45, 2993-3003

128. Wehrhahn, C., Poggio, T., and Bülthoff, H. (1982). Tracking and chasing in houseflies (*Musca). Biological Cybernetics* 45, 123-130.

129. Wiederman, S. D., and O'Carroll, D. C. (2011). Discrimination of features in natural scenes by a dragonfly neuron. *The Journal of Neuroscience* 31. 7141-7144.

130. Wiederman, S. D., and O'Carroll, D. C., (2013). Selective attention in an insect neuron. *Current Biology* 23, 156-161.

131. Wiederman, S. D., Shoemaker, P. A., and O'Carroll, D. C. (2008). A model for the detection of moving targets in visual clutter inspired by insect physiology. *PLOS ONE* 3, e2784.

132. Wiederman, S. D., and O'Carroll, D. C. (2013). Biomimetic target detection: Modeling 2nd order correlation of OFF and ON channels. *Proceedings of the 2013 IEEE Symposium Series on Computational Intelligence for Multimedia, Signal and Vision Processing (Singapore).*

133. Zanker, J. M (1994). Modelling human motion perception II. Beyond Fourier motion stimuli. *Naturwissenschaften* 81, 200-209.

134. Zawarzin, A. (1914). Histologische Studien über Insekten. IV. Die optischen Ganglien der Aeschna-Larven. *Zeitschrift fur wissenschaftliche Zoologie* 108, 175-257.

135. Zirnsak, M, Steinmetz, N.A., Noudoost, B., Xu, K. Z., and Moore, T. (2014). Visual space is compressed in prefrontal cortex before eye movements. *Nature* 507, 504–507.

2 Methods

The detailed methodologies used in different projects are described within each results chapter. Here I focus on describing some general principles of the methods used to acquire and analyse the data presented in this thesis.

2.1 Animals and electrophysiology

Intracellular electrophysiological recordings from dragonfly STMD neurons make up the vast majority of the data presented in this thesis. All recordings were performed in wild-caught male *Hemicordulia* dragonflies, either *Hemicordulia tau* or *Hemicordulia australiae*. These species are highly amenable to electrophysiological recording, and have been studied since the 1970s. These species are also amongst the most abundant species in South Australia, usually available for approximately 9 months of the year. My recording seasons ranged between September and May, with a mid-season dip in dragonfly availability in December and January.

Dragonflies were immobilised with a 1:1 wax/rosin mixture on an articulating magnetic stand, before dissecting a small hole in the posterior surface of the head capsule. Aluminosilicate electrodes were filled with a 2M KCl solution, and placed into a medial location in the lobula complex. Across the duration of my PhD I recorded from 298 dragonflies, gathering data from 406 neurons (figure 1A, B). Only a small number of these neurons fit our strict recording quality standards for publication. Data from cells was discarded if the health of a neuron was deemed sub-standard, due to unstable resting membrane potential, reduced spike amplitude or unusually high or erratic spontaneous spiking activity. Our recording site targets axon tracts leaving or entering the lobula complex, a location containing many cell types with favourable axon diameters (figure 1C). While my PhD targeted STMD neurons, specifically CSTMD1 and SF-STMDs, I encountered a large number of cells with different physiological properties. Most of these other cell types were tuned to larger patterns or features, which we generally classified as either bar-sensitive or wide-field motion sensitive. I also occasionally encountered cells that responded to transient flicker, and even one cell class that primarily responded to mechanosensory stimuli such as wind.

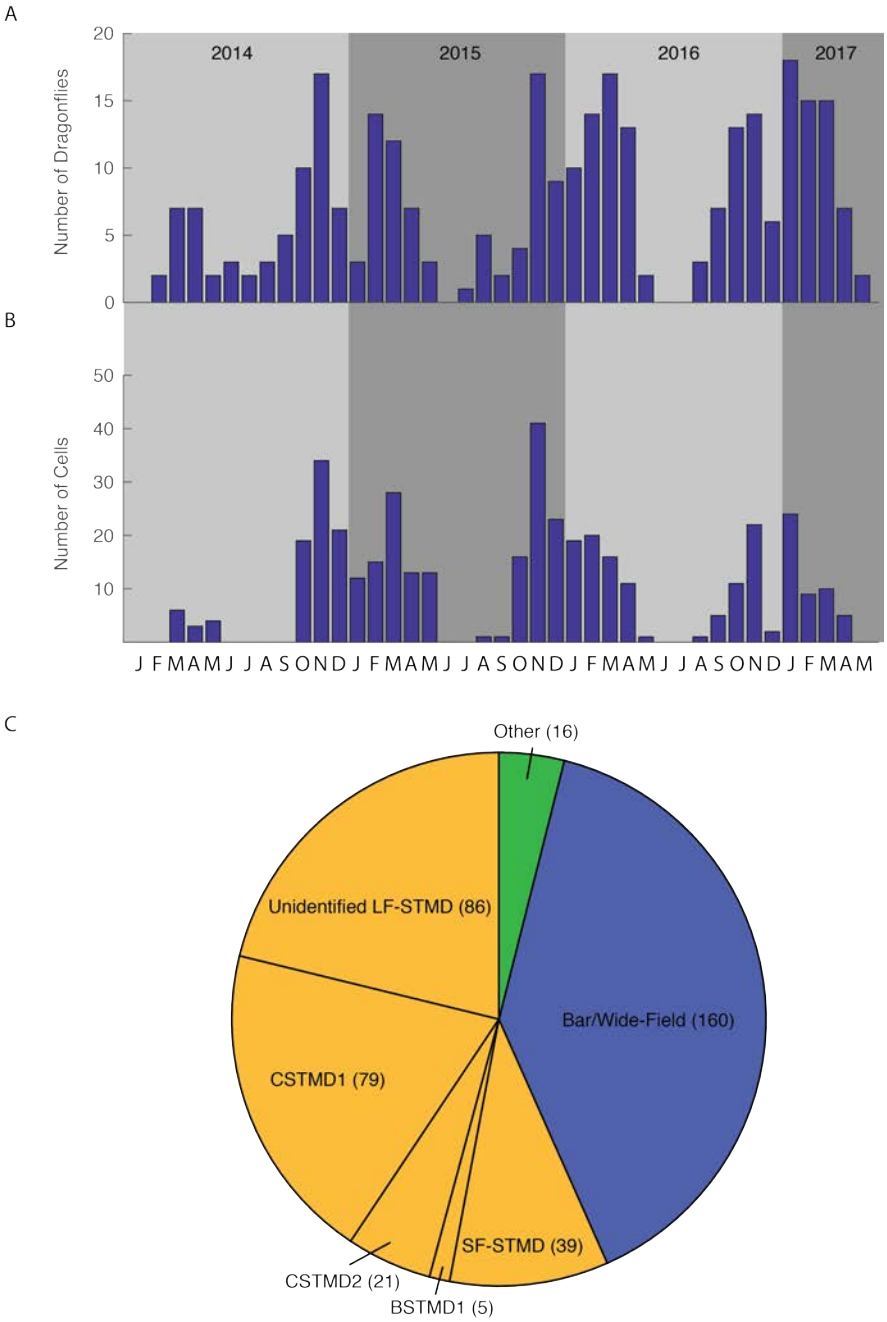

Figure 2-1: A summary of my electrophysiological recordings across the duration of my PhD. A) The number of animals recorded from over time. B) The number of cells for which data was obtained over time. C) A break-down of the different cell types recorded from.

Most of my experiments required lengthy recordings from one specific identified neuron, CSTMD1, across many animals. A standard experiment lasted at least 3-4 hours, and I encountered CSTMD1 in approximately 26% of my experiments before accounting for quality control. These challenges were compounded by the fact that the

responses of STMD neurons become habituated if stimuli are repeatedly presented in the same position over a short period of time. The individual experimental paradigms presented in this thesis required the presentation of a sequence between 30 and 200 trials in length. To ensure that responses were not strongly affected by habituation we had to allow for rest periods of 8-10 seconds between every trial. This means that gathering a single repeat of a single experiment could require holding a healthy intracellular recording from CSTMD1 for more than 30 minutes at a time. For these reasons, gathering the data presented in this thesis required a substantial amount of work and patience.

2.2 Visual stimulus design

All our visual stimuli were presented on an LCD display placed 20 cm away from the animal and centred on the animals frontal midline. Data from the first two and a half seasons used a 120 Hz monitor (Eizo FORIS FG2421, 400 cd / m^2), while in late 2016 we transitioned to 165 Hz monitors (350 cd / m^2). Unless we were specifically investigating the effects of target size, all experiments were performed with 1.5x1.5° targets dark targets on a white background. STMD neuron responses quickly saturate when presented with a maximum contrast target, which can potentially mask the effects of facilitation. To avoid this saturation we used stimuli in the range of 0.2-0.4 weber contrast wherever possible.

2.3 Data analysis

STMD neurons commonly have a spontaneous spiking activity of 10-20 spikes/s. When presented with a small dark target drifting through the receptive field, the spike frequency increases to as much as 400 spikes/s depending on the cell (figure 2a). Varying the salience of a stimulus by decreasing contrast results in reduced spike frequency (figure 2b). This suggests that STMD neurons are using a rate code to convey stimulus strength. For this reason we use the rate of action potential firing to quantify neuronal response.

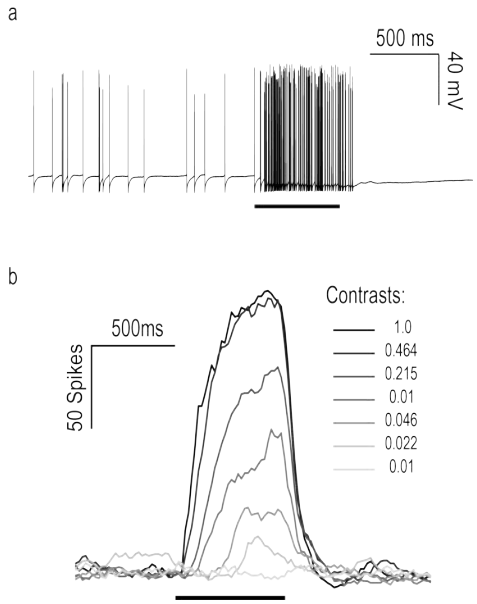

Figure 2-2: STMD neurons utilise a rate code. a) A raw data trace from an STMD neuron during the presentation of a maximum contrast black target drifting within the receptive field. The stimulus bar displays Peristimulus duration. b) Instantaneous spike frequency plot showing responses of an STMD neuron to targets of different contrasts.

To quantify neuronal response we counted the number of spikes in a given analysis window. Most experiments in this thesis aimed to quantify the strength of facilitation across different conditions. Since facilitation appears to be a continuous phenomenon that begins to slowly build at stimulus onset (Nordström et al. 2011), it is impossible to observe the true unfacilitated response of an STMD neuron. Instead we must analyse neuronal response in an analysis window timed shortly after stimulus onset, where the effects of facilitation are minimised. The timing and duration of this window is a trade-off between improving signal robustness and minimising the 'self facilitation' or our probe targets. Through experimentation we find that the optimal solution to this compromise is a 100 ms window, starting 50 ms following stimulus onset. This window is long enough that it includes a representative number of action potentials in the majority of trials, while the 50 ms offset accounts for the absolute response latency of STMD neurons, giving us confidence that we are not misinterpreting responses elicited by a prior stimulus as facilitation.

3 The complex optic lobe of dragonflies

Context

A recent review of the insect brain grouped the dragonfly with dipteran flies, moths and beetles, as insects with a lobula complex formed by a lobula and lobula plate (Ito et al. 2014). However, this statement provided no citation and to our knowledge no published work has described a lobula plate in dragonflies. Members of our lab have been recording from the lobula complex of dragonflies for more than 25 years, and had always assumed the dragonfly lobula was a single fused neuropil. If the dragonfly does have a lobula plate, knowing its position is crucial for our interpretation of the morphology and function of the neurons we study. This encouraged us to utilise modern immunohistochemical techniques to image the synaptic organisation of the lobula complex. Our pilot data revealed an incredibly complex optic lobe and lobula complex. We undertook a more detailed investigation, in an attempt to answer the following research questions:

1. How are the synaptic neuropil of the dragonfly optic lobe organised?
2. Is this organisation plesiomorphic amongst dragonflies?
3. Are the synaptic layers of the medulla and lobula similar to those described in other species?
4. What are the physiological properties of neurons housed in different lobula complex structures?

Statement of Authorship

Title of Paper	The complex optic lobe of dragonflies
Publication Status	☐ Published ☐ Accepted for Publication ☑ Submitted for Publication ☐ Unpublished and Unsubmitted w ork w ritten in manuscript style
Publication Details	Fabian, J. M. F., el Jundi, B., Wiederman, S. D., and O'Carroll., D. C. (2017). The complex optic lobe of dragonflies. Current Biology, in resubmission

Principal Author

Name of Principal Author (Candidate)	Joseph Fabian		
Contribution to the Paper	Experiment conceptualisation, caught all animals, performed dissection, performed immunohisotochemical processing, aided in imaging, analysed all data, wrote the manuscript.		
Overall percentage (%)	65%		
Certification:	This paper reports on original research I conducted during the period of my Higher Degree by Research candidature and is not subject to any obligations or contractual agreements with a third party that would constrain its inclusion in this thesis. I am the primary author of this paper.		
Signature		Date	28/8/2017

Co-Author Contributions

By signing the Statement of Authorship, each author certifies that:

i. the candidate's stated contribution to the publication is accurate (as detailed above);

ii. permission is granted for the candidate in include the publication in the thesis; and

iii. the sum of all co-author contributions is equal to 100% less the candidate's stated contribution.

Name of Co-Author	Basil el Jundi		
Contribution to the Paper	Aided in immunohistochemical processing, tissue sectioning and imaging. Provided substantial input into data interpretation and manuscript evaluation.		
Signature		Date	21.08.2017

Name of Co-Author	Steven Wiederman		
Contribution to the Paper	Experiment conceptualisation, aided interpretation of the data and manuscript evaluation.		
Signature		Date	28/8/2017

Name of Co-Author	David O'Carroll		
Contribution to the Paper	Experiment conceptualisation, immunohistochemical processing, performed imaging, aided in data analysis, data interpretation and manuscript writing.		
Signature		Date	25-AUG-2017

The complex optic lobe of dragonflies

IN RESUBMISION: Fabian, J. M., el Jundi, B., Wiederman, S. D., and O'Carroll., D. C. (2017). The complex optic lobe of dragonflies. ***Current Biology***

Joseph M Fabian[1], Basil el Jundi[2,3], Steven D Wiederman[1], and David C O'Carroll[2].

[1]Adelaide Medical School, The University of Adelaide, Adelaide, Australia.

[2]Department of Biology, Lund University, Lund, Sweden.

[3]Biocenter, Behavioural Physiology and Sociobiology, University of Würzburg, Würzburg, Germany.

3.1 Summary

Dragonflies represent an ancient lineage of visual predators, which last shared a common ancestor with insect groups such as dipteran flies in the early Devonian, 406 million years ago (Misof et al. 2014; Letch et al. 2016). Despite their important evolutionary status, and recent interest in them as a model for complex visual physiology and behavior, the most recent detailed description of the dragonfly optic lobe is itself more than a century old (Zawarzin. 1914). Many insects process visual information in optic lobes comprising 4 sequential, retinotopically organized neuropils: the lamina, medulla, lobula and a posterior lobula plate devoted to processing information about wide-field motion stimuli (Cajal and Sanchez. 1915; Strausfeld. 2009). Recent reports suggest that the dragonflies also follow this basic plan, with a divided lobula similar to those of flies, moths and butterflies (Ito et al. 2014; Strausfeld. 2005). Here we refute this claim, showing that dragonflies have an unprecedentedly complex lobula comprising at least 4 sequential synaptic neuropils, in addition to two lobula plate like structures located on opposite sides of the brain. The second and third optic ganglia contain approximately twice as many synaptic layers as any other insect group yet studied. Using intracellular recording and labeling of neurons we further show that the most anterior lobe contains wide-field motion processing tangential neurons similar to those of the posterior lobula plate of dipteran flies. In addition to describing what is probably the most complex and unique optic lobe of any insect to date, our findings provide interesting insights to understanding the evolution of the insect optic lobe and serve as a reminder that the highly studied visual circuits of dipteran flies may represent a derived form of these brain structures.

3.2 Materials and Methods

Animals

Male dragonflies were caught in the wild, either from the Adelaide Botanical Gardens, Australia (*Hemicordulia tau, Adversaechna Brevistyla*) or various wetlands in Lund, Sweden (*Aeshna mixta, Sympetrum striolatum*). Animals were stored in small, moist plastic bags at 4°C until use, normally not exceeding 5 hours.

Wholemounts

To visualise neuropil in wholemount specimens, we followed the staining protocol by Ott (2008). We carefully dissected and removed the brain from the head capsule under HEPES buffered saline (HBS; 150 mM NaCl; 5 mM KCl; 5 mM CaCl2; 25 mM sucrose; 10 mM HEPES; pH 7.4) before fixation for 24 hours at room temperature (RT) in zinc-formaldehyde solution (ZnFA; 0.25% [18.4 mM] ZnCl2; 0.788% [135 mM] NaCl; 1.2% [35 mM] sucrose; 1% formaldehyde). Following fixation, brains were rinsed in HBS (8 x 20 minutes), before treatment in 80/20 DMSO/methanol solution for 55 minutes at RT. Brains were then rinsed in Tris-HCL (3x10 minutes) and preincubated in 5% Normal Goat Serum (NGS) for 3 hours at RT or overnight at 4°C. Primary antibodies (anti-synapsin, RRID:AB_528479) were diluted 1:50 in PBT and 1% NGS, and incubated for 5 days at 4°C under gentle agitation. Brains were then rinsed (8x20 minutes) in PBT, and treated with secondary antibodies (Goat anti-mouse CY5, RRID:AB_10895546) diluted 1:300 in PBT and 1% NGS for 3 days at 4°C under gentle agitation. Brains were then rinsed (6x20 minutes) in PBS, and dehydrated by ascending ethanol series (50%, 70%, 80%, 90%, 100%, 15 minutes each). Dehydrated brains were cleared in Methyl salicylate, (50% Methyl salicylate 50% ethanol for 15 minutes, 100% Methyl salicylate for 1 hour). Finally brains were mounted in Permount between two #1.5 coverslips, separated by plastic adhesive spacer rings (~500µm).

Sections

Sections for synapsin staining followed the exact same protocol as above, with the following exceptions: Following primary fixation, brains were embedded in a gelatin-albumin mixture (4.8% gelatin and 12% ovalbumin in milliQ water), and allowed to set at RT before post-fixing overnight in 4% Paraformaldehyde at 4°C. 200µm horizontal sections were cut on a vibratome before rinsing (6x20 minutes) in PBS. No DMSO step was included due to the reduced thickness of tissue. Sections were either incubated with anti-synapsin alone, or in combination with anti-serotonin or anti-lucifer yellow (*H. tau* only). Primary antibody incubation was reduced to 3 days. For sections that included intracellularly labelled neurons, synapsin was visualised with a Goat anti-mouse CY3 secondary antibody. For sections co-labelled for serotonin, this was visualised with a Goat anti-rabbit Alexa Fluor 546 secondary antibody.

Additional thick sections for osmium staining were prepared from from one individual of *Hemicordulia* from a brain fixed in 2% glutaraldehyde, 4% paraformaldehyde in 0.2 M phosphate buffer (+5% sucrose) at pH 7.4 for 2 h. Tissue was rinsed in PBS (2x10 minutes) before embedding in 4% agarose (in buffer), allowed to cool to just above setting point (ca. 25°C). After cooling, the block was cut into 100 μm sections on a vibratome, which were then post-fixed in 1% aqueous OsO_4 for 30 min before dehydration through an ethanol series, and mounting under coverslips in unpolymerized araldite.

Electrophysiology and intracellular neuron labelling

Hemicordulia tau dragonflies were immobilised with a 1:1 wax/rosin mixture, and fixed to an articulating magnetic stand. A small hole was dissected on the posterior surface of the head capsule directly above the left lobula complex. Aluminosilicate electrodes were pulled on a Sutter Instruments P-97 electrode puller, and tip filled with 4% Lucifer Yellow in 1M LiCl solution. Electrodes had typical resistances of 150-200 MΩ. Electrodes were placed in the medial portion of the lobula complex, and stepped through the brain from the posterior to anterior lobula complex using a piezo-electric stepper (Marzhauser-Wetzlar PM-10). Intracellular responses were digitized at 5 kHz with a 16-bit A/D converter (National Instruments) for off-line analysis with MATLAB. Following physiological characterisation, neurons were injected with approximately -2nA of current for up to 30 minutes. Immediately following injection the brain was carefully dissected under PBS, before fixation overnight in 4% paraformaldehyde at 4°C. Brains were then processed in accordance with published protocols (Gonzalez-Bellido and Wardill. 2012). Brains were rinsed (3x10 minutes) in PBS, before permeabilization in 80/20 DMSO/Methanol solution for 55 minutes. Brains were then rinsed (3x30 minutes) in PBT, and preincubated in 5% NGS in PBT for 3 hours at RT under gentle agitation. Brains were incubated in 1:50 dilution of primary antibody (anti-lucifer yellow, RRID:AB_2536190) in universal antibody dilution solution (Sigma Aldrich) for 3 days at 4°C under gentle agitation. They were then rinsed (3x30 minutes) in 10% NGS, before incubation with a 1:50 dilution of NeutraAvadin DyLight 633 for 3 days at 4°C under gentle agitation. The samples were then rinsed, dehydrated and mounted identically to wholemount synapsin labelled samples described above. Following confocal imaging brains were retrieved

from coverslips with xylene, rehydrated by an inverted ethanol series (90%, 80%, 70%, 50%, 0%), and sectioned through an identical protocol as described above.

Visual Stimuli and Physiological Characterisation

Recordings obtained were during ongoing experiments aimed at classifying feature selective neurons such as the small target motion detecting (STMD) neurons described in our recent work (Wiederman et al. 2017), from more than 300 dragonflies over a 3 year period. Upon establishing a healthy recording, all neurons were characterized using a range of stimuli presented on an LCD monitor (either an Eizo Foris FG2421 LCD at a frame rate of 120 Hz, or an Asus ROG Swift PG279Q IPS LCD at 165 Hz). Stimuli included a sequence of drifting texture patterns, drifting sinusoidal gratings with varying directions, spatial and temporal frequency, and discrete features (e.g. targets, bars) of different sizes and contrast. In addition to hundreds of recorded neurons that were primarily selective for discrete features such as small targets and which gave weak responses to optic flow stimuli, we obtained reasonably complete data sets for 56 lobula neurons that provided robust responses to wide-field motion stimuli. Despite all giving strong responses to optical flow stimuli, these neurons nevertheless display very diverse physiological properties, with some displaying non-directional responses or strong responses to discrete edges or features, so ongoing work is required to establish a classification of their basic properties. One subset, however, gave robust, direction opponent responses to wide-field texture patterns and gratings, with little to no response to small moving features. Most of this subset of neurons also show the sensitivity to contrast and the tuning and selectivity for spatial and temporal frequency very similar to neurons classified as lobula plate tangential cells (LPTCs) in dipteran flies and other taxa (Hausen. 1982).

Tracer injection

Aeshna mixta dragonflies were immobilised with a 1:1 wax/rosin mixture, and fixed to an articulating magnetic stand. A large hole was cut in the posterior head capsule, allowing visualisation of the optic lobe. The neural sheath was carefully removed, and any excess liquid was absorbed with tissue paper. Aluminosilicate microelectrodes had their tips manually broken and were then dipped in Vaseline, before dipping into fluorescent dextran 488 (3000 mw.) crystals. The electrode was then inserted into the posterior part of the left medulla by hand. After thoroughly rinsing the head capsule

with PBS to ensure that no crystals remained on the brain surface, animals were placed in a small moist container, and left overnight at 4°C. The following day, the brain was carefully dissected under PBS and fixed overnight in 4% PFA. Brains were then washed, dehydrated, cleared and mounted as described previously.

Imaging, Image Processing and 3D Reconstruction

Samples were imaged on a confocal microscope (Zeiss LSM 510 Meta), using a 10x (Zeiss C-Apochromat, NA=0.45 water immersion) or 25x (Zeiss LD LCI Plan-Apochromat, NA=0.8, with correction for oil immersion) objectives. Samples were scanned using either a 561 (Cy3) or 633 (Cy5, Neutravadin Dylight 633) laser line. All samples were imaged as a Z-series at a resolution of either 1024x1024 or 2048x2048, with Z step sizes ranging from 1-3 μm. Most samples required multiple overlapping image stacks, which were then fused using ImageJ's grid collection stitching plugin using the 'unknown positions' option (Preibisch et al. 2009). Image stack downsampling, 3D segmentation and reconstruction were performed using the software Amira 6.1. For 3D reconstructions, pixels of each image stack were assigned to individual brain structures in the segmentation editor. We used the grey-value information of the anti-synapsin image stacks to define the boundaries of the neuropils in all three dimensions. The resulting voxel skeleton was then interpolated using Amira's 'wrap' function, before generating a polygonal surface model to visualise the optic lobe in 3D. To improve clarity, all final images were adjusted for brightness and contrast in Adobe Photoshop CS6.

Layering analysis

We defined layers using confocal image stacks of a horizontal section through the optic lobe of *Hemicordulia tau*, co-labelled for synapsin and serotonin. A 45 μm z-stack was segmented into 6 maximum intensity projections of equal thickness, separating synapsin and serotonin channels. Two regions of interest were selected, one over the medulla and the other over the primary lobula. Care was taken to place these regions of interest in a position that minimised any shifts in structures across the X and Y planes at different depths. We used the plot profile tool in ImageJ to generate intensity plots for each region of interest, across both channels and at all 6 depths. Layers were segmented manually, defined by consistent changes in either synapsin or serotonin intensity across multiple depths of the sample.

3.3 Results and Discussion

The dragonfly optic lobe

The major divisions of synaptic neuropil in the dragonfly optic lobe (*Hemicordulia tau*) are clearly evident from confocal images of thick horizontal sections labelled using antibodies against the presynaptic vesicle protein synorf1 (Fig. 1A). Here fluorescence corresponds to regions of high synaptic density within neuropil, while darker areas represent dividing layers of cell bodies or the major axon tracts that serially interlink neuropils (Klagges et al. 1996). On this basis, the large and complex optic lobes can be readily segmented into 11 distinct neuropils; the lamina, the outer medulla, serpentine medulla, inner medulla, an anterior accessory medulla (not visible in Fig. 1A), and a lobula complex with 6 distinct subdivisions (Fig. 1A,B).

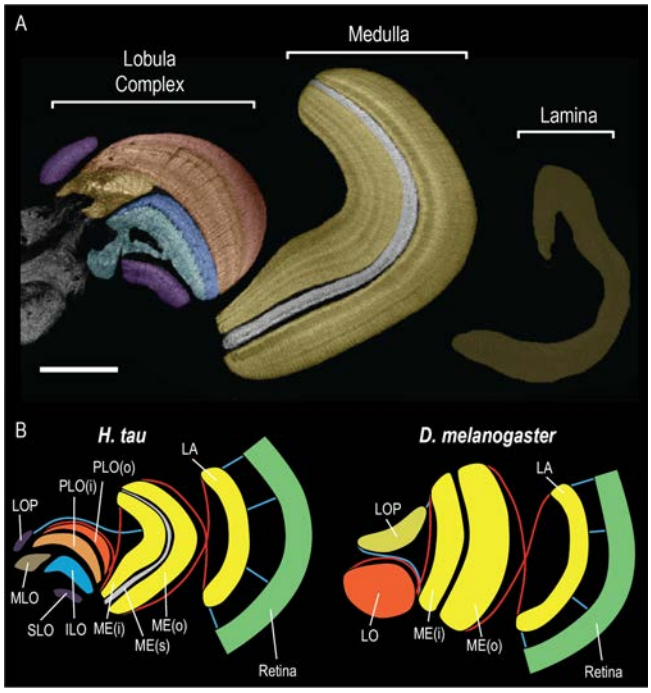

Figure 3-1: The complex optic lobe of *Hemicordulia tau*. (A) A synapsin stained horizontal section through the optic lobe of *H. tau*, defining the segmentation of different neuropils based on anti-synapsin immunoreactivity. Scale bar = 200 µm. (B) An diagrammatic view of the optic lobe of *H. tau* (left) and *Drosophila melanogaster* (right). LA = Lamina, ME(o), ME(s) and ME(i) = outer, serpentine and inner medulla, PLO(o) and PLO(i) = outer and inner subunit of the Primary Lobula, ILO = Inner lobula, SLO = Sublobula, MLO = Medial Lobula and LOP = Lobula Plate. Blue lines indicate major uncrossed serial connections, while red lines indicate crossed connections (chiasmata), see also Figure S1.

We observed this same basic plan in synapsin stained sections and whole-mount brains of species from 3 families: the Corduliidae (Fig. 1, S1), Libellulidae, and the Aeshnidae (Fig. 2). We segmented confocal image stacks from wholemount preparations in three-dimensions (3D) to produce digital reconstructions of identifiable neuropils (lamina removed during wholemount preparation) in individual brains across all three species (Fig. 2B). In relative terms, the dragonfly medulla is extremely large, as is expected given the compound eye holds up to 24000 facets (Pritchard. 1966). Although absolute brain size differs across this group (correlated with obvious large differences in body size) the optic lobe organisation observed in *Hemicordulia* (Fig. 1) is conserved across all three families. These families last shared a common ancestor in the early Triassic, some 250 million years ago (Letch et al, 2016), with the Aeshnidae representing the most ancient lineage of extant dragonflies, so this complex lobula organisation is likely plesiomorphic in odonates.

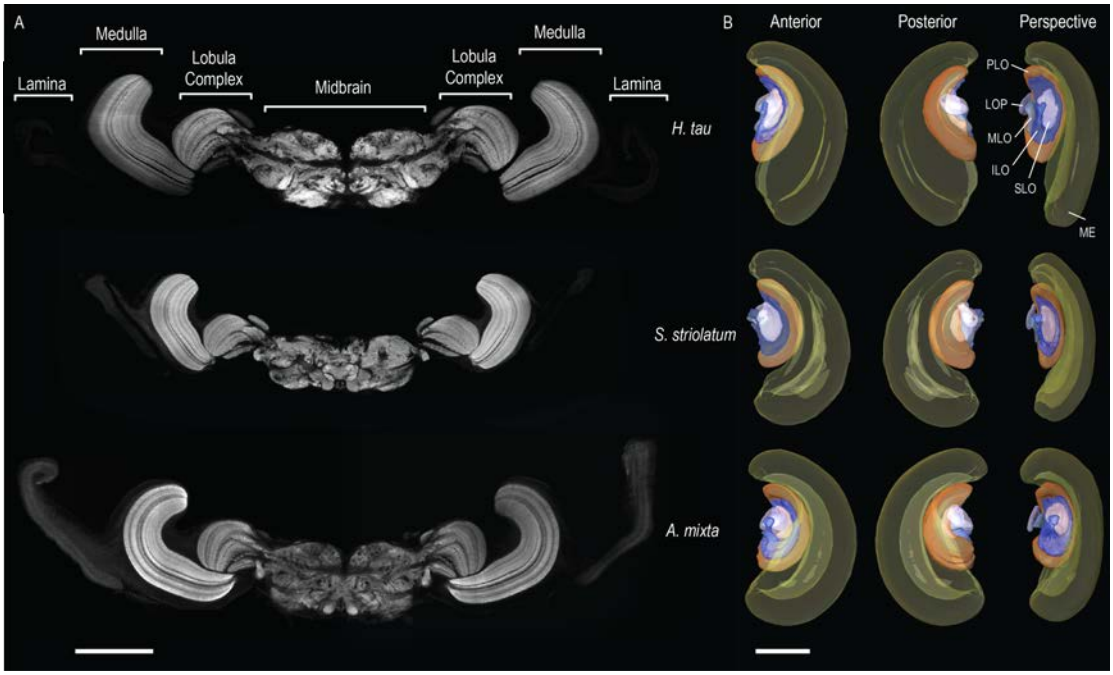

Figure 3-2: Similarity of the optic lobes in three dragonfly species. (A) Synapsin stained horizontal sections through the brain of dragonflies. Each section displays the left and right optic lobes, flanking the central protocerebrum. Depths within the optic lobe are similar across sections, however the corresponding protocerebral depth varies. (B) 3-dimensional reconstructions of the optic lobe across all three species. Reconstructions were produced by segmenting identified structures from confocal images of individual wholemount brains stained for synapsin. Structures were labelled in accordance with figure 1B, however the inner and outer subunits of the medulla and primary lobula are reconstructed as a single structure for clarity. Scale bars = 500μm.

The organisation of the dragonfly lobula, traditionally considered as the 3rd optic ganglion, is clearly more elaborate than those of holometabolous insects including dipteran flies such as *Drosophila melanogaster* (Rein et al, 2002; Ito et al, 2014, Fig 1B), Coleoptera (Dreyer et al. 2010; Immonen et al. 2017) and Lepidoptera (Kvello et al. 2009; el Jundi et al. 2009; Heinze and Reppert. 2012; Montgomery and Ott. 2015; Stöckl et al. 2016). In its more typical form, the insect lobula is divided into two subunits, a posterior lobula plate that receives direct projections from the inner medulla (ME(i)) and a larger anterior lobula that receives inputs that cross over at a chiasm with the inner medulla (ME(i), fig. 1B). In the dragonflies, this prominent chiasm is also present between the medulla and the outermost and largest of a series

of at least 4 concentric lobula neuropils. The primary lobula (PLO, fig 1B), spanning the entire distal surface of the lobula complex is divided into striate outer (PLO(o)) and inner (PLO(i)) regions by a prominent dark serpentine layer very similar to those seen in the medulla of many insects (Fischbach and Dittrich. 1989). Nested within the proximal surface of the PLO(i) there are then two smaller structures that we term the medial and inner lobula (MLO, ILO, fig. 1B). The wedge-shaped MLO intrudes between the posterior portions of the primary and the inner lobula. The inner lobula lies anterior to this medial unit, and is further divided into outer and inner subunits by a thin layer of lower synaptic density, with the innermost part extending further medially into additional synaptic structures which may be contiguous with those of the lateral mid-brain (Fig. 1A). The columnar appearance of both the MLO and ILO and the absence of obvious additional tracts linking these structures directly to medulla projections suggests that they are postsynaptic to the primary lobula and retinotopically organised, thus forming two additional 4^{th} optic ganglia.

Moreover, lying anterior and medial to the inner lobula, is a further distinctive structure that we term the sublobula (SLO, Fig 1 A,B), by analogy to a term originally proposed by Cajal and Sanchez (1915) for the inner part of the lobula in honeybees. Strausfeld (2005) suggests that the sublobula of bees may be functionally equivalent to the dipteran lobula plate as a site of wide-field motion processing in the dragonfly. In the honeybee it is fused to the outer lobula as a single, large, synaptically dense structure (Ribi and Scheel. 1981; Brandt et al. 2005), but in the dragonfly this structure is clearly segregated from the inner lobula by a thick band devoid of synapsin immunoreactivity. Finally, a small 6^{th} subunit sits on the posterior surface of the lobula complex, at the medial margin of the outer lobula. Osmium stained frontal sections and injections of neuronal tracer into the posterior medulla (Fig. S1) reveal direct projections of a population of columnar neurons into this subunit, posterior to the second optic chiasm (OCH2, Fig S1), so it likely lies at a similar level of hierarchical processing to the outer primary lobula (PLO(o)) and the lobula plate of holometabolous insects (Ito et al. 2014; Strausfeld. 2005). Outside the holometabola, relatively small satellite neuropils that receive uncrossed axons and lying to one side or beneath the lobula have also been observed in Mantoidae and plecopterans (stone flies)(Strausfeld. 2005).

Layering of the Medulla and Lobula complex

One of the most striking differences between the dragonfly optic lobes and those of other insect species is in the extreme degree of horizontal stratification seen in each of the major divisions of the optic lobes. We further investigated the complexity of individual neuropils by identifying individual synaptic layers and attempting to compare these with the layers identified in the medulla and lobula of other insect species. This is complicated by the fact that recent work has numbered layers of different species based on inconsistent criteria (Heinze and Reppert. 2012; Kinoshita et al. 2015; Rosner et al. 2017). Perhaps the most robust numbering of layers comes from classical studies using Golgi and other techniques to identify 10 key strata in the fly medulla based on apparent common synaptic layers of key classes of columnar and tangential neurons (Fischbach and Dittrich. 1989; Strausfeld. 1970). In an attempt to provide a more robust basis for identifying layers than used in prior work, we computed pixel intensity plots from confocal images of sectioned *H. tau* brains co-labelled with antibodies against synapsin and serotonin. These two labels are complementary since synapsin is widely expressed in areas of high synaptic density (Klagges et al. 1996), allowing visualisation of key input and output layers, while extensive anti-serotonin immunoreactivity has been observed in large tangential cells that arborize across the medulla of insects (Nässel and Klemm. 1983) providing a general stain that selectively highlights tangential neuronal structures, greatly improving layer discriminability (see fig S2 for a complete section). To minimise the possibility of subjective errors we generated six maximum intensity projections of local 7.5 μm confocal stacks at different depths from thick horizontal sections through the medulla (Fig 3 A-C) and primary lobula (Fig 3 D-E). Synaptic layers were defined by contrast boundaries in either anti-synapsin or anti-serotonin immunoreactivity observed across multiple depths in the sample.

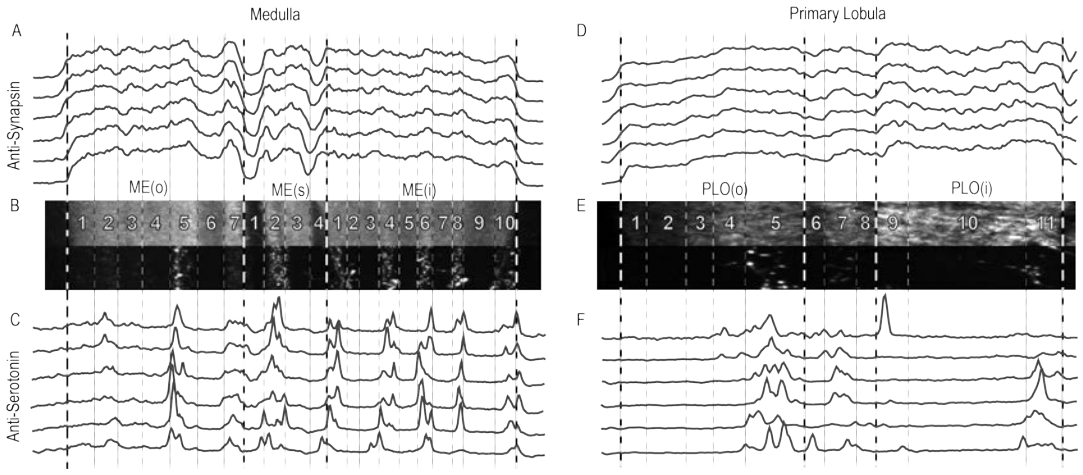

Figure 3-3: The synaptic layers of the medulla and lobula in *Hemicordulia* (A) Synapsin immunoreactivity intensity plots from a series of maximum intensity projections through the medulla obtained from different depths of a confocal image stack from a horizontal section obtained from *Hemicordulia*. (B, E) Example confocal images of anti-synapsin (top) and anti-serotonin (bottom) immunoreactivity, used to generate intensity plots. (C) Serotonin immunoreactivity intensity plots from the corresponding positions in A. (D) The synapsin immunoreactivity of the lobula. (F) Serotonin immunoreactivity intensity plots from the corresponding positions in D.

Based on this analysis, we can distinguish 21 layers in the dragonfly medulla, compared to the 8-11 layers observed in all other insects studied (Heinze and Reppert. 2012; Kinoshita et al. 2015; Rosner et al. 2017; Strausfeld. 1970; Wendt and Homberg. 1992). Given this unprecedented complexity, specific comparisons between individual layers and those of other insects is difficult. For example, the 9th and 10th medulla layers lie within a mid-band of synapsin staining between 2 dark bands that may be homologous with the dipteran serpentine layer (M7), but we then see a highly complex subdivision of 10 additional layers in the inner medulla (compared with 2-3 in Diptera). Therefore, while we adopt the naming conventions recently recommended for the major divisions of these ganglia (Ito et al. 2014), we implement a separate numbering system for the layers of the outer medulla, serpentine region and inner medulla.

We identify a total of 7 layers (MEO1-MEO7) in the outer medulla, 10 in the inner medulla (MEI1-Mi10) and 4 in a ‘serpentine’ region (S1-S4) that separates the inner from the outer medulla. This region is bounded by dark layers S1 and S4 which show

little, if any synapsin staining, and likely contain the axons and major dendrites of tangential and amacrine processes that feed into the medulla in many insects (Fischbach and Dittrich. 1989). Whilst these layers are not technically 'synaptic', we include them in our analysis to be consistent with other studies where a single serpentine layer is commonly reported as medulla layer M7 (Heinze and Reppert. 2012; Fischbach and Dittrich. 1989). The purpose of the dragonfly dual serpentine layer and the two synaptic layers within it, are currently unknown, although anti-serotonin immunoreactivity is especially prominent in layer S2. Indeed, of the 21 layers in the dragonfly medulla, 9 show consistent anti-serotonin immunoreactivity (Fig 3).

Whilst the absolute number of layers is striking, their distribution is equally abnormal. In most insects the outer medulla houses 6 synaptic layers, compared to just 2-3 in the inner medulla. Our findings show that the synaptic organisation in the dragonfly medulla is the opposite, with an extremely elaborate inner subunit consisting of 10 layers - the same as the total number of layers observed in the *Drosophila* medulla. No studies have yet investigated the physiological function or cell types present in these layers of dragonflies, but in other species these are the major input sites for retinotopic columnar neurons that project to the lobula complex. The large number of such layers in the dragonfly may prove to be linked to the larger number of possible post-synaptic targets in the highly divided inner layers of the lobula complex.

The highly layered organisation evident from the medulla is repeated within the lobula. Within the primary lobula alone we observed 11 layers (L1-L11). As with layers S1 and S4 of the medulla, Primary Lobula layers L6 and L8 are serpentine-like 'dark' layers, with weak anti-synapsin immunoreactivity that separates the inner and outer Primary Lobula. Indeed the shape, size and number of synaptic layers in the primary lobula is so exaggerated that it resembles the medulla of many other insect species. While there has not yet been any complete description of all the cell types present, the outer layers of the Primary lobula host the dendrites of several previously described target-detecting neurons (Geurten et al. 2007; Wiederman et al. 2017). While we did not quantitatively analyse layering of the higher-order lobula subunits, the inner lobula (Fig. 1) and sublobula also show a serpentine-like dark mid-bands so

could potentially be segregated further into outer and inner divisions. Hence the total number of lobula layers is certainly more than the 11 of the primary lobula.

The sub-lobula and wide field motion analysis

In considering the substantial differences between the dragonfly lobula complex and that of other insects, one interesting question that emerges is that of which subunit serves the role served by the lobula plate of other species. To date, most research on the lobula plate of species such as dipterans supports it having a primary role in visual motion analysis, while other visual tasks (e.g. polarization vision, pattern analysis, colour processing or feature detection) may be handled by neural circuits of the lobula and mid-brain (Gilbert and Strausfeld. 1991; Maddess and Yang. 1997; Nordström and O'Carroll. 2009; el Jundi et al. 2014). The widely studied Lobula Plate Tangential Cells (LPTCs) are an important group of motion-sensitive neurons found in a variety of flying insect species (Hausen et al. 1982) and which mediate responses to optic-flow cues. This is a visual sub-modality that dragonflies would also encounter during their spectacular hovering flight and acrobatic aerial pursuits of conspecifics and prey, which in many respects rival those of territorial Diptera with advanced visual abilities. However, despite their ancient lineage - among the oldest of the extant insect groups – the most obvious structure that we identified as a posterior lobula plate in the dragonfly (Fig. 1, S1) is approximately 12 fold smaller in volume terms (Table S1) than the lobula plate of other insects with similar sized eyes and brain, such as the male sphingid moth *Manduca* (el Jundi et al. 2009) (e.g. total brain volume, excluding the lamina = 6.81×10^8 in *Hemicordulia*, 6.95×10^8 in *Manduca*).

Are LPTC analogues, then, distributed within other lobula subunits in the dragonfly? To address this question, we used intracellular recording techniques to characterise the anatomy and physiology of a number of lobula complex neurons that produce LPTC-like physiological responses when presented with classical optic flow stimuli (fig. 4). Fig. 4A shows the responses of one such neuron to stimulation with a sinusoidal grating. Motion in the preferred direction elicits a robust depolarisation and increase in spiking activity, whilst gratings moving in the opposite direction produce hyperpolarisation. These responses strongly resemble those seen in direction-selective HS or VS neurons of the fly lobula plate (Hausen. 1982). Wholemount confocal images of intracellularly labelled neurons reveal broad spiny input dendrites that span

the medial and anterior portion of the lobula complex (fig 4B, D). Horizontal sections from these same brains were subsequently immunolabelled with anti-synapsin antibodies to reveal the synaptic sites of these inputs. This reveals that both neurons receive inputs in the sublobula (fig 4C, E).

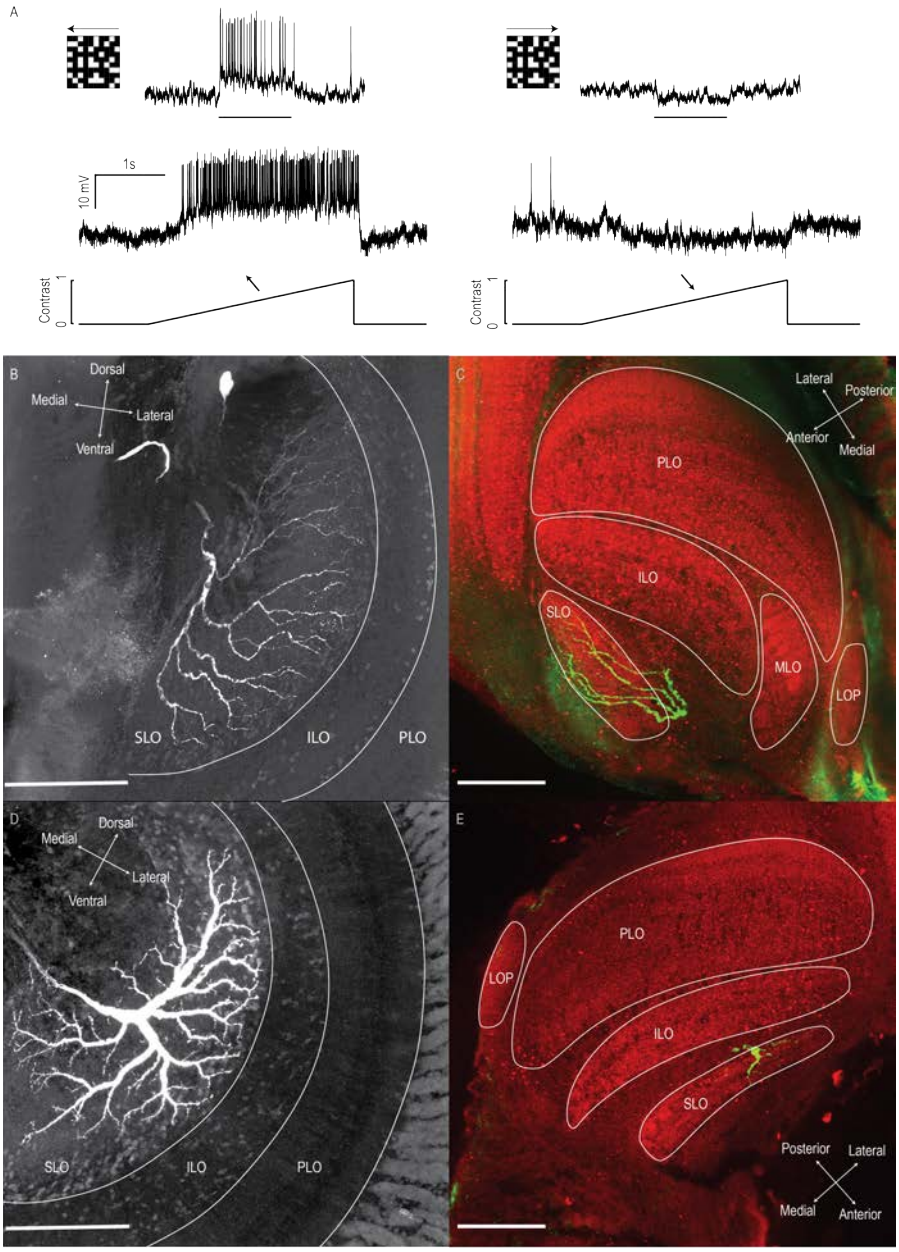

Figure 3-4: Motion-sensitive neurons of the dragonfly sublobula. (A) A subset of neurons in the dragonfly lobula complex provide robust, direction opponent responses to drifting gratings. (B) A wholemount montage of a dye-filled bar-sensitive neuron labelled by intracellular lucifer yellow injection. (B) Horizontal Sections through the lobula complex confirm the input dendrites of this motion sensitive neuron lies within the Sublobula. (C) A wholemount montage of an optic flow sensitive neuron. (D) Neurons sensitive to optic flow also receive inputs in the sublobula.

Evolution of the divided lobula

Strausfeld (2005) has suggested that a lobula plate (or an equivalent 'visual tectum') is an ancestral trait in insects and indeed that the only two optic lobe neuropils of entomostracan crustaceans are homologous with the lamina and lobula plate of insects and malacostracan crustacea. However, assuming that the ancestors of insects had visual behaviours that required additional neural circuits to those involved in motion analysis, the ancestral visual tectum must have been a multi-function structure. Hence the motion-specialised organisation of the lobula plate that we see in more recent insect groups such as dipteran flies and other Holometabola could be a derived trait. This is supported by recent studies of polyneopteran insects including the locust, mantis, and cockroach (Rosner et al. 2017) which all have lobula complexes formed by up to 5 relatively small subunits with different functional roles (O'Shea and Rowell. 1975) and no obvious homologue of the lobula plate. In Malacostracan crustaceans, the lobula plate is reduced, as we also see in the dragonfly, and motion processing may be handled instead by neurons at deep levels of the lobula (Sztarker et al. 2005). However, analysis of deep neuropils in crabs failed to identify neurons with properties consistent with their optomotor behaviour.

We have yet to record from neurons in the dragonfly posterior lobula plate and thus cannot preclude them from also displaying similar properties to those of the sublobula. Nevertheless, our results conclusively demonstrate that the dragonfly sublobula most certainly contains a population of tangential neurons closely resembling those of LPTCs in dipteran flies. It is therefore difficult to reconcile our findings with recent neuroanatomical studies (Strausfeld. 2005) and a review of the invertebrate brain (Ito et al. 2014) that grouped dragonflies along with holometabolous Diptera, Lepidoptera and Coleoptera as having a divided lobula with a lobula plate. We did indeed find a lobula plate-like structure on the posterior surface of the optic lobes. However, our observation that a functional role equivalent to that of the lobula plate of more recent insect groups is instead handled by a separate structure on the other side of the brain brings into some doubt the idea that the lobula plate of holometabolous insects is synapomorphic with those of some crustaceans, and thus an ancestral form for the insect optic lobe. Importantly, wide-field motion sensitive neurons have also been described from the honeybee lobula (DeVoe et al. 1982; Ibbotson. 1991). While Strausfeld (2005) previously argued that the sublobula

may be supplied by homologues of the medulla T4 neurons that feed the lobula plate in other holometabolous insects, this view of the sublobula as a homologue of the dipteran lobula plate seems at odds with our finding that the dragonfly has both structures, on opposite sides of the brain. Dragonfly equivalents of the dipteran medulla T4 and lobula T5 neurons have yet to be identified. Since these can be considered to be sibling cells that might have arisen by the duplication of progenitors in a common ancestor (Shinomiya et al. 2015), further analysis of the columnar neurons that project from the proximal medulla to different lobula subunits in the dragonfly may shed further light on whether the sublobula is indeed a homologue of the lobula plate.

Acknowledgements

This research was supported financially by the Swedish Research Council (VR 2014-4904), the Australian Research Council (DE150100548, DP130104572) and STINT, the Swedish Foundation for International Cooperation in Research and Higher Education. We thank the manager of the Adelaide Botanic Gardens for allowing insect collection, and staff of Adelaide Microscopy and the Lund University Biology Microscopy facility for confocal microscope support.

4 A predictive focus of gain modulation encodes target trajectories in insect vision

Context

The data presented in this chapter are the result of recordings that date as far back as 2012. In early 2014 when I started my PhD project Steven Wiederman and our labs recently completed PhD candidate James Dunbier intended to publish a dataset describing a predictive 'focus' of gain modulation that builds within the receptive field of CSTMD1 during a continuous trajectory. These experiments expanded on the initial characterisation of a facilitation mechanism described in our labs earlier work (Nordström et al. 2011; Dunbier et al. 2011; Dunbier et al. 2012).

These results formed the main inspiration for my first experimental paradigms. These experiments aimed to address the following research questions:

1. Does the focus of gain cross visual hemifields when a primer drifts in the contralateral eye?
2. Does the position of the focus shift depending on the duration of an occlusion?
3. Does a drifting target induce any bias in target direction?
4. Does a drifting target effect contrast gain ahead of its path?
5. Do Small-Field STMD neurons, and other uncharacterised Large-Field STMD neurons also display facilitated responses to targets on long trajectories?

Pilot data obtained during my first recording season encouraged us to hold off publishing the previous results, instead choosing to combine the original datasets with what would have been the first publication of my PhD thesis. Of the final results presented here, figure 4 was the product of work by James Dunbier, while figure 2, 3a and 3b was mostly a result of work by Steven Wiederman. Data presented in figures 1, 3c-d, 5, 6, 7 and 8 are the products of my PhD work. Steven Wiederman and I co-drafted the manuscript and are co-first authors on the final work.

Statement of Authorship

Title of Paper	A predictive focus of gain modulation encodes target trajectories in insect vision
Publication Status	☑ Published ☐ Accepted for Publication ☐ Submitted for Publication ☐ Unpublished and Unsubmitted work written in manuscript style
Publication Details	Wiederman, S. D*., Fabian, J. M*., Dunbier, J. R., and O'Carroll., D. C. (2017). A predictive focus of gain modulation encodes target trajectories in insect vision. eLife26478

Principal Author

Name of Principal Author (Candidate)	Joseph Fabian
Contribution to the Paper	Experiment conceptualisation, caught animals, collected data, analysed data, interpreted data, generated figures and co-wrote the manuscript.
Overall percentage (%)	55%
Certification:	This paper reports on original research I conducted during the period of my Higher Degree by Research candidature and is not subject to any obligations or contractual agreements with a third party that would constrain its inclusion in this thesis. I am the primary author of this paper.
Signature	Date 28/8/2017

Co-Author Contributions

By signing the Statement of Authorship, each author certifies that:

i. the candidate's stated contribution to the publication is accurate (as detailed above);

ii. permission is granted for the candidate in include the publication in the thesis; and

iii. the sum of all co-author contributions is equal to 100% less the candidate's stated contribution.

Name of Co-Author	Steven Wiederman
Contribution to the Paper	Experiment conceptualisation, caught animals, collected data, analysed data, interpreted data, generated figures and co-wrote the manuscript.
Signature	Date 28/8/2017

Name of Co-Author	James Dunbier
Contribution to the Paper	Experiment conceptualisation, caught animals, collected data and analysed data,
Signature	Date (28/8/2017)

Name of Co-Author	David O'Carroll
Contribution to the Paper	Experiment conceptualisation, data interpretation and contributed to writing the manuscript.
Signature	Date 25-AUG-2017

A predictive focus of gain modulation encodes target trajectories in insect vision

PUBLISHED: Wiederman, S. D., Fabian, J. M., Dunbier, J. R., and O'Carroll., D. C. (2017). A predictive focus of gain modulation encodes target trajectories in insect vision. *eLife* 6, e26478.

Steven D Wiederman[1]*, Joseph M Fabian[1]*, James R Dunbier[1], and David C O'Carroll[2].

[1]Adelaide Medical School, The University of Adelaide, Adelaide, Australia.

[2]Department of Biology, Lund University, Lund, Sweden.

*These authors contributed equally to this work

4.1 Abstract

When a human catches a ball, they estimate future target location based on the current trajectory. How animals, small and large, encode such predictive processes at the single neuron level is unknown. Here we describe small target-selective neurons in predatory dragonflies that exhibit localized enhanced sensitivity for targets displaced to new locations just ahead of the prior path, with suppression elsewhere in the surround. This focused region of gain modulation is driven by predictive mechanisms, with the direction tuning shifting selectively to match the target's prior path. It involves a large local increase in contrast gain which spreads forward after a delay (e.g. an occlusion) and can even transfer between brain hemispheres, predicting trajectories moved towards the visual midline from the other eye. The tractable nature of dragonflies for physiological experiments makes this a useful model for studying the neuronal mechanisms underlying the brain's remarkable ability to anticipate moving stimuli.

4.2 Introduction

A diverse range of animals are capable of visually detecting moving objects within cluttered environments. This discrimination is a complex task, particularly in response to a small target generating very weak contrast as it moves against a highly, textured background. The neural processing underlying this behavior must enhance a localized, weak and variable signal, which may only stimulate one or two photoreceptors in turn. Rather than simply respond reactively, some animals even anticipate a target's path by predicting its future location. In the vertebrate retina, high initial gain combined with neuronal adaptation and sensitization allows responses from a network of overlapping ganglion cells to 'keep up' with the current target location and account for sluggish neuronal delays (Berry et al. 1999; Kastner & Baccus 2013). This encoding anticipates targets moving in a straight line, with trajectory reversals eliciting a synchronous burst of activity from a population of ganglion cells (Schwartz et al. 2007; Chen et al. 2014). However, this anticipation does not use the recent trajectory to extrapolate likely target locations at future times. Rather, the last observed location remains sensitized after the target disappears. This differs from studies of human observers, where a temporarily occluded target results in improved sensitivity at the extrapolated forward location (Watamaniuk & McKee

1995). This predictive encoding of future target locations indicates the presence of additional processing mechanisms beyond the retina.

Like human ball players, dragonflies also estimate target location, capturing single prey in visual clutter, even amidst a swarm of potential alternatives (Corbet 1999). We recently described a 'winner-takes-all' neuron in the dragonfly likely to subserve such competitive selection of an individual target, whilst ignoring a distracter (Wiederman & O'Carroll 2013). In other animal models, inhibitory circuits drive the selection of salient stimuli (Mysore & Knudsen 2013) and the direction of attention towards targets is evidenced by modulation of contrast gain (Moran & Desimone 1985; Reynolds et al. 2000). How prediction relates to the selection of salient stimuli is unknown (Zirnsak et al. 2014) and how selection, prediction and attention are encoded at the neuronal level is an intense topic of scientific investigation.

Here we used intact, *in vivo*, recordings from the system of small target-selective neurons in predatory dragonflies to reveal local changes in sensitivity elicited during target tracking. We show that this involves a large increase in contrast gain just ahead of the target's most recent location, with suppression in the surround. We investigated the spatial extent, temporal persistence and direction tuning within this region of enhancement. Our data shows that a local increase in gain spreads forward after a delay, even anticipating the path of primers presented to the contralateral eye and moved towards the visual midline. Moreover, the direction tuning shifts to match the prior path. Such response attributes differentiate this neuronal processing from typical models of direction selectivity and are ideally suited for a dragonfly's predictive pursuit of prey (Mischiati et al. 2015).

4.3 Materials and Methods

Electrophysiology

We recorded from a total of 63, wild caught male dragonflies, *Hemicordulia*. Animals were immobilized with a wax-rosin mixture (1:1) and fixed to an articulating magnetic stand. The head was tilted forward and a small hole dissected in the posterior surface, exposing the left optic lobe.

We pulled Aluminium silicate electrodes on a Sutter Instruments P-97 electrode puller, and backfilled them with 2M KCl solution. Electrodes were inserted through the neural sheath into the proximal lobula complex using a piezo-electric stepper

(Marzhauser-Wetzlar PM-10), with typical resistance between 50-150 MΩ. Intracellular responses were digitized at 5 kHz with a 16-bit A/D converter (National Instruments) for off-line analysis with MATLAB.

Freshly penetrated cells were presented with small targets, bars and wide-field gratings for classification. Neurons were classed as STMDs when responding robustly to visual stimuli composed of small, moving targets and not responsive to bars or gratings. CSTMD1 was identified by its characteristic receptive field, response tuning and action potentials. STMD neurons were categorized into small or large-field by mapping their receptive fields with drifting targets (a half-width either less than, or greater than 25°).

Visual Stimuli and Data Analysis

We presented stimuli on high definition LCD monitors (120 Hz and above). The animal was placed 20 cm away and centered on the visual midline. Contrast stimuli were presented at screen center to minimize off-axis artefacts. Stimulus scripts (https://github.com/swiederm/predictive-gain) were written using MATLAB's Psychtoolbox and integrated into the data acquisition system. Unless stated otherwise all targets were 1.5°x1.5° black squares drifted at 40°/s. A minimum of 7 seconds rest between trials was implemented to avoid habituation or facilitation from prior trials. Data were only ever excluded due to pathological damage of the neuron or extensive habituation (experiment cessation). All means are calculated from biological replicates (i.e. repeated measurements from identified neurons in different animals). Each biological replicate represents the mean of between 1 and 10 technical replicates

Statistical Tests: We report exact P (unless miniscule). Due to the small sample sizes, all tests are nonparametric, two-sided and account for multiple comparisons. All box and whisker plots indicate median, interquartile and full minimum-maximum range (whiskers).

Predictive focus of gain modulation: We mapped the spatial extent of this focus with a series of 200 ms probe targets randomly presented across a 10x10 grid of locations within CSTMD1's excitatory receptive field. We calculated spike rate within an analysis window (50-150 ms) following probe onset at each location. We randomly interleaved unprimed probe stimuli with (in 50% of trials) corresponding probes that followed a 1 second-long primer target (n=9 dragonflies). Priming targets moved vertically up the screen at 32°/s, pseudo-randomly presented within a 5° wide region

(white outlined box) to minimize local habituation induced by the primer. For each spatial location (100 in total), we calculated the difference between probe response (following primer) with probe response (no primer). Inter-trial and inter-neuronal noise in the focus colormaps was reduced by averaging across dragonflies interpolated and slightly smoothed (Gaussian, σ=0.5) matrices. This noise-reducing method effectively portrays the result of adding the primer target, however, may slightly blur the focus region due to averaging across samples. A second experiment followed the same protocol except with a 300 ms pause inserted between primer and probe (n=7 dragonflies). A third experiment had the primer moving horizontally within the visual field of the contralateral eye with care taken to avoid the frontal region of 10° binocular overlap. This experiment also included a 300 ms pause inserted between primer and probe (n=7 dragonflies). To examine the significance of these maps, we created Cohen's d versions. For each spatial location (*loc*), we calculated the mean difference (primer & probe – probe alone) across the sample size (n, number of dragonflies) and divided by the standard deviation of these differences across the sample size. This effect size represents the mean observed change at each location (across dragonflies) normalized by the standard deviation at each location (across dragonflies). Note that to avoid divide by zero errors, we did not calculate the Cohen's d values for the inhibitory hemifield (map for Figure 3c) which has no activity, and thus minimal standard deviation. For specific locations of interest, we tested for statistical significance by calculating the paired t-statistic and two-tailed P-value.

$$\mu_{loc} = \sum_{i=1}^{n} ((\text{primer \& probe})_i - (\text{probe alone})_i)$$

$$\sigma_{loc} = \sqrt{\frac{1}{n-1}\sum_{i=1}^{n} ((\text{primer \& probe})_i - (\text{probe alone})_i) - \mu)^2}$$

$$Cohen's\ d_{loc} = \frac{\mathrm{u}_{loc}}{\sigma_{loc}}$$

$$t_{loc} = Cohen's\ d_{loc} \cdot \sqrt{n}$$

Further experiments were conducted along a 1-dimensional path. Firstly, with a constrained location of the primer (n=12 dragonflies) and then with a constrained

location of the probe (n=8 dragonflies). For the time courses, we normalized responses by dividing by fully-facilitated controls (corresponding spatial locations), thus accounting for spatial inhomogeneity in the receptive field. Statistical comparisons applied either Wilcoxon or Friedman's tests with multiple comparisons.

Contrast Sensitivity: We varied the contrast (7 values) of a probe target drifted upwards through CSTMD1's receptive field (n=9). Target contrast (Weber) was defined as:

$$c_w = \frac{I_{target} - I_{background}}{I_{background}}$$

Probes drifted upwards for 600 ms at two possible locations separated horizontally by 20°. For each probe contrast, we measured responses in an analysis window (50-150 ms) following onset. Primers drifted upwards for 600 ms, either towards the probe location (primer) or displaced 20° to the side (distant primer). Primer contrast was either 1.0 (high contrast) or 0.2 (low contrast). Primer responses were quantified over the last 100 ms of primer motion. We inserted a 50 ms pause between primer and probe and primer to ensure that the residual primer response was not attributed to the probe. Trial order across all contrast sensitivity experiments was randomized. The parameters (top, bottom, logIC50 and hill-slope) of each contrast sensitivity function were compared with an extra sum-of-squares F test, whilst responses to primers were compared by Wilcoxon test. To define a detectability threshold for estimating contrast sensitivity, we measured spontaneous activity in the 1 second pre-stimulus period across all 630 trials (n=9 dragonflies). For each neuron, responses were binned (20 ms) before calculating the upper 95^{th} percentile of binned responses.

Direction Selectivity: We measured CSTMD1's direction selectivity by drifting probes in 8 directions from a central point in CSTMD1's excitatory receptive field (n=9). Primers drifted for 1 s in each of 4 cardinal directions terminating at the probe location. In a separate experiment, vertically drifted primers terminated 4° below the probe location, placing all probes within the center of focus (n=5). Probe responses were analyzed in a window (40-100 ms) following probe onset. This window is shorter and earlier than in other experiments to account for the rapid establishment of probe direction selectivity.

We quantify direction selectivity in two ways. We regress responses onto the sinusoidal model $R(\theta) = b_0 + b_1 \sin(\theta + \varphi)$, where R is the response at direction θ, b_0

is the offset, b_1 *is* the directional component of the response and φ is the phase (preferred direction). We also quantify the mean polar vector for each condition, calculating 95% confidence intervals for both vector direction and vector magnitude across all cells.

Differences in b_1/ b_0 ratio between trials that were primed upward, and upward following a forward jump were compared with a Mann-Whitney test. The variance of responses to targets that turn back in the opposite direction to the primer were analyzed by a Kruskal-Wallis test, followed by Dunn's multiple comparisons. We applied the Kruskal-Wallis test because the direction tuning data with (figure 7C, condition J) and without (Figure 7 C, conditions P U R L D) a forward jump was obtained from different independent samples.

SF-STMD Facilitation: Responses were elicited by 400 ms probe trajectories, commencing motion within the classical receptive field and drifted in the neuron's preferred direction. Primers were either drifted for 800 ms 'towards' the excitatory receptive field, or from within the excitatory receptive field moving 'away'. Primers terminated at least 8° away from the classical receptive field, and were followed by a 200 ms pause before the appearance of the probe stimulus. Primer responses were analyzed in a window 300-800 ms following onset, whilst the probe was 50-150 ms following probe onset.

The remaining large-field and small-field experiments were performed across populations of neurons with varying overall activity. To normalize, neuronal responses for a given neuron were divided by a factor equal to the neuron's mean response to probes across all priming conditions. To convert responses back into spikes/s, we multiplied the normalized response by the mean factor for all neurons in the dataset. As all conditions were paired across independent samples, we compare responses across conditions by a Friedman test, followed by Dunn's multiple comparisons. All statistical tests presented are two-tailed.

Dye filling

The morphology of an SF-STMD neuron was visualized by intracellular labelling with Lucifer Yellow. Iontophoresis was achieved by passing 3nA negative current through electrodes tip-filled with 4% Lucifer Yellow solution in 0.1M LiCl. Brains were then carefully dissected, fixed overnight in 4% paraformaldehyde at 4°C,

dehydrated in ethanol series (70%,90%,100%,100%), cleared in methyl salicylate and mounted on a cavity slide for fluorescence imaging.

Data availability

Data obtained is managed per the ARC/NHMRC Australian Code for the Responsible Conduct of Research. Raw data from experimental testing and numerical simulation is stored on a locally managed server. Processed experimental and numerical data is available on the eResearchSA data management server.

4.4 Results

Receptive fields are modulated by stimulus history

'Small target motion detector' (STMD) neurons in the dragonfly, *Hemicordulia tau*, are tuned to target size and velocity and are highly sensitive to contrast (O'Carroll 1993, Wiederman et al. 2008, Wiederman et al. 2013). One identified STMD, CSTMD1, responds selectively to a small, moving target, even when embedded within natural scenes (Wiederman & O'Carroll. 2011). CSTMD1 also exhibits a sophisticated form of selective attention. The neuronal response to the presentation of two simultaneously moving targets does not simply result in either neuronal summation or inhibition. Instead, CSTMD1 responds in a winner-takes-all manner, selecting a single target as if the distracter does not even exist (Wiederman & O'Carroll. 2013).

We mapped CSTMD1's receptive field by measuring spiking activity in response to a single, black, square target (1.5°x1.5°) moving along trajectories at varying spatial locations in the visual field. In one region, a gridded array (10x10) of short, vertical, target trajectories evoke weak neuronal responses (Figure 1A). For each short 200 ms trajectory, we plot mean spike rate over a 100 ms analysis window (from 50 to 150 ms). This colormap represents the spiking activity in response to short trajectories for each of the 100 corresponding spatial locations. In comparison, we present an identical square target moved along long, vertical trajectories (Figure 1B, Video 1) and segment responses at the same corresponding spatial locations of the short paths in Figure 1A (mean spike rate over 100 ms bins). This reveals higher overall spiking activity in response to the long, continuous target trajectories. Here we investigate this effect of stimulus history by separating trajectories into components; a primer and a probe. Each elicit responses when presented alone, however, the probe's initial

response is affected by the gain induced by a *preceding* primer (Figure 1C). We note that neuronal responses build slowly over hundreds of milliseconds - a property we have previously termed facilitation (Nordström et al. 2011). For the primer & probe condition (where a primer always precedes the probe stimulus) responses to the probe are facilitated (green region, cf. black with blue time courses). This facilitatory effect is not simply due to slow kinetics, as both responses have a rapid decay time course when the stimulus ends (Dunbier et al. 2012).

Previously, we have reported receptive fields in their facilitated state (Dunbier et al. 2012), mapped using targets moving along either long horizontal (Figure 1D) or vertical trajectories (Figure 1E). These reveal CSTMD1's excitatory receptive field which extends from the dorsal, visual midline to the periphery. Spatial inhomogeneity within this receptive field (interpolated to reduce binning artefacts) likely results from underlying dendritic integration and local spatiotemporal tuning differences. In the other visual hemifield (midline at 0° azimuth), a drifting target generates inhibition (Figure 1D,E), with activity suppressed to below spontaneous levels (0 spikes/s from a spontaneous activity of 11 ± 4 spikes/s, mean ± std.).

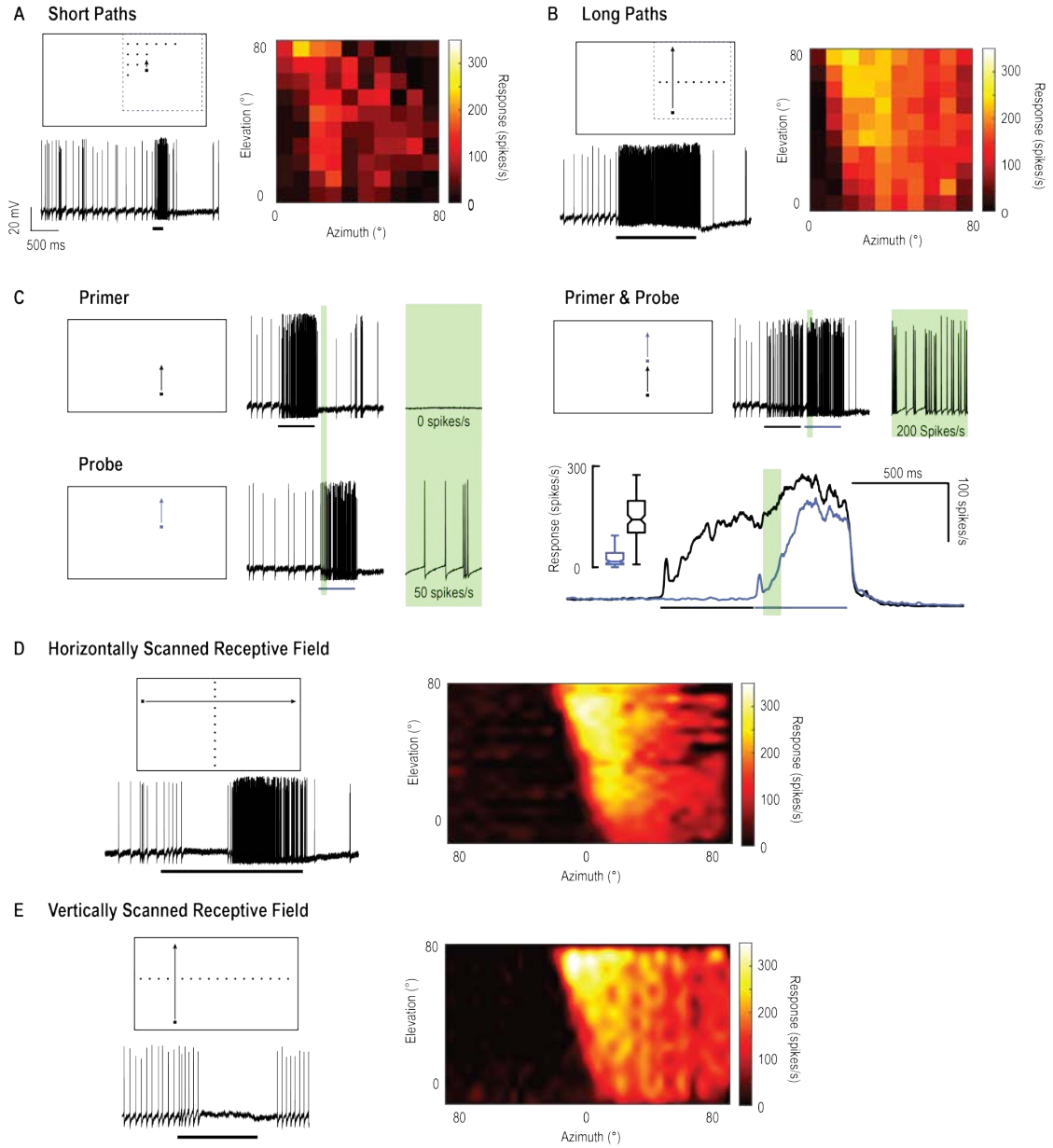

Figure 4-1: CSTMD1's receptive field mapped with drifting targets. (A) Small targets (black squares, 1.5°x1.5°) move along short trajectories (200 ms) that are both vertically and horizontally offset on a 10x10 grid. Pictograms are illustrative and not to scale. The colormap reveals CSTMD1 responses to these stimuli producing an 'unfacilitated' receptive field (50-150 ms analysis window). (B) Horizontally offset targets are drifted vertically up the monitor display along long, continuous trajectories eliciting strong, facilitated responses (100 ms bins to corresponding spatial locations in A). (C) Separating long paths into two components (primer followed by probe), allows us to examine the facilitatory effects within a short analysis window (before the probe self-primes, green region). In a single neuron, we examined response time courses (mean of 140 replicates over two hours) to repeated probe alone (blue line)

and primer & probe (black line) conditions (D) We have previously described facilitated receptive fields in response to targets drifted across the entire visual display. Targets moving rightwards (vertically offset) reveal inhibition in one eye's visual field (in response to motion from the periphery towards the frontal area) and excitation in the other (from frontal to periphery). (E) The facilitated receptive field (B,D) mapped with upwards moving targets is stronger than the weaker, though similarly shaped, unfacilitated receptive field in A.

What is the effect on a 2D array of 'probe' responses (short paths in Figure 1A) when a long primer is presented along a single, *constrained*, trajectory immediately preceding each probe? Such an experiment would provide us with a snapshot of the effect of stimulus history (the primer target) on the current receptive field. Figure 2 provides examples of individual, neuronal responses to short target trajectories (probes, blue arrows), both with and without a preceding 1 second duration target trajectory (primer, black arrow). For each probe location (in a 10x10 grid), we measured the spike rate within a 100 ms time window (the green shaded regions in Figure 2). The effect of priming was calculated as the difference (Δ spike rate) between the probe response when preceded by the primer ('primer & probe', black and blue arrows) and the probe alone (blue arrow) conditions. In this paradigm, we changed the spatial offset (jumps) between primer and probe without any delay (Figure 2A,B) or following a 300 ms pause (Figure 2C,D). We also tested a condition where the primer target drifted toward the dragonfly's midline, through the visual field of the other eye (Figure 2E,F). By ensuring primers did not enter the region of binocular overlap, any changes elicited in the probe locations (in the opposing eye) must have traversed brain hemispheres.

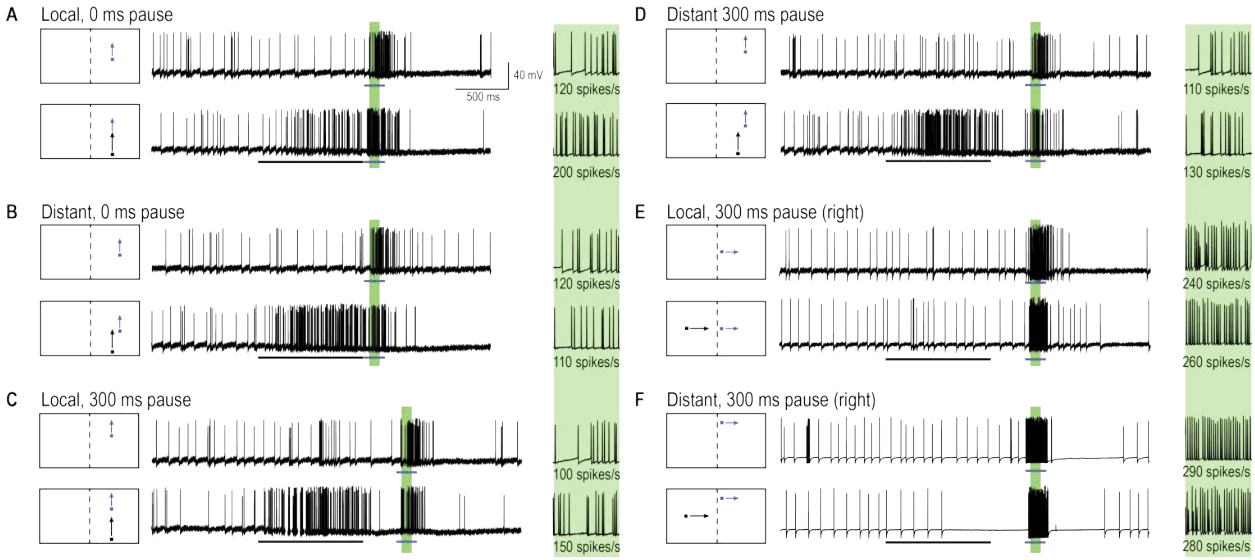

Figure 4-2: A primer target changes probe responses. (A) Example traces of CSTMD1's response to a probe target alone (blue arrow) or following a primer target (black arrow). The effect of the primer is measured as the difference (Δ spike rate) in response activity (primer & probe – probe alone) in the corresponding 100 ms window (green shaded region, with enlarged view on right). (B) With the primer spatially constrained, we repeat primer & probe and probe alone trials in a gridded array of 100 locations (200 trials in total, randomly interleaved). (C, D) A pause of 300 ms is inserted between the conditions where the primer disappears before probe onset (i.e. simulating a target occlusion). (E, F) A primer placed in the visual field of the other eye and moved toward the visual midline tests for information traversing the brain hemispheres.

Predictive modulation of gain

Figure 3 shows the complete two-dimensional map of primer-induced gain modulation, averaged across repeated intracellular recordings from CSTMD1 in different animals. Receptive fields are perspective-corrected from the dragonfly's point of view to a dragonfly eye map (mirrored along the vertical midline) and smoothed using bicubic interpolation to remove binning artefacts. The contour lines in Figure 3A-C indicate the average unfacilitated responses to the probe alone condition. In primer & probe trials, the primer target moved upwards (Figure 3A,B, Video 2) or rightwards (Figure 3C) along different paths in each trial but constrained within a region 5° wide (indicated by the white outlined box). To the CSTMD1 we

recorded from (with its excitatory inputs located in the right mid-brain), upward and rightward moving targets represent progressive stimuli (i.e. moving from front-to-back). The small variation in primer path decreased local habituation from a repeating primer running over the exact same trajectory. Probe alone and primer & probe trials were randomly interleaved. The color map reveals the average change in neuronal activity (Δ spike rate) elicited by the spatially constrained primer for each probe location (primer & probe – probe alone). Figure 3A reveals a pronounced 'focus' of increased sensitivity just ahead of the final location of the priming target and an extensive region of suppression in surrounding locations (mean, n=9 dragonflies). Thus, what we have previously referred to as facilitation is a more complex phenomenon - local enhancement with spike rate *suppression* elicited by probes jumped into the surround. Here we use the term 'focus' to refer to both the local enhancement and widespread concomitant inhibition. Such neuronal processing may be indicative of an attentional mechanism, rather than a global arousal or sensitization (Slagter et al. 2016). In Figure 3A, we observed a large mean change in spike rate – over 50% increase within the focus center (P=0.0007, n=9) and up to 50% decrease in surrounding locations (P=0.005, n=9).

If the primer disappears for 300 ms before each probe, a similarly intense focus is still evident (Figure 3B, Video 2), but now spread forward in spatial extent (P=0.005, n=7 dragonflies). The focus seems to account for the expected target location had it continued on its original trajectory (to a position as indicated by the white cross-hair in Figure 3B,C), albeit with an increased uncertainty given its broader spatial extent (mean, n=7 dragonflies). Moreover, if we move a horizontal primer toward the visual midline in the contralateral eye before it disappears for 300 ms, the focus transfers across the brain to the ipsilateral hemisphere (Figure 3C). We then observed enhancement (red) localized to a broad region ahead of the primer trajectory (P=0.004, n=7 dragonflies), but strong suppression (blue) at higher elevations (P=0.02, n=7 dragonflies). Dragonflies have a small area of binocular overlap between the two eyes corresponding to the frontal/dorsal visual field (Horridge, 1978). Our stimulus was carefully designed to avoid this region, disappearing just before entering the area of overlap. Therefore, our result cannot be explained by facilitation being regenerated in the ipsilateral eye. Rather it must involve a localized, inter-hemispheric transfer of information. Furthermore, a localized and spatially

segregated combination of enhancement and suppression (red and blue regions in Figure 3C) cannot be explained by a simple global mechanism, such as, a post-inhibitory rebound following a strong inhibitory stimulus (Bolzon et al. 2009). This transfer of a predictive focus between brain hemispheres is likely to play a crucial role in the prediction of target location during pursuit flights where the pursuer attempts to fixate the target frontally (Mischiati et al. 2015). Prolonged pursuit flights of conspecifics involve highly convoluted paths in which the target may readily cross from one visual field to the other (Land & Collett, 1974). In Figure 3D, we show the effect sizes of the three maps (Figure 1A-C) at all spatial locations. These Cohen's d values are the mean differences between primer & probe and probe alone (Δ spike rate), divided by the standard deviation of these differences. Cohen's d values over 0.5 are considered large effect sizes, thus our values of up to 1.8 in both excitatory and inhibitory directions are considerable. For particular points in these maps (Figure 3C, +'s) we calculate the paired, two-tailed P-values, highlighting the statistically significant effect of the primer.

Figure 3E shows data from an additional 12 dragonflies, where we mapped the forward-spreading focus following a delay of either 100 ms or 300 ms along a single dimension. These data (mean ± SEM) show that a small (6°) jump backwards precisely over the previously primed path already resets the response magnitude to that of the unfacilitated response (dashed line), whilst larger jumps backwards (12°) reveal potent suppression. Considering that the largest jump in this case is stimulating a part of the receptive field that last saw the target up to 700 ms earlier, the profound inhibition seen for this stimulus suggests that the prior primer target exerts long-lasting effects on the surrounding receptive field. Targets that jump forward after a delay reveal a shift in facilitation, spreading further forward after 300 ms (green line), compared to 100 ms (yellow line). Examining the mean difference combined across all forward jumps (6°, 12° and 18°) reveals a statistically significant difference between 100 ms and 300 ms pauses ($P = 0.03$, Cohen's $d = 0.7$). Here the probe target followed directly 'on path' to the priming stimulus, without the small horizontal offsets (up to 5°, Figure 3A-C white priming region) used previously to limit local habituation.

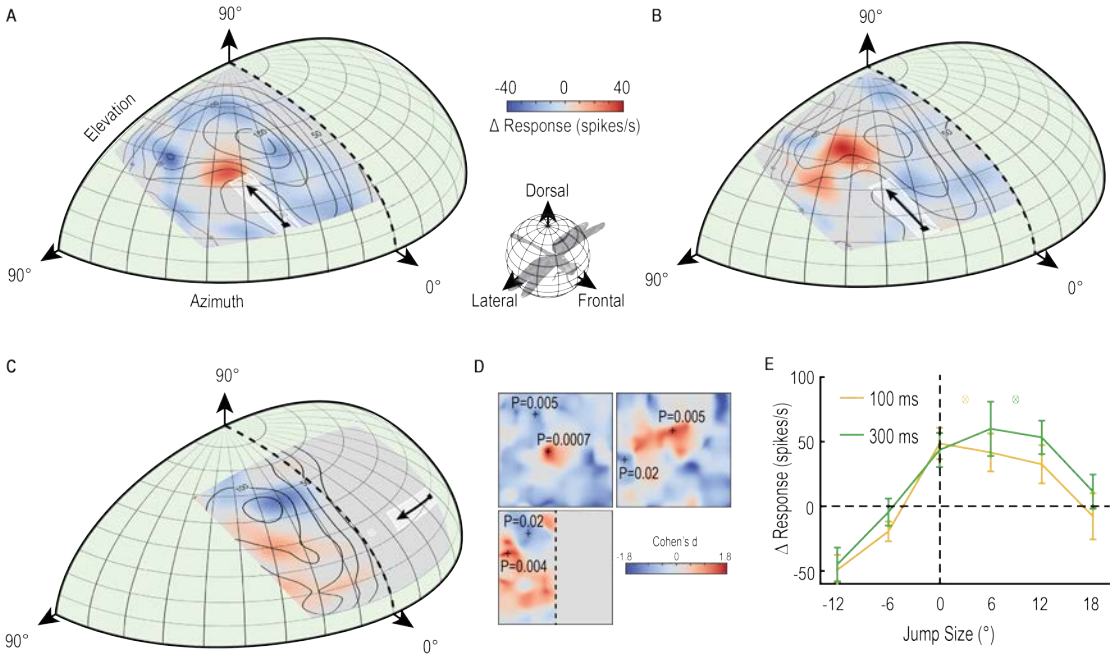

Figure 4-3: A predictive focus facilitates responses to a moving target. (A) The probe receptive field in response to short, vertical trajectories is indicated by contour lines (mean, n=9 dragonflies). The color map shows change in spike rate (for each location) due to the immediately preceding primer trajectory that is presented within the white outlined box. The change in spiking activity in the corresponding analysis window reveals >50% enhancement in front of the moving target (red), but suppression in the surround (blue). (B) With a 300 ms delay introduced after the primer, the focus spreads forward (color map, n=7 dragonflies), estimating the theoretical future target location (white crosshairs). (C) The primer moves toward the midline in the other eye's visual field, whilst avoiding binocular overlap. The focus transfers between brain hemispheres, with a spatially-localized enhancement in front of the target and suppression at higher elevations (color map, n=7 dragonflies). (D) We examined the statistical significance of all three mappings (Figure A-C) by calculating the effect size at each spatial location (Cohen's d). We see values within the range ± 1.8, well above those considered as large effect sizes (>0.5). For spatial points of interest (+), we calculate the corresponding statistical significance (P value) between the primer & probe and probe alone versions (E) There is a forward shift in the focus region (mean ± SEM, P=0.03, n=12 dragonflies) following an occlusion (cf. 100 ms pause, yellow line with 300 ms pause, green line). The expected target locations following occlusions are indicated with color crosshairs (3° for 100 ms and 9° for 300 ms).

In another eight dragonflies, instead of constraining the position of our primer, we instead tested responses to probes that always landed at the same location following different primers. This stereotyped probe followed either a jump in space, a pause in time, or a combination of both tests. Figure 4A-D show normalized response time-courses from individual CSTMD1 examples. The small 4° instantaneous jump ahead of the primer leads to a response time course with a very rapid rise to a level similar to the fully facilitated state (Figure 4A). However, a 12° instantaneous jump elicits a similar (slower) response time course to the unfacilitated probe (grey line), confirming the limited extent to which facilitation initially extends ahead of the target path. A large 20° jump ahead (Figure 4A) bypassing the focus-region entirely, again reveals surround suppression, with a much slower response time course than the control. Instantaneous backwards jumps (Figure 4B) also reveal potent suppression.

Pauses without a jump (0°), show that facilitation strength slowly decays over time at the last seen location of the target (Figure 4C,E, Cohen's d=4.48). With no pause (0 ms), the strongest responses occur 4° in front of the moving target (Figure 4E) as observed in the 2D receptive fields (Figure 3A). Given that the target moves at 40°/s, it would have traversed 4°, 12° and 20° during pause 'occlusions' of 100 ms, 300 ms and 500 ms respectively. When larger jumps are matched to their respective pauses as might be expected during trajectory occlusions (12° and 300 ms; 20° and 500 ms) there is a statistically significant increase in the resultant spiking activity (Figure 4E, Cohen's d=2.0 and 2.32 respectively).

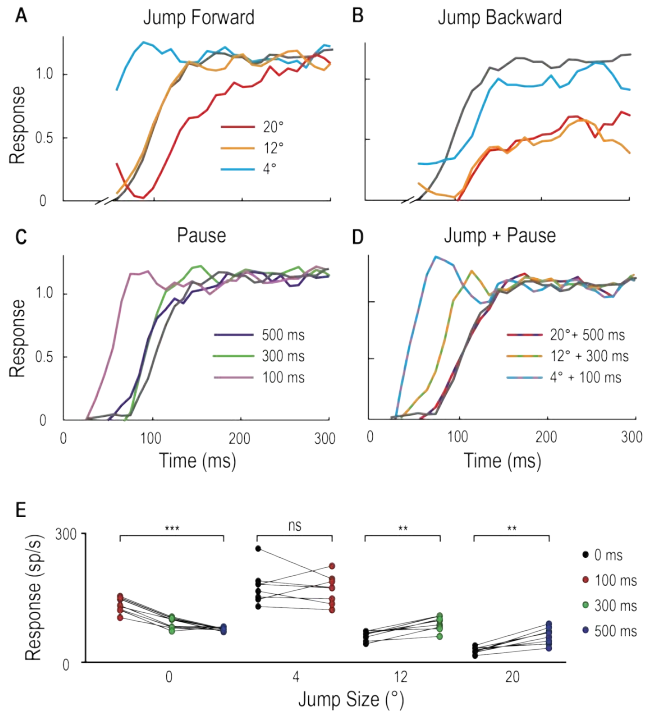

Figure 4-4: Spatial jumps and temporal pauses in target trajectories. (A) CSTMD1's normalized response to a short probe trajectory builds over several hundred milliseconds (grey line) and is changed by the position and timing of a 500 ms priming target. Probes jumped forward immediately following the primer, reveal facilitated responses (4° ahead), unfacilitated responses (12° ahead) and suppression (20° ahead), indicative of the focus-region in Figure 3. (B) A jump immediately back over the primer path exhibits unfacilitated (4° behind) or strongly inhibited (12° or 20° behind) responses. (C) Inserting a temporal pause between primer and probe shows that weaker facilitation persists at the primed location for over 500 ms, diminishing as the pause duration increases. (D) Combining a short pause with a jump reveals a forward spread of facilitation that could account for an occlusion. (A-D, n=9 technical replicates from 1 dragonfly) (E) At the target's last seen position (jump size 0°), probe responses decrease at times following the primer's disappearance (P=0.0005). In comparison, responses to probes jumped 12° and 20° ahead increase when matched to their corresponding occlusion durations of 300 ms (P = 0.008) and 500 ms (P = 0.008). Asterisks indicate significance, n=8 dragonflies.

Primers increase contrast sensitivity

The data presented so far make a strong case for a complex predictive mechanism working to boost responses in a region where a target seen in the recent past is likely

to move to in the near future. In primates, one known effect of such attentional or expectation effects is an upregulation of local contrast sensitivity (gain control) (Reynolds et al. 2000; Carrasco et al. 2000). To quantify changes in gain, we measured responses to varying contrast probes, preceded by either a low or high contrast primer (Figure 5A,B, Video 3). Both primers induced a large increase in response, with a larger output range (increased maximum response) and a greater than 5-fold increase in contrast sensitivity (Figure 5C, contrast threshold reduced from 0.071 to 0.013 for near threshold stimuli, C_{50} from 0.36 to 0.13, n=9 dragonflies). Lower contrast primers themselves induce less overall activity during the priming stimulus (Figure 5D, Cohen's d=0.97), yet their effect on subsequent responses to stimuli presented at the expected location is remarkably similar to high contrast primers (cf. pink with red lines in Figure 5C). This suggests that the gain modulation is not elicited solely by the stimulus contrast or the neuronal activity induced by the primer per se, but rather by target presence. This may indicate a 'switch' process, such as that suggested for neural circuits in the auditory brain stem of the barn owl (Mysore et al. 2011), rather than a simpler, activity-dependent gain control mechanism. Another interesting feature of the facilitated contrast sensitivity is that the boost of response gain is largest at mid-contrast, with softer saturation at high contrasts, extending the range of contrasts over which the response is modulated by a full order of magnitude. Both observations make sense considering the natural context for target detection. During pursuit flights, resources could thus be directed to the expected target location independent of its varying contrast as it moves across a cluttered background. Moreover, the reduction in slope of the contrast sensitivity function would reduce overall response variance to changes in the contrast of the selected target, a phenomenon also observed in humans (Avidan et al. 2002).

Our results also show that the increased contrast sensitivity is localized to the focus-region evident in Figure 3. A more distant primer displaced 20° to the side of the probe does not evoke facilitation of the contrast sensitivity function (Figure 5C). Instead, the contrast sensitivity function reveals a weaker effect of the surround suppression observed in the 2-D receptive fields (Figure 3). These contrast experiments used a shorter primer duration (600 ms vs. 1 s), suggesting that suppression could result in part from CSTMD1's global activity, rather than presynaptic processing. Facilitating stimuli certainly increase the firing rate against a

steadily hyperpolarizing membrane potential (Figure 5D). Following a high contrast primer, this hyperpolarizing motion-after-effect (MAE) reaches almost 4 mV and suppresses subsequent spiking activity for several hundred milliseconds (Figure 5D,E), an attenuation that may compete with spatially-localized facilitation. Interaction between the facilitation time course and longer-term suppression with slow kinetics may be analogous to the 'inhibition of return' observed in human reaction time experiments (Posner & Cohen 1984).

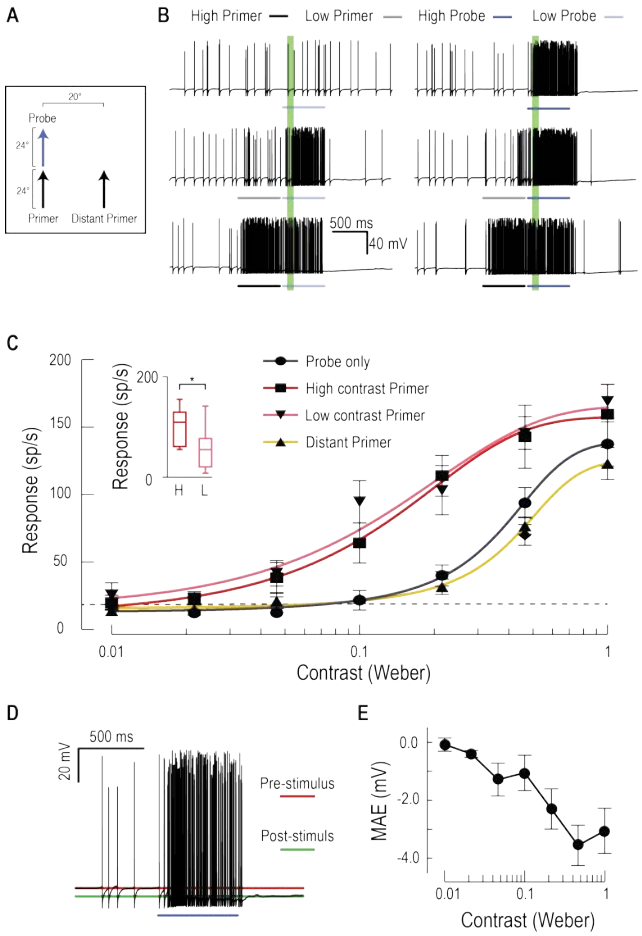

Figure 4-5: Low or high contrast primers increase probe contrast sensitivity. (A) Either a low or high contrast primer is presented before varying contrast probes (contrast sensitivity function). These either continue the path trajectory or jump to a distant location. (B) Example data traces of responses to either low (grey) or high (black) contrast primers that are presented before a series of varying contrast probes (light, medium and dark blue) (C) CSTMD1's sensitivity to varying contrast probes exhibits a sigmoidal function (grey), with the dashed line indicating a detection threshold above spontaneous levels. Following either a nearby low contrast (pink) or high contrast (red) primer, contrast sensitivity is substantially increased (n=9

dragonflies, P<0.0001). A distant primer (yellow) does not elicit facilitation, even though spiking activity during low and high contrast primers (final 100 ms) is significantly different (inset, n=9 dragonflies, P=0.02). (D) In response to an excitatory stimulus (e.g. high contrast stimulation), the underlying membrane potential is hyperpolarized, a form of motion-after-effect (MAE). (E) The hyperpolarizing motion-after-effect is related to the strength (e.g. target contrast) of the stimulus.

Primers induce directionality

The facilitated response of CSTMD1 appears to be only weakly direction-selective when stimulated with targets moving along prolonged paths. Within each hemifield, CSTMD1 has a weak preference for progressive motion upwards and away from the midline (rightwards for the neurons recorded here) (Nordström et al. 2011). To test whether the focus also anticipates the *direction* of a moving target, we presented a primer moving along one of four cardinal directions, followed by a probe that moves in eight possible directions (Figure 6A,B, Video 4). Probe responses alone are both weak and weakly direction selective (Figure 6C, grey dots). But all four primers facilitate responses maximally in the direction of the primer's path, shifting the direction tuning to match that of the primer (Figure 6C). The b_1/b_0 ratio is a measure of the strength of directionality which is similar for each of the conditions (Figure 6D). However, the magnitude of facilitation (Figure 6E) is considerably larger in CSTMD1's weak preferred, direction (upwards and rightwards for this hemisphere's CSTMD1). Such targets would be those moving away from the dragonfly's own heading (Olberg 1986) with the mirror-symmetric CSTMD1 expected to exhibit directional preference to progressive targets moving upwards and to the left. This suggests that the preference of both the underlying tuning and the recruitment of facilitation may be linked to a control role in downstream processing of target trajectories for pursuit. Following a reversal of the target trajectory (Figure 6F, blue and purple lines), CSTMD1's response is strongly inhibited compared to the corresponding probe alone response (grey lines). This contrasts with findings in the vertebrate retina, where a subset of ganglion cells respond strongly and synchronously to motion reversals (Schwartz et al. 2007).

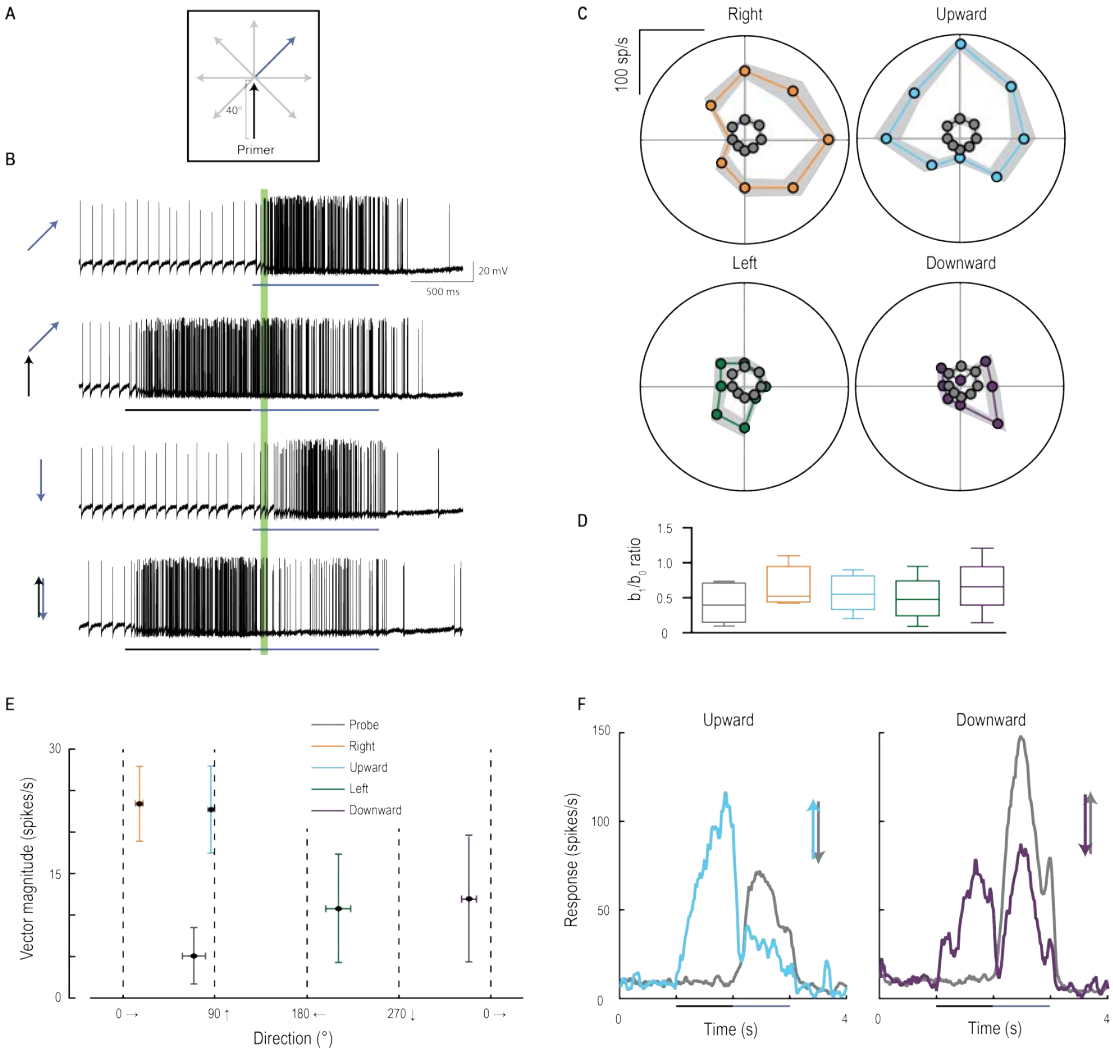

Figure 4-6: Primer direction establishes probe direction selectivity. (A) Primers of four possible directions (right, upward, left, downward) preceded probe responses in each of eight possible directions. (B) Examples of individual traces to a subset of the experiment conditions. The analysis period is indicated in green. (C) Probe responses are weak (grey points) until following a primer (in one of four cardinal directions) and are most facilitated in the primer's direction (mean ± SEM, n=9 dragonflies). (D) The b_1/b_0 is an index showing the strength of directionality. (E) Polar plot vector magnitude and direction (mean± 95% CI), shows that probe direction selectivity generally aligns with the primer direction. (F) Either upward or downward probe alone (grey lines) evoke robust responses. However, 'reversals' (probes opposite in direction to a preceding primer) generate strong and long-lasting inhibition (mean time course, n=9 dragonflies).

Does the recruitment of enhanced responses in the direction of travel represent an alteration of the direction selectivity in underlying local motion detectors, or does it result from the offset position of the focus of gain modulation located just ahead of the most recent target location (Figure 3A)? We tested this by jumping the probe stimulus 4° forward into the predicted center of the focus region (Figure 7A, Video 5). This stimulus induced much weaker direction selectivity (Figure 7B) than those that radiate away from the end of the same priming path (b_1/b_0 ratio of 0.32 vs. 0.50, P=0.04). Probes that reverse direction relative to the primer are not facilitated, except when the probe jumps 4° into the focus center (Figure 7C, Cohen's d=3.90). Thus, the predictive focus of gain modulation is a spatial phenomenon, established by the past trajectory. This suggests that the apparent direction selectivity induced by primers is not due to any change in the local bias of underlying motion detectors to any one stimulus direction, but rather from the overall displacement of the focus *ahead* of the target location. Over a target's developing trajectory, direction selectivity (quantified here as vector magnitude) is established even more rapidly than the gain in the facilitated response (Figure 7D). The emergence of directional tuning raises the intriguing possibility that the modulation assists anticipation of target trajectories - promoting the expectation of a continued path. How such tuning matches closed-loop pursuits of the hawking dragonfly with its prey or conspecifics is not yet known.

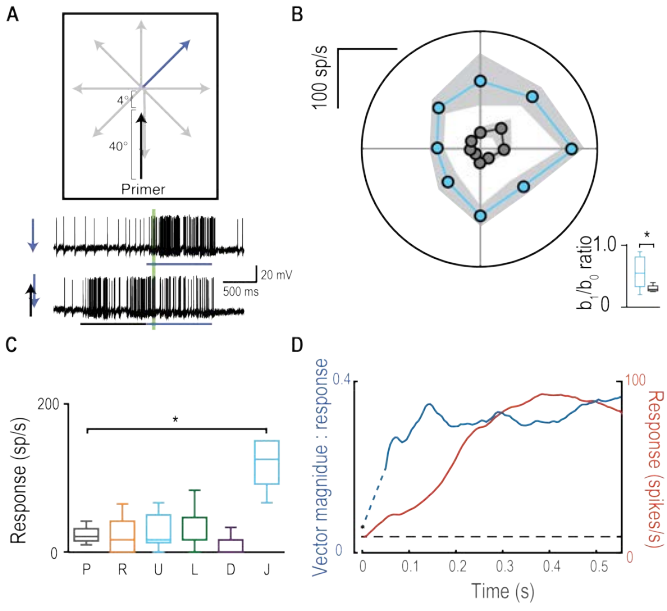

Figure 4-7: Direction selectivity is a result of spatial facilitation. (A) The direction experiment is repeated, now with a 4° jump forward into the spotlight. (B) Responses

are facilitated for all directions (mean ± SEM, n=5 dragonflies) with decreased direction selectivity (b_1/b_0). (C) Probes in the opposite direction to their corresponding primer reveal no facilitation or inhibition, except when jumped [J] into the spotlight (P=0.03). (D) The magnitude of direction selectivity builds on a faster timescale than the response onset.

Facilitation in earlier retinotopic neurons

CSTMD1 is a higher-order neuron with inputs in the anterior optic tubercle, a midbrain output destination of optic lobe interneurons. We also tested for the facilitatory component of the predictive gain modulation in likely pre-cursor neurons: small-field (SF) STMDs located at an earlier stage of visual processing (Barnett et. al., 2007). Retinotopically organized SF-STMDs have inputs in the outer lobula, a region akin to mammalian primary visual cortex (Okamura & Strausfeld 2009, O'Carroll 1993). They have properties similar to end-stopped (hypercomplex) cells (Nordström & O'Carroll 2009), which are modulated by contextual stimuli presented outside their classical receptive field (Polat et al. 1998). We presented primers outside SF-STMD receptive fields, that themselves induce no activity above spontaneous levels (Figure 8A,B, Video 6, n=13 dragonflies), with probe stimuli that are limited to the classical (excitatory) receptive field. Primers moving toward the receptive field facilitate the probe responses by over 40%, whilst those heading away elicit no facilitation. This predictive gain modulation may be inherited and improved downstream, since we also observe facilitation in other large-field STMD neurons, with an average gain of over 80% (Figure 8C, Cohen's d=1.02). Individual responses of both small and large field STMDs vary in facilitation strength, as well as overall activity. The retinotopic organization (Figure 8D) and facilitation observed in SF-STMD's make them ideal candidates for mediating an interhemispheric transfer of localized predictive gain modulation. Supporting this hypothesis, at least one identified (dye-filled) SF-STMD axon traverses the brain with an output arborization located within a limited area of the contralateral lobula (Figure 8D). Neurons such as this are thus perfectly suited for the spatially localized inter-hemispheric modulation, both excitatory and inhibitory shown in Figure 3C.

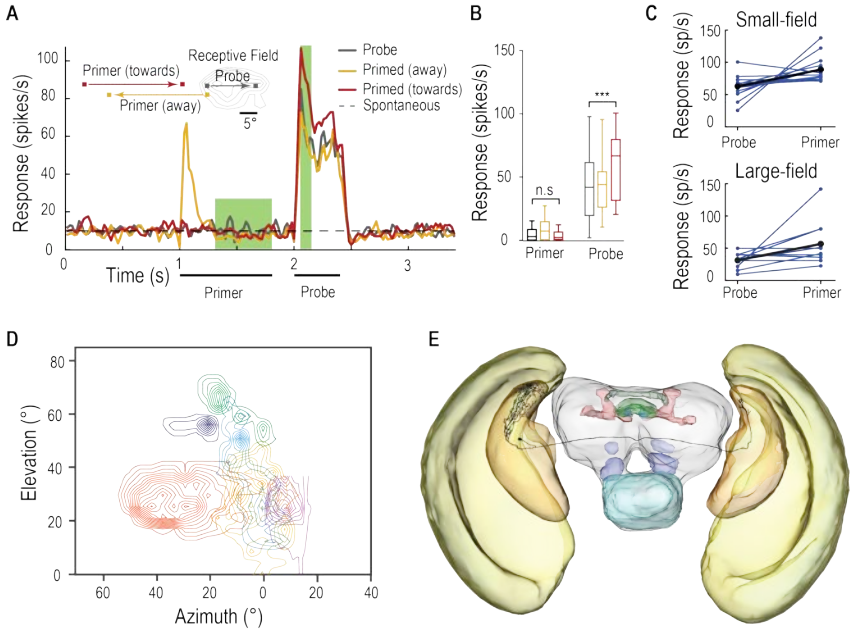

Figure 4-8: SF-STMDs are facilitated by a primer that moves toward the receptive field. (A) Primers move either toward (red) or away (yellow) from the classical receptive field (RF), preceding a probe target within the RF (mean, n=13 dragonflies). (B) Outside the receptive field, primer responses do not significantly differ from spontaneous activity. Primers that move towards the receptive field increase probe responses by over 40% (P=0.0004, n=13 dragonflies). (C) Individual STMDs, with either small or large receptive fields, exhibit varying degrees of facilitation (blue). Mean facilitation (black) increase responses by over 40% in small-field (n=13 dragonflies), 80% in large-field STMDs (n=11 dragonflies) and 50% in CSTMD1 (data not shown). (D) Six small-field STMD receptive fields (RF) are predominantly fronto-dorsal and exhibit variation in overall size and spatial locations. Contour lines represent 25 spikes/s. The SF-STMD with light purple contours is the same neuron in E, with inputs in the binocular region of the dragonfly's right visual field, whilst input dendrites are in the left hemisphere (E) An SF-STMD's axon traverses the brain, potentially underlying transfer of local predictive gain modulation.

4.5 Discussion

Neuronal receptive fields are defined by their excitatory and inhibitory responses to stimulation. Populations of such responses elucidate network function, for example, as control systems in insect flight behavior (Gonzalez-Bellido et al. 2013; Maisak et al. 2013). However, our results show that in addition to stimulus selectivity (contrast, size, velocity), a neuron's receptive field is also a dynamic representation of the

spatial (Wiederman & O'Carroll 2013) and temporal context. Here modulation of the dynamic receptive field represents anticipatory coding, a more complex influence of history than simple neuronal adaptation, sensitization, habituation or fatigue. Indeed, such complexity in processing is also evident in the 'omitted stimulus response' in the vertebrate retina, where an omitted component of a periodic pattern predictively elicits robust neuronal activity (Schwartz et al. 2007). These examples highlight that the brain is a 'predictive machine' (Rao and Ballard 1999). However, instead of encoding novelty or the unexpected, STMD neurons predict consistency of a selected target's trajectory, all whilst suppressing distracters.

Direction selectivity is, in effect, a simple form of prediction. For example, the Hassenstein-Reichardt correlator provides a nonlinear, facilitated response when an adjacent point is stimulated within a future period (Hassenstein and Reichardt 1956). However, such direction selective models cannot explain the observation of a traveling gain modulation that spreads further forward, the longer the occlusion. Neither can these models account for changes in preferred direction, determined by the target's previous direction of travel. Such models do not result in a contrast invariant 'switch' establishing the focus strength, nor the presence of a large suppressive surround. Furthermore, the effects described here are on larger scales either spatially (tens of degrees) or temporally (hundreds of milliseconds) compared with local motion detection processes, such as optic flow analysis (tens of milliseconds, Guo & Reichardt, 1987). Finally, our results show a local, predictive focus of facilitation that traverses across brain hemispheres, which is an attribute more reminiscent of higher order attentional networks, rather than local motion encoding circuitry.

Our findings of over a 400% increase in contrast sensitivity is consistent with studies that cue spatial attention in vertebrates, albeit with a significantly larger increase. For example, the contrast gain of human observers is increased by approximately 40% for stimuli presented at an attended location (Carrasco et al. 2000), with concurrent decreased contrast gain for stimuli presented elsewhere (Pestilli & Carrasco 2005). Similar results are also observed in single unit recordings from macaque V4, where gratings presented at attended locations elicit responses equivalent to a 51% increase in stimulus contrast (Reynolds et al. 2000). Whilst there is ongoing debate over whether attention produces contrast gain (Reynolds et al. 2000) or response gain

(Lee & Maunsell 2010), the facilitation in CSTMD1 reveals a combination of both (Figure 5C). CSTMD1's gain modulation could be an inherent component of the prediction mechanism, or the result of the priming target acting as a cue directing attention to the targets predicted location.

We have previously reported that CSTMD1 selectively attends to one target when presented with a pair of competing stimuli, completely ignoring the distracter (Wiederman & O'Carroll 2013). In repeated trials, the selected target was not always the same and even occasionally switched mid-trial. This raises the intriguing possibility that the predictive focus 'locks on' to a single target, suppressing distracters. The anticipatory gain control measured here provides a possible explanation for this behavior – a positive feedback that allows the neuron to lock onto a single object while other mechanisms, including global inhibition may help suppress competing objects. Future experiments will address the parameters of the stimuli (e.g. timing, salience) that permit the predictive focus to switch between alternative targets. Furthermore, we are currently investigating whether the predictive focus and competitive selection is elicited bottom-up by the stimuli (exogenous) or includes a top-down component (endogenous). That is, for a dragonfly feeding in a swarm, are target saliency attributes driving pursuit selection, or is the dragonfly choosing its prey from more complex internal workings?

For decades, scientists studied the neuronal basis of 'elementary motion detection' in true flies (*Diptera*). With morphological (Takemura et al. 2013) and physiological (Maisak et al. 2013) experiments making significant progress at elucidating this circuitry, increasing attention is now shifting towards other visual tasks such as feature discrimination (Aptekar et al. 2015, Keles & Frye, 2017). Until now, there has been a divide between such 'simple' visual operations and higher-order processing observed in mammals. Our results reveal the dragonfly as a surprisingly sophisticated, yet tractable model, permitting investigation of fundamental physiological and morphological principles underlying neuronal prediction and selective attention.

Acknowledgements

This research was supported by the Australian Research Council (DP130104572, DE150100548) and the Swedish Research Council (VR 2014-4904). We thank the manager of the Adelaide Botanic Gardens for allowing insect collection and behavioral recordings.

5 The parameters underlying predictive gain modulation in target-detecting neurons

Context

In the previous chapter I described a complex predictive gain modulation mechanism that utilises the predictable nature of target trajectories to enhance the robustness and sensitivity of STMD neurons during target detection. This work included descriptions of a 'focus' of gain produced by the continuous motion of targets through the receptive field. This focus shifts forward over time, predicting the future location of a target following occlusions. However to this point we had not performed detailed experiments that investigate how different parameters of a priming trajectory affect the strength of gain produced. Here I have varied a series of primer parameters to investigate the following research questions:

1. How does the duration of a priming target and the angular distance it covers affect the strength of gain modulation?
2. Does the velocity of a priming target affect the rate at which the focus of gain spreads following an occlusion?
3. How does the angular size of a primer affect the strength of gain modulation, and does this have any effect on target height tuning?
4. How does a primers contrast affect the strength of gain modulation?

This chapter is not a published manuscript, but rather a less formal results chapter. For this reason it lacks a broad and detailed introduction that is covered in previous chapters. The results presented here will form the basis of a first authored manuscript.

5.1 Introduction

Dragonflies are predatory insects that detect and capture small moving prey and conspecifics. During this behaviour prey rarely span more than 1° of visual space, stimulating two or three ommatidia of the compound eye (Lin and Leonardo 2017). A population of neurons that respond to these targets have been identified in the lobula of dragonflies, Small Target Motion Detectors (STMDs) (O'Carroll 1993; Geurten et al. 2007). Visual neurons that detect the motion of larger patterns or objects integrate the response of many presynaptic units that view different portions of the same feature (Bausenwein et al. 1992). This integration over space produces a robust visual signal that allows impressive contrast sensitivity. Neurons that underlie small-target detection cannot pool inputs across space and are faced with a minute and noisy signal. Despite this, some STMD neurons can detect targets with contrast as low as 1.3%, sensitivity that matches blowfly HS neurons (Harris et al. 2000; Wiederman et al, 2017). Here a small hyperpolarisation in just a few photoreceptors is sufficient to generate robust neuronal response and behaviour (Rigosi et al. 2017).

What processes allow STMD neurons to extract reliable target information from weak inputs? Following the sudden onset of a stimulus, neuronal responses are weak (Nordström et al. 2011). These responses build in strength over several hundred milliseconds if a stimulus is continuous in space and time (Dunbier et al. 2012), a property classified as facilitation. This build-up of response is matched by a large improvement in contrast gain, with the detectability threshold at stimulus onset more than 5-fold poorer than that following several hundred milliseconds of target motion (Wiederman, Fabian et al. 2017). This facilitation is expressed as a local gain increase situated slightly ahead of a targets current position, surrounded by global suppression. The 'focus' is predictive in nature, shifting forward in space following an occlusion, and matching the direction of a targets motion. As a result, signal strength is greatly improved for 'natural' target trajectories, while simultaneously decreasing the signal of background distracters or false positives.

Psychophysical experimentation shows that humans also use prior trajectory information to improve their ability to detect and track targets (Watamaniuk et al. 1995; Watamaniuk and McKee 1995). When humans predict the position and

movements of an occluded object, they account for properties such as its velocity or direction (Bennet and Barnes 2003), but a clear neuronal correlate of these predictions remains elusive. Here we have studied the strength and propagation of predictive gain modulation within the receptive field of STMD neurons in response to different parameters of a prior trajectory. This allows us to identify which stimulus parameters control these mechanisms, and test the accuracy of its predictive functions.

5.2 Results and Discussion

Spatiotemporal tuning of gain modulation

In order to investigate which target parameters effect the magnitude of gain modulation, we present target trajectories that are segmented into two sections; a primer and a probe (Figure 1a, b). Responses to 'probe' targets are weak when presented alone, and enhanced by varying amounts when preceded by a 'primer' of different durations or distances (Figure 1c).

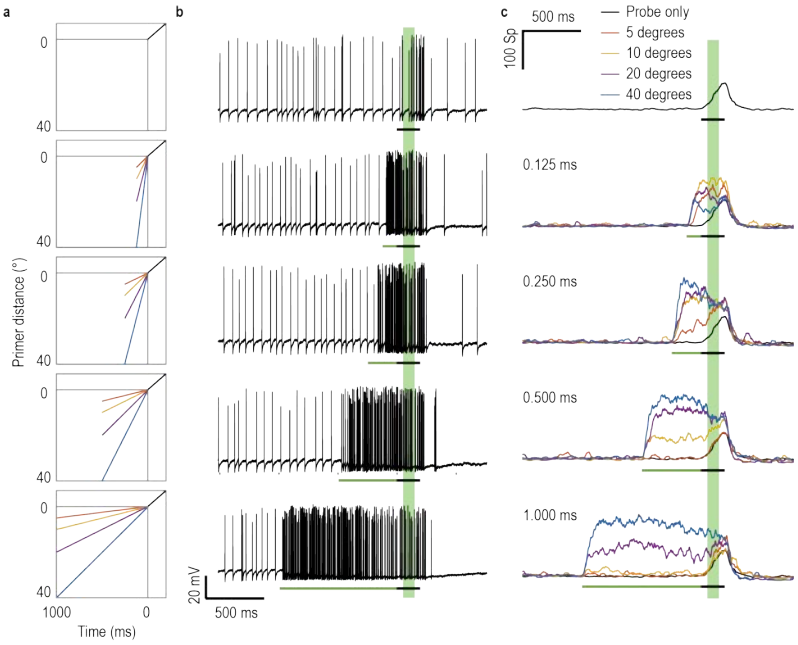

Figure 5-1: Priming targets facilitate the response to a probe. a) Probes drift on a short trajectory, preceded by primers that covers 16 combinations of distances and durations. b) Responses to probes are analysed across different conditions in a 100 ms window (green shaded area). Green and black stimulus bars represent primer and probe presentation respectively. c) The response to the same probe varies in strength dependent on the primer that proceeds it.

All previous studies of facilitation in STMD neurons presented priming targets that drifted for similar durations and covered similar distances (Nordström et al. 2011; Dunbier et al. 2012; Wiederman et al. 2017). While each of these experiments demonstrated consistent increases in local gain, they confound the duration of a priming stimulus with the space it traversed. Because of this it is still unclear whether gain modulation is a result of a target stimulating a certain number of detectors across space, or whether it simply requires constant stimuli over sufficient time. To answer this question we present 'primer' targets that drift for different combinations of space and time, each terminating at the start position of a uniform probe stimulus. The change in probe response elicited by each primer represents the strength of gain modulation (figure 2a).

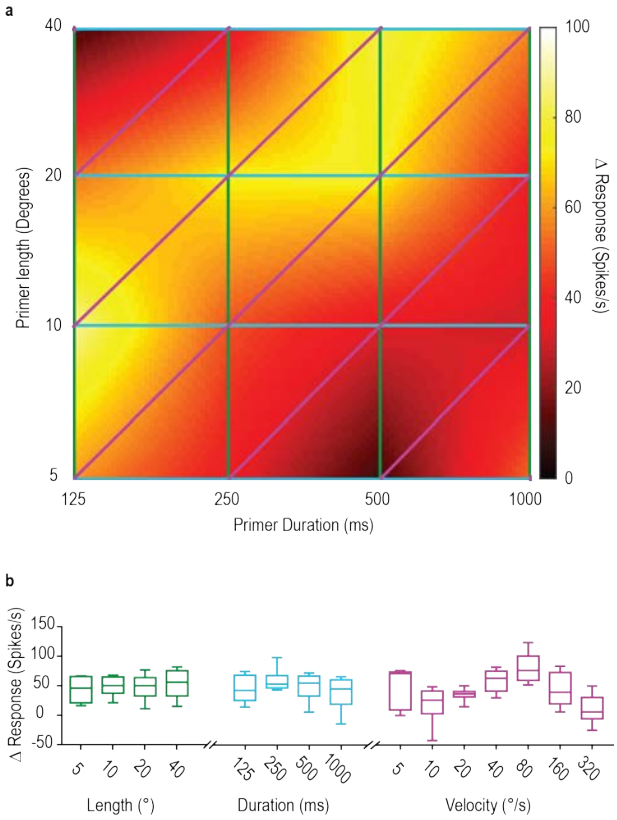

Figure 5-2: The relationship between primer parameters and response gain. a) A 2D representation of the strength of gain modulation for primers presented across different combinations of space and time. b) Each datapoint in (a) can be arranged into groups of equal primer length, primer duration or primer velocity (n = 6 dragonflies).

If gain modulation only required the stimulation of several adjacent motion detectors, we should observe strong facilitation irrespective of the duration of the target that passes that space. Conversely, if gain is modulated by the duration of a stimulus, primers of equal duration but varying distance should produce equal facilitation. Our results show that all primers produce an increase in gain (figure 2b). Pooling trials where the primer covered an equal length or duration reveals no net effect on the amount of facilitation generated. However if we sort trials by primer velocity (primer length/primer duration) we observe what resembles a tuning function. Primers that drift at 80°/s produced the strongest increase in gain, irrespective of their duration or length. It is important to note that this does not mean primer space or distance have no effect. Gain is derived from the difference in response from the probe stimulus, in a window of 50-150ms following termination of the primer. Thus, even the shortest duration primer (125 ms) reflects analysis window that begins after 175 ms of continuous target motion. Had we presented even shorter trajectories, at some point effects of stimulus duration will be observed.

Target velocity and the spread of gain

A distinguishing property of dynamic gain modulation is that when a drifting priming target is temporarily occluded, the 'focus' of gain modulation shifts forward in space (Wiederman et al. 2017). This forward shift in the focus accurately matched the distance the target would have drifted had it continued moving at the same velocity. However since this experiment was only performed at a single velocity, it is unclear whether the shifting focus shifts at a target-matched velocity, or a constant 'hardwired' velocity that happened to match the primer velocity. To investigated further we present two primers of equal duration, one drifting at 30°/s and the other at 60°/s (Figure 3a). The faster primer covers twice the distance of the slow primer, but terminates at the same position. Following termination of the primer, we introduce a pause of either 100 ms or 300 ms to allow gain to spread, before presenting probes at different locations ahead and behind of the primers final position (Figure 3b). If the 'focus' spreads at a primer matched velocity over the same time period the gain elicited by the faster primer should spread twice as far as the gain elicited by the slower primer.

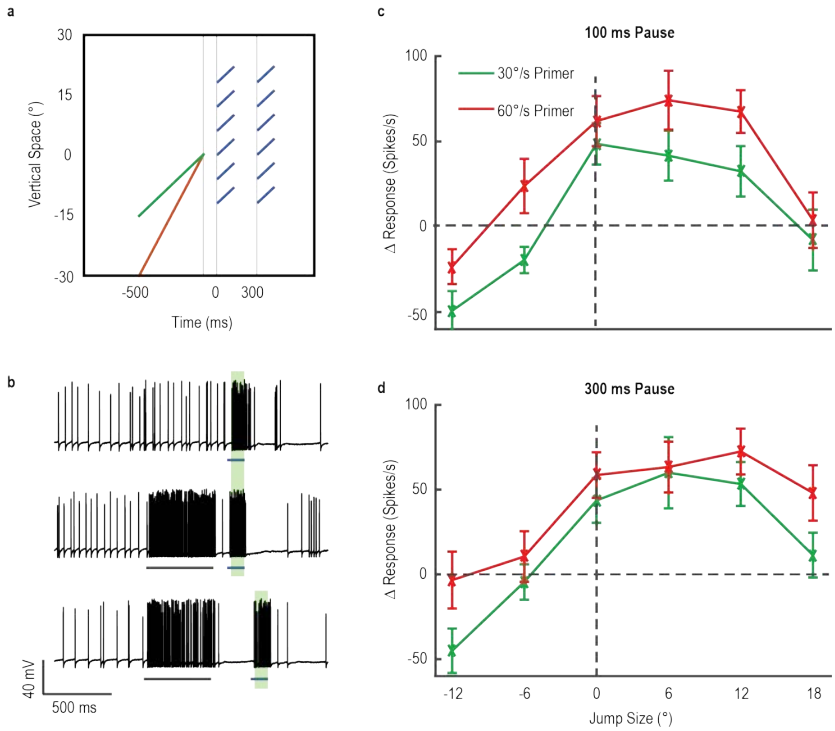

Figure 5-3: Primer velocity and the shifting focus of gain. a) The change in response to a series of probes (blue) in different locations is mapped following primers of different velocity (green and red), following a 100 and 300 ms pause. b) Responses to probes are quantified in a 100 ms window, presented alone or following different primers. Changes in probe response at different positions are displayed 100 ms (c) or 300 ms (d) following the termination of a primer (n = 12 dragonflies).

Figure 3c and 3d show one-dimensional maps of gain modulation following the two primers following 100 ms and 300 ms pauses. As observed in figure 2, primer velocity alters the magnitude of gain modulation. Since the 60°/s primer lies closer to the velocity optimum, it generates stronger effects at all positions relative to the 30°/s alternative. This global increase in gain complicates our analysis, as we lack the data to distinguish between forward and upward shifts in the 'focus' map. Thus, based on this data we do not observe a significant velocity dependency on the forward shift in spread. Now that we know the effect of primer velocity on gain magnitude (figure 2b), I will design a follow-up experiment that uses primer velocities on opposing sides of the velocity-tuning curve (perhaps 60° and 120°), to isolate forward shifts.

This data also allows us to observe the inhibition that builds behind a targets last seen position. Wiederman et al (2017) show that strong facilitation is observed at the last seen position of a terminated target for at least 500 ms. Similarly, here we see that

300 ms following the end of a priming stimulus, we maintain strong facilitation at its last seen position (0° jump).

Based on this result, we would expect probes that jump backwards to recently observed target locations (< 500 ms) to elicit facilitated responses. However as with previous work, when we jump backwards by 12° following either 100 or 300 ms pauses we observe strong inhibition. This suggests that continuous stimulation during a target trajectory generates inhibitory feedback that abolishes any gain increase along the targets prior path. This results in lingering gain enhancement at a terminated targets last seen position, but prevents gain from accumulating behind a target on a continuous trajectory. This could be functionally useful, as it allows a 'memory' of the location a target was lost, but does not affect ongoing target tracking.

Gain modulation across target height

Dragonflies are highly selective for the angular size of prey, with pursuit rarely initiated for targets spanning >1° on the retina (Combes et al. 2013; Lin and Leonardo 2017). The tuning range of STMD neurons is usually much broader, with CSTMD1 producing optimal responses to targets spanning 2-3° (Geurten et al. 2007). In the past, target height tuning has been measured with targets that drift across the entire visual display and are therefore 'self-facilitated' (Geurten et al. 2007). This means that these tuning curves represent not only the underlying size tuning of CSTMD1, but also any potential size tuning of gain modulation itself.

Here we investigated whether gain modulation produced by primers of different height affects CSTMD1's height tuning. We present a series of probes with different heights, either alone or following the presentation of primers of two heights, 0.5° or 5° (Figure 4a). These sizes lay either side of CSTMD1's optimal height range, and are expected to elicit responses of similar magnitude (Geurten et al. 2007). However, one target represents an ideal pursuit candidate for a behaving dragonfly, whilst the other would be ignored (Lin and Leonardo. 2017). Does the ideal target elicit more gain than the larger, equally salient but less behaviourally relevant target? Furthermore, similarly to a primers effects on direction tuning (Wiederman et al. 2017), does gain modulation produced by a target of a certain height result in any shifts in height tuning?

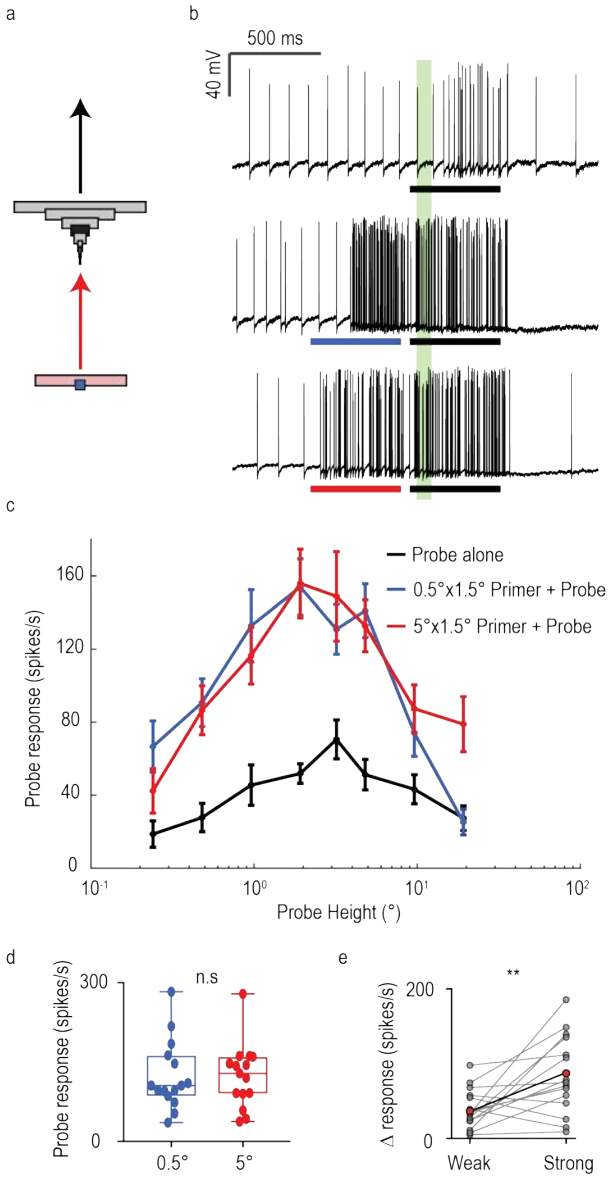

Figure 5-4: Target height tuning following different height primers. Probes of different height measure target height tuning, presented alone or primed by a small (0.5°x1.5°) or large (5°x1.5°) targets. b) Probe responses are quantified in a 100 ms window (green shaded region). c) Responses to probes of different heights, presented alone or following different priming conditions (n = 15 dragonflies). d) The mean response to both primers across all probe conditions. e) The strength of gain produced by identical primers for 'weak' probes (0.24°, 0.48°, 9.6° and 19.2° probes pooled) and 'strong' probes (0.96°, 1.92°, 3.2°, and 4.8° probes pooled).

Our results show that CSTMD1's optimum target height remains at 2-3°, irrespective of whether or not the target is primed, or the size of the primer itself (Figure 4c). Both primers produced responses of equal strength (Figure 4d, 123.4 ± 16.9 for 0.5°, 123.7

± 15.6 for 5°, P = 0.84). However, the strength of gain was not equal across all probe sizes. Instead, the gain produced by a given primer is greatest when the probe is at an optimal size (39.6±6.8 for weak probe sizes, 84.8± 13.5 for strong, p=0.007). Given that the same primers generate different amounts of facilitation across different probes, gain modulation cannot be a simple additive operation. Instead, the magnitude of gain modulation is dependent on both the salience of a priming stimulus, and the salience of the probe that follows. We are currently developing some simple computational models that could explain these primer-probe interactions.

Target contrast gating

But how does this relate to primer contrast? Wiederman et al (2017) demonstrated that a primer produces a large increase in contrast gain and response gain. Importantly, reducing the contrast of a primer produced identical results, despite the fact that the weaker primer generated significantly weaker responses. This suggests that the strength of gain does not necessarily match the salience of a primer, but instead transitions rapidly in a binary operation once the salience of a primer reaches a threshold. To confirm this concept, instead of studying the effect of a primer on probes of different contrasts, we modulated the contrast of primers preceding a constant contrast probe (Figure 5a). We choose to present probes of intermediate contrast (0.1 and 0.22 Weber), where the strength of modulation is most evident. Responses were analysed in a 100 ms window following probe onset (Figure 5b, green shaded area).

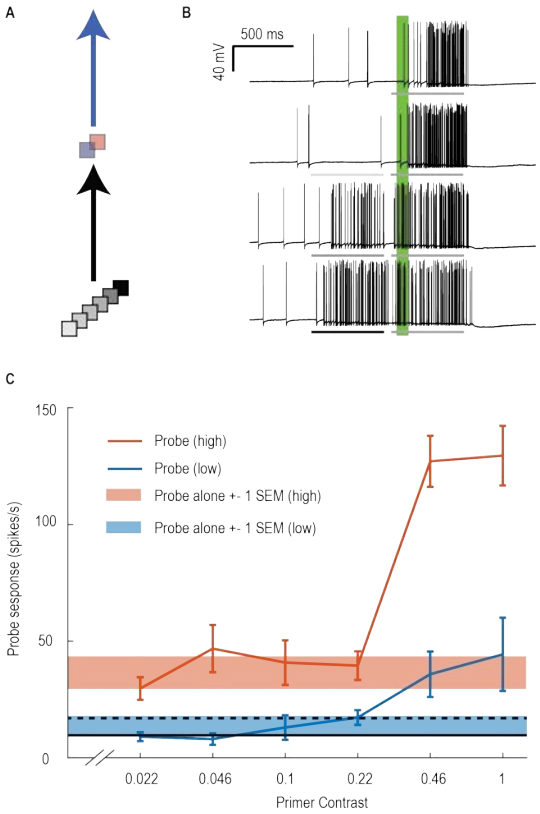

Figure 5-5: The contrast dependence of gain modulation. a) Two probes of intermediate contrast (0.1 and 0.22 Weber) were preceded by a series of primers of varying contrast. b) Probe response was quantified in a 100 ms window, shown by the green shaded box. c) Responses to the two probes following priming by different contrast primers (n = 11 dragonflies).

Probes presented alone produce moderate responses (Figure 5c, 31.9 ± 6.8 and 56.1 ± 9 Spikes/s). When primers of varying contrast preceded the probe, response was only affected by primers of 0.46 contrast or above (Figure 5c). While the strength of gain remains equal across suprathreshold primers of different saliency, for the same primer we again observe stronger facilitation for more salient probes. This result is consistent with previous findings, however the contrast threshold which gates gain modulation is noticeably higher than in our previous work (where a 0.2 weber contrast primer produced strong gain). Given that these recordings were performed from the same identified neuron in the same species of dragonflies, these differences are must be due to either the stimulus positioning within the receptive field, neuronal habituation or the stimulus presentation hardware. CSTMD1's excitatory receptive field is significantly smaller when mapped by a low contrast target (Wiederman and O'Carroll 2013). While all stimuli were presented within the receptive field, it is

possible that in some cases this location was not sensitive to the lower contrast priming targets. In addition, stimuli were presented on a monitor with lower maximum luminance intensity than the prior work (350 cd/s vs 400 cd/s). Weber contrast is a relative measure independent of absolute intensity, but the sensitivity of STMD neurons to targets of equal contrast but varying intensity has never been investigated.

5.3 Conclusion

The responses of individual STMD neurons are generated by complex interactions between the parameters of a stimulus and the spatiotemporal dynamics of the receptive field (Wiederman et al. 2017). Previous descriptions of gain modulation have proposed that receptive field sensitivity builds occur over hundreds of milliseconds of target motion (Nordström et al. 2011). This work suggests that the absolute duration of prior stimulation is just one of many parameters that controls this process. We demonstrate that the magnitude of predictive gain modulation is dependent on the parameters of both priming targets and probes. While these parameters have clear effects on gain magnitude, we were not able to observe any velocity dependency in the spread of gain over time. Whether this is because the spread is velocity independent, or because of limitations of our experimental paradigms is yet to be seen. However it is clear that in practice if this dependency did exist it would be strongly confounded by the velocity dependency of gain magnitude. Using neuronal response alone, downstream pathways could not distinguish between a target that perfectly matched the location predicted by a slower primer, and a target that poorly matched the location predicted by a faster primer.

The advantages of such a non-linear stimulus-stimulus interaction is that robust tracking of targets can be obtained amidst dynamically changing conditions. A target that temporarily drops out of an optimal range in size, contrast or velocity will still elicit strong responses due to gain generated during its prior path. Conversely, in contrast to our previous ideas, a target that abruptly enters the visual field can be detected in a reasonably short time if it accurately matches the systems tuning parameters. Such a stimulus-stimulus interaction is favourable for improving signal-to-noise ratio when extracting small moving targets from cluttered backgrounds.

6 The interactions between target selection and predictive gain modulation

Context

Previous work from our lab described selective attention in CSTMD1 when presented with multiple targets simultaneously (Wiederman and O'Carroll. 2013). Up until this point the experiments in my PhD focussed on the dynamic receptive field properties induced by individual targets. While detailed two-target experiments are beyond the scope of my PhD, one of my major aims was to investigate whether selective attention is an inherent result of predictive gain modulation, or whether the two phenomena represent unique and parallel properties of STMD neurons. In the final year of my PhD a newly commencing PhD student, Benjamin Baden, worked on developing methods of 'tagging' a stimulus, allowing us to identify which of multiple targets was selected in any trial. The method he developed has allowed me to perform the experiments presented in this chapter.

This chapter is not a published manuscript, but rather a less formal results chapter. For this reason it lacks a broad and detailed introduction that is covered in previous chapters. This work will be combined with additional work performed by Benjamin Baden (not presented here), in a second authored manuscript.

6.1 Introduction

One of the central aims of this thesis was to determine whether the previously described dynamic gain modulation within the receptive field of STMD neurons represented a mechanism of selective attention. When CSTMD1 is presented with two targets drifting on long simultaneous trajectories (T1 and T2), the neuron responds robustly, with each individual trial accurately matching the responses observed when either T1 or T2 was presented alone (Wiederman and O'Carroll 2013). This suggests that CSTMD1 selects one target in a scene and ignores others; a property classified as selective attention. As reported in previous chapters, gain modulation involves local enhancement of response, surrounded by global suppression elsewhere. We have proposed that such a mechanism might underlie target selection, where the receptive field is modulated such that the focus of gain 'locks on' to one target, whilst responses to the other is abolished by the surround suppression. Alternatively, this gain modulation may work in parallel with a separate selective attention mechanism, implemented either before or after target selection is made.

If gain modulation is the mechanism that underlies selective attention in STMD neurons, we would expect that presenting two primers simultaneously would generate enhanced responses for probes located ahead of the selected primer and reduced responses for primers located ahead of the 'loser'. However such an experiment requires a robust method of identifying which of the two primers were selected in each trial. Previous work identified the selected target by comparing the different 'signature' peri-stimulus time histograms for targets that drifted across different parts of the receptive field. This method was effective when targets drifted for 2+ seconds across the entire display monitor in locations with different sensitivities. Unfortunately such a stimulus is not effective for use as a primer, as excessively long target trajectories introduce separate inhibitory influences and also limit the space available for probe trajectories. This technique is also highly sensitive to minor changes in local sensitivity caused by habituation over a long experiment. Luckily a recently commencing PhD student, Benjamin Baden, was set to task to identify and optimise new techniques for identifying which target is selected. From this work, a promising frequency tagging method was developed. The basic premise of this method is that if the contrast of a drifting target is modulated in a sinusoidal pattern at

a given frequency, the response of an STMD neuron should also contain a sinusoidal component at the same frequency. This technique is robust across a reasonably large range of modulation frequencies (Figure 1a, Benjamin Baden, Personal communication). Furthermore, when two targets of different frequencies are presented simultaneously, we observe significant modulation of spike rate at the frequency of the selected target, and no modulation at the frequency of the other (Figure 1b). This allows us to determine which target is selected from a given trial with much more confidence than in the past, and is readily implemented into priming experiments that investigate gain modulation.

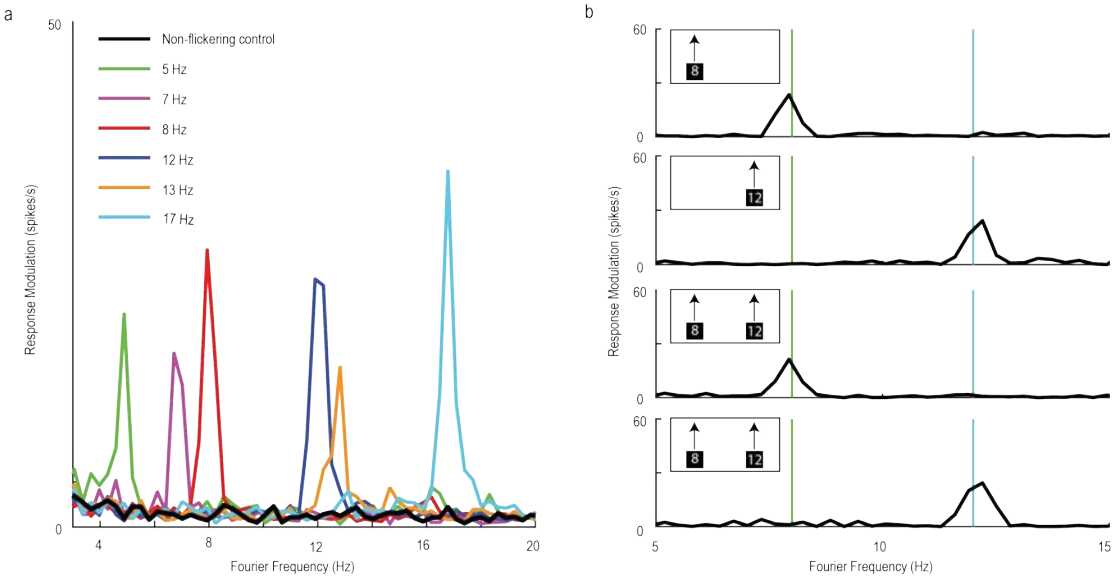

Figure 6-1: Frequency tagging allows the identification of an attended stimulus. (Benjamin Baden, personal communication) a) Targets that drift through the receptive field of CSTMD1 have their contrast modulated at different frequencies. The responses elicited by each target contain a robust frequency component that matches the modulation frequency (mean from 71 trials in 4 dragonflies). b) If we present two targets with different modulation frequencies simultaneously, the modulation of neuronal response from any individual trial matches the frequency of the selected target.

6.2 Methods

Our protocol for animal preparation and electrophysiology was identical to that described in previous chapters.

Neuronal identification

Upon establishing a healthy intracellular recording, all neurons were presented with a series of stimuli that included moving patterns, gratings, bars, full-screen flicker and small drifting targets. STMD neurons were classified by their selectivity to small targets, with CSTMD1 identified by its characteristic receptive field and biphasic action potentials.

Visual Stimuli

All stimuli were presented on high definition LCD monitors (120 Hz and above). All targets were 1.5°x1.5° degree dark squares presented on a white background. The intensity of tagged targets was modulated at frequencies of 8, 11, 12 or 15 Hz, with target contrast transitioning between 0.22 and 1.0 (weber contrast) in a sinusoidal pattern. The frequencies chosen were matched to the monitor refresh rate in order to avoid unintended aliasing effects.

Priming targets drifted upwards for 1 second within the receptive field of CSTMD1, either presented alone or as a pair separated by 20° of horizontal space (T1 = left primer, T2 = right primer). Following a 50 ms pause, we presented one of two possible probes, one in-line with T1 and the other in-line with T2. Probes had a contrast of 0.4 in order to reduce the effects of saturation. Each probe is presented alone, as well as following priming by T1 alone, T2 alone and T1 and T2 presented together.

Analysis

From each trial we calculate the instantaneous spike frequency for the duration of the priming stimulus. This data was then subjected to a continuous 1-D wavelet transform, where we extract the relative modulation at the frequency of T1 and T2. To determine which target was selected we subtract the modulation at T2's frequency from the modulation at T1's frequency, such that positive values suggest T1 is being

tracked and negative values suggest T2 is being tracked. Choosing the duration of our analysis window was a compromise between signal robustness and temporal resolving power. Wavelet transforms are the most accurate when pooling across a large time window, but larger windows increase the risk of mid-trial attentional switches (Wiederman and O'Carroll 2013). For this reason we use a 500 ms window from 450 ms to 950 ms following primer onset. To ensure habituation was not a major factor, we exclude any trials where the mean primer response during this 500 ms window was less than 50 spikes/s.

From each animal we calculated the mean response to probe stimuli presented alone in an analysis window of 50-150 ms following probe onset. This value was then subtracted from the response to probes following each priming condition from the same animal, providing a difference measure (Δ spikes/s) that represents the effect of priming, directly comparable to the measures used in our previous work (Wiederman et al. 2017). Trials were pooled based on the spatial relationship between the primer and probes presented (figure 2).

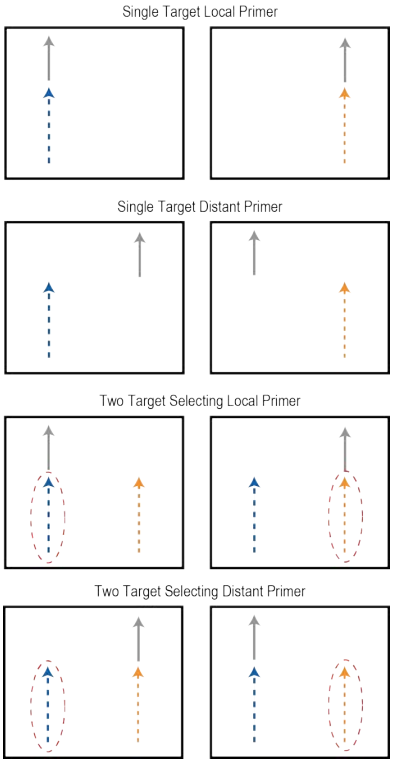

Figure 6-2: The different experimental conditions presented, and their pooling in the subsequent analysis. Red dashed oval lines highlight the attended target in trials where two primers are presented simultaneously.

For trials primed by a single target, 'Local Primer' represents trials where T1 preceding the left probe or T2 preceded the right probe, while 'Distant Primer' represents trials where T1 preceded the right probe and T2 the left probe. For trials

where both primers are presented simultaneously we pool trials based on the spatial relationship between the target that was selected and the probe presentation. This provides a total of 4 different conditions, ‘Single Target Local Primer’, ‘Single Target Distant Primer’, ‘Two Target Selecting Local Primer’ and ‘Two Target Selecting Distant Primer’(figure 2). All experimental conditions were randomly interleaved, with each trial followed by a rest period of at least 8 seconds to minimise habituation.

6.3 Results

My previous work demonstrated that following the motion of a primer, probes presented directly ahead of the primed path show increased responses, while probes presented elsewhere are inhibited (Wiederman et al. 2017). When two targets are presented simultaneously, one target will be selected and the other ignored (Wiederman and O’Carroll 2013). Here we presented a series of probes, either alone, preceded by a local primer, preceded by a distant primer or preceded by both primers simultaneously (Figure 3a). In agreement with prior work, in the single target paradigm local primers facilitate responses to a probe stimulus whilst distant primers produce inhibition. If this gain modulation were a mechanism of selective attention, in a two-target paradigm if the ‘local’ primer were selected we would expect facilitation of probe responses, whilst if the ‘distant’ primer were selected we would expect inhibition. Instead, we observed significant facilitation of responses irrespective of whether the selected primer was local or distant (Figure 3b, $P < 0.0001$). This suggests that gain is modulated across both trajectories simultaneously, even though only one is eliciting a response. This finding effectively rules out predictive gain modulation as a mechanism underlying selective attention, suggesting that its primary role is to enhance weak signals by integrating target motion signals across a trajectory. However this result helps explains the rare examples of ‘attentional switching’ observed in previous work (Wiederman and O’Carroll. 2013). If the ‘losing’ target did not produce its own gain enhancement, when the attended target switches CSTMD1’s response should fall to a naïve unprimed state, and take several hundred milliseconds to re-build. Instead, in examples where the attended target switches mid-trial, responses seamlessly switched to the fully facilitated level for the previously unattended path.

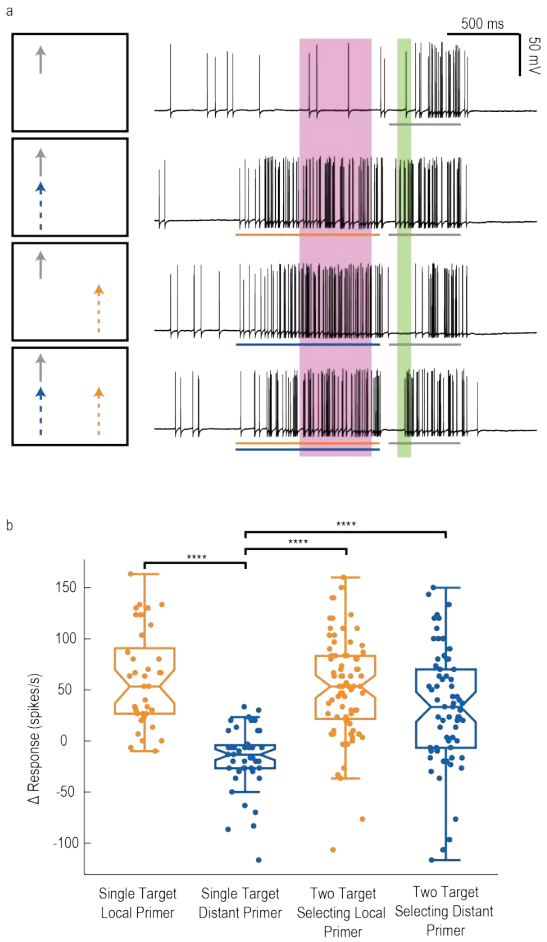

Figure 6-3: Facilitation of probe responses following two simultaneous primers. a) Examples of stimulus paradigms and neuronal responses from intracellular recordings in CSTMD1. Probes are presented either alone, or following one of three priming conditions. Primer selection is determined by continuous 1-D wavelet transform across a 500 ms window (pink shaded area), and the magnitudes of probe responses are quantified in a 100 ms window (green shaded area). b) The effects of different priming conditions on responses for CSTMD1 to a uniform probe stimulus. Boxplots represent mean, interquartile range, max and min (excluding outliers) while notches show our 95% confidence interval. **** displays p value < 0.0001 (263 trials from 9 dragonflies).

While on average we observe strong facilitation of probe responses when the more distant of the two primers was selected, we do note an increase in variability relative to other conditions. To investigate this further, we plot relative frequency histograms for the data presented in figure 3b (Figure 4a). In single target trials our results were very consistent; local primers almost invariably resulted in an increase in probe

response while distant primers cause a decrease. Increases in response had a broader distribution, possibly because in some neurons response saturation can limit the strength of facilitation observed. When two primers are simultaneously presented and the local primer is selected the distribution of probe responses closely matches that of single local primer examples (Yellow solid and dashed lines). However when the distant primer is selected, the distributions are less accurately matched, with an increased frequency of inhibited responses. This could be explained if in some cases an unselected primer enhanced responses, and in other cases inhibited them. To support this idea we performed a linear combination fit, where different weightings of the distributions of single primer trials, either local or distant, were combined to identify the best fit to our two-target distributions (figure 4b, fit = a*(Single Target Local Primer) + b*(Single Target Distant Primer). This process produced a model distribution that accurately fits our observed data (a = 0.7336 and b = 0.2471, R-squared = 0.984). While a conclusive description of this effect will require more experimentation, the current dataset hints that gain modulation by an unselected primer may be gated by an additional unidentified variable.

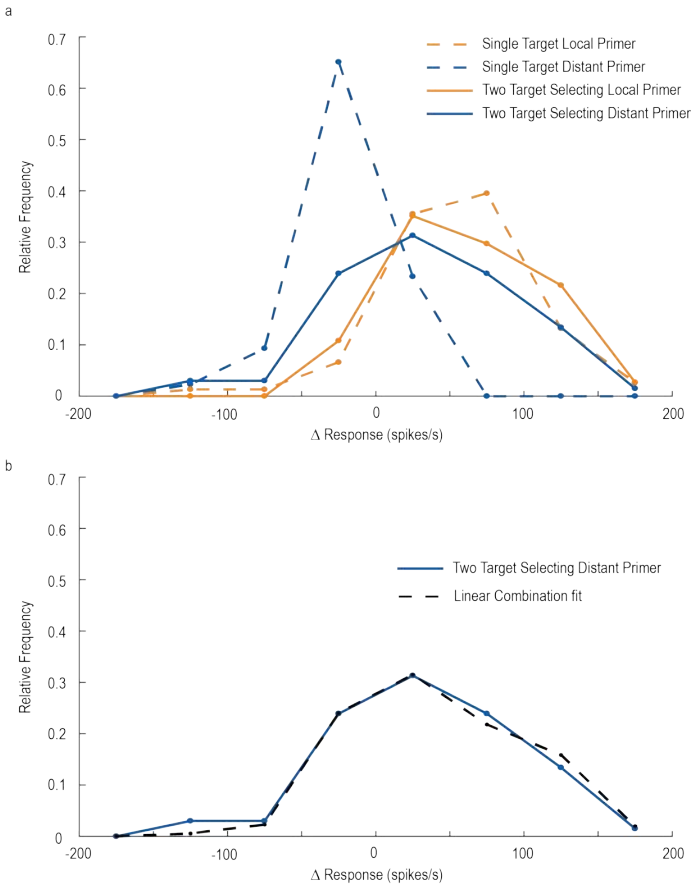

Figure 6-4: Relative frequency histograms for probe responses following different priming conditions. a) Data from each priming condition in figure 2b was grouped into 50 spike/s bins. Histogram values are plotted as lines to allow comparison between different distributions. b) Data for the Two Target Selecting Distant Primer condition plotted against a linear combination fit (data = 0.7336*Single Target Local Primer + 0.2471* Single Target Distant Primer, R-squared = 0.984).

6.4 Conclusions

Predictive gain modulation has been studied in detail within single target paradigms. Whilst the relationship between this effect and selective attention in CSTMD1 has been a fascinating discussion point in our recent work, our ability to design experiments that explore this relationship have been limited by our inability to identify which priming target had been selected.

The recent development of a frequency tagging technique for intracellular recordings in STMD neurons has allowed us to answer this question. Our data for single-target paradigms accurately matches findings in previous studies, where CSTMD1's

receptive field is dynamically re-organised to enhance targets presented in ‘expected’ locations. However, when we present two primers simultaneously we observe strong gain modulation for probe targets irrespective of whether the ‘local’ or ‘distant’ priming target is selected. This suggests that target selection and gain modulation are separate, decoupled processes. Thus, gain modulation most likely serves as a mechanism for improving signal-to-noise ratio during target detection, whilst target selection occurs at a later stage of visual processing. However, future work should investigate the facilitation of probe responses by unattended stimuli in more detail. Ideally, these experiments would bias attention towards a distant primer by using temporal offsets in primer presentation.

7 Bar-sensitive neurons in the dragonfly lobula

Context

Visual features come in many shapes and sizes. The dragonfly lobula contains separate feature detecting neurons sensitive to small features and elongated bars (O'Carroll 1993). Unlike their small target-sensitive counterparts, bar-sensitive neurons have not been studied in detail since their initial description 24 years ago. While STMD neurons were the primary target of my electrophysiological recordings, in the process of gathering this data I commonly encountered bar-sensitive neurons (see figure 1, chapter 2). I took this opportunity to build a dataset that characterised the basic physiological properties of these neurons. The experiments presented in this chapter aimed to answer the following research questions:

1. How much variability do we observe in the basic physiological properties of bar-sensitive neurons?
2. How do bar-sensitive neurons respond to bars of different velocity and width?
3. How do bar-sensitive neurons respond to bars of different contrasts, and contrast polarities?

This chapter is not a published manuscript, but rather a less formal results chapter. For this reason it lacks a broad and detailed introduction that is covered in previous chapters. These data will form the basis of a first authored manuscript that will include additional datasets contributed by co-authors Karin Nordström, David O'Carroll, Steven Wiederman, Douglas Bolzon and Bernard Evans.

7.1 Introduction

The first report of feature detecting neurons in the dragonfly lobula described two fundamentally different classes of cells; Small target-sensitive (now known as STMDs) and bar-sensitive (O'Carroll 1993). In the 24 years since this description STMD neurons have been studied in detail, yet there has been no additional description of the bar-sensitive class in dragonflies.

As their name suggests, a bar-sensitive neuron provides optimal responses to an elongated bar drifting in its preferred direction and orientation. Unlike an STMD neuron, bar-sensitive neurons also commonly respond weakly to a grating stimulus (O'Carroll 1993). We certainly observe other neurons sensitive to gratings, which we previously classified as wide-field motion sensitive neurons similar to the wide-field motion sensitive Lobula Plate Tangential Neurons of flies (see chapter 3). Until now the key property used to distinguish between bar-sensitive and wide-field motion sensitive neurons was their relative responses to discreet bars and gratings. Wide-field motion sensitive neurons integrate input across 2 dimensions of a pattern, with responses increasing as the size and number of cycles in a pattern increases (Dvorak et al. 1980). However bar-sensitive neurons of dragonflies are stimulated optimally by the motion of the leading and trailing edges of a single feature. Here I have attempted to provide a description of bar-sensitive neurons in the dragonfly lobula.

7.2 Methods

Electrophysiological preparations were identical to those described in previous results chapters.

Visual Stimuli

All visual stimuli were presented on a LCD monitor (165 Hz). Upon establishing a health recording, all cells were presented with a characterising stimulus that included a moving texel pattern (a full-screen pattern of randomly distributed 1x1° black and white squares), drifting bars, and full screen flicker. Any cell that responded robustly to the drifting bars in this stimulus were defined as 'bar-sensitive' and included in our further analysis.

To measure velocity and width tuning we drifted black bars across a white background, with stimuli crossing the entire display in the preferred direction. To quantify contrast sensitivity we drifted 12x86° bars of different intensity at 50°/s against a background of mean intensity, allowing us to investigate responses for both positive and negative contrast polarities. We also presented an individual cell with edges (60x86°) and bars (6°) of 1.0 or -1.0 contrast, in order to isolate responses to the leading and trailing edges of a stimulus.

Data analysis

We fit a sinusoid to responses elicited by bars and patterns drifting in different directions. From this sinusoid we take the maximum (preferred direction response), minimum (anti-preferred direction response) and the phase (direction preference). We use these values, along with the mean spontaneous activity quantified in a 1 s pre-stimulation period preceding each stimulus presentation, to calculate direction opponency and direction selectivity indexes. Where R represents the spiking response, these indexes are defined as the following:

$$Direction\ Opponency\ Index = \frac{R_{Spontaneous} - R_{Anti-preferred}}{R_{Preferred} - R_{Spontaneous}}$$

$$Direction\ Selectivity\ Index = \frac{R_{Preferred} - R_{Anti-Preferred}}{R_{Preferred} + R_{Anti-Preferred}}$$

Analysis of our velocity and width tuning experiment was more complex, as there is no perfect way of choosing the correct analysis window across trials of different duration, especially across cells with different receptive field widths. We chose to quantify responses in a flexible time window matched to the duration a stimulus spent within any individual cells receptive field. This means that cells with broader receptive fields used longer analysis windows, and that within a given cell faster bars had shorter analysis windows than slower bars. Given the broad range of velocities presented, this method is more appropriate than using a window of fixed duration.

For our contrast experiment we analyse the first 200 ms of neuronal response, and attempted to avoid including any responses to the bars trailing edge which had the opposing contrast polarity.

7.3 Results

Bar-sensitive neurons represent a highly diverse population. Although our morphological data for bar-sensitive neurons is limited, anatomical similarities between the neurons we have observed are scarce (figure 1a). Bar-sensitive neurons can be efferent (cell 1) or afferent (cell 2). Both neurons presented here have broad arborisations in the sublobula similar to that of wide-field motion sensitive neurons (see chapter 3), however cell 1 also sends major projections into the outer layers of the primary lobula, and both cells have extensive projections within the lateral midbrain. The responses of bar-sensitive neurons can be spiking only, but often contain significant graded components (figure 1b). While by definition all bar-sensitive neurons respond to an elongated bar, the slope of a target height tuning curve of bar-sensitive neurons varies considerably between cells (figure 1c).

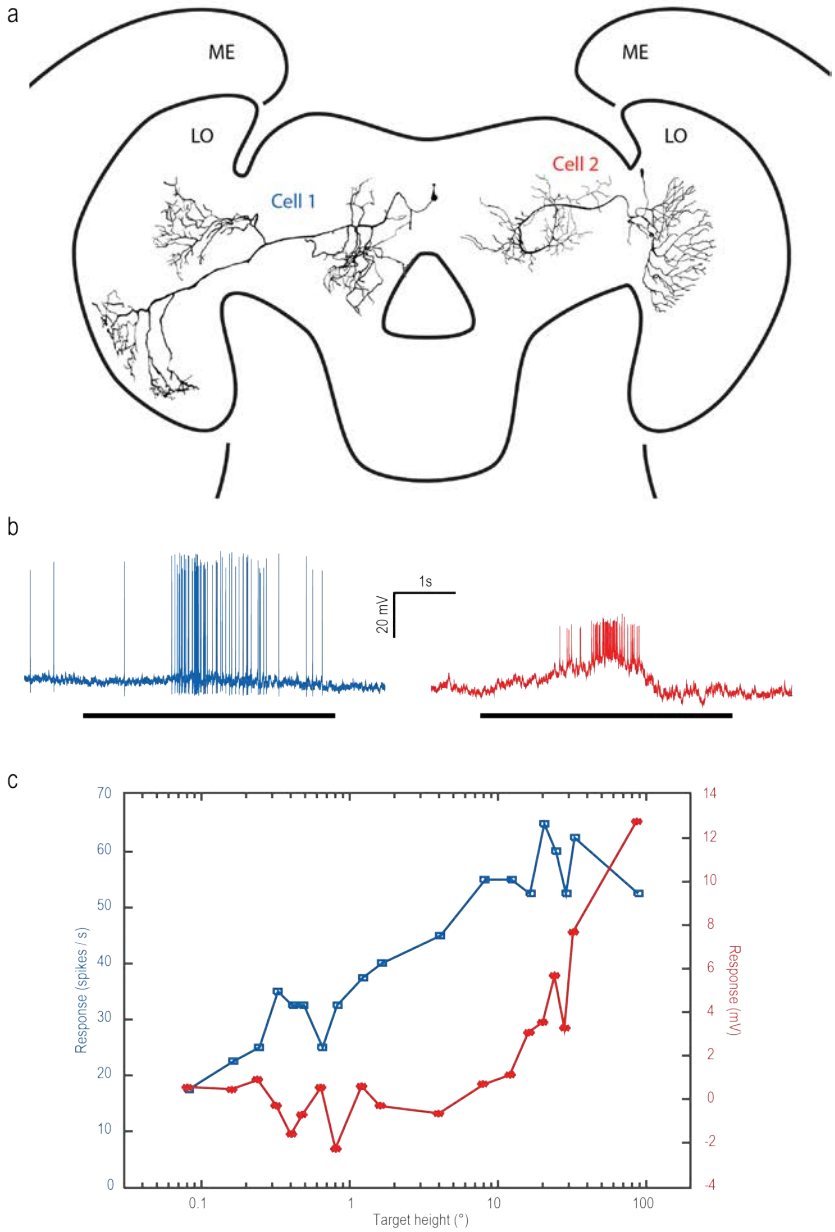

Figure 7-1: The morphology and physiology of two example bar-sensitive neurons. a) 2-D tracings of two lucifer yellow filled bar-sensitive neurons in the dragonfly lobula. b) Raw responses from the neurons shown in (a) in response to a 2x86° bar drifting in the neurons preferred direction. c) Height tuning curves from each neuron, produced by drifting a series 2° wide bars of varying height through the receptive field.

Given the diverse nature of bar-sensitive neurons, we attempted to classify a variety of cells into different subpopulations based on basic tuning properties. We presented 56 cells with a series of drifting bars, full-screen texel patterns and full screen flicker (figure 2a). While all cells in this dataset are sensitive to bars, we expect that some

may be better classified as wide-field motion sensing neurons. We initially expected that these cell types would be clearly distinguished by comparing responses to a full-screen texel pattern and single drifting bar. However instead of two distinct classes of cells, we observe a continuous distribution of cells with various sensitivities to each stimulus class (figure 2b). This suggests that the distinction between bar-sensitive and wide-field neurons may not be as clear as previously thought. Many of these neurons also give transient responses to full screen flicker (figure 2c). Individual cells often preferred one polarity of flicker to another, independent of their preference for bars or texel patterns. A key feature of both bar-sensitive neurons and wide-field motion sensitive neurons is their tuning for the direction of motion. To determine the direction preference of each cell we compare responses to bars and texel patterns moving in different directions (figure 2d). Points represent the preferred direction and the magnitude of response for a given stimulus in that direction. Direction preferences are relatively evenly distributed, covering all directions of motion. We calculated metrics for direction selectivity and direction opponency, for both bar and texel stimuli (figure 2e). Our opponency index (OI) quantifies the strength of inhibition in the anti-preferred direction, relative to the strength of excitation in the preferred direction. When a cell is stimulated in its anti-preferred direction, cells that are inhibited below spontaneous levels will have positive opponency values, while cells that are excited will have negative values. Conversely, our direction index (DI) compares the difference in response for stimuli in preferred and anti-preferred directions, relative to their sum. Almost all cells were at least weakly direction selective, with similar results observed when using a bar or texel pattern. Approximately half the cells were direction opponent, while the others were excited by motion in either direction (31 cells $OI > 0$, 25 cells $OI < 0$).

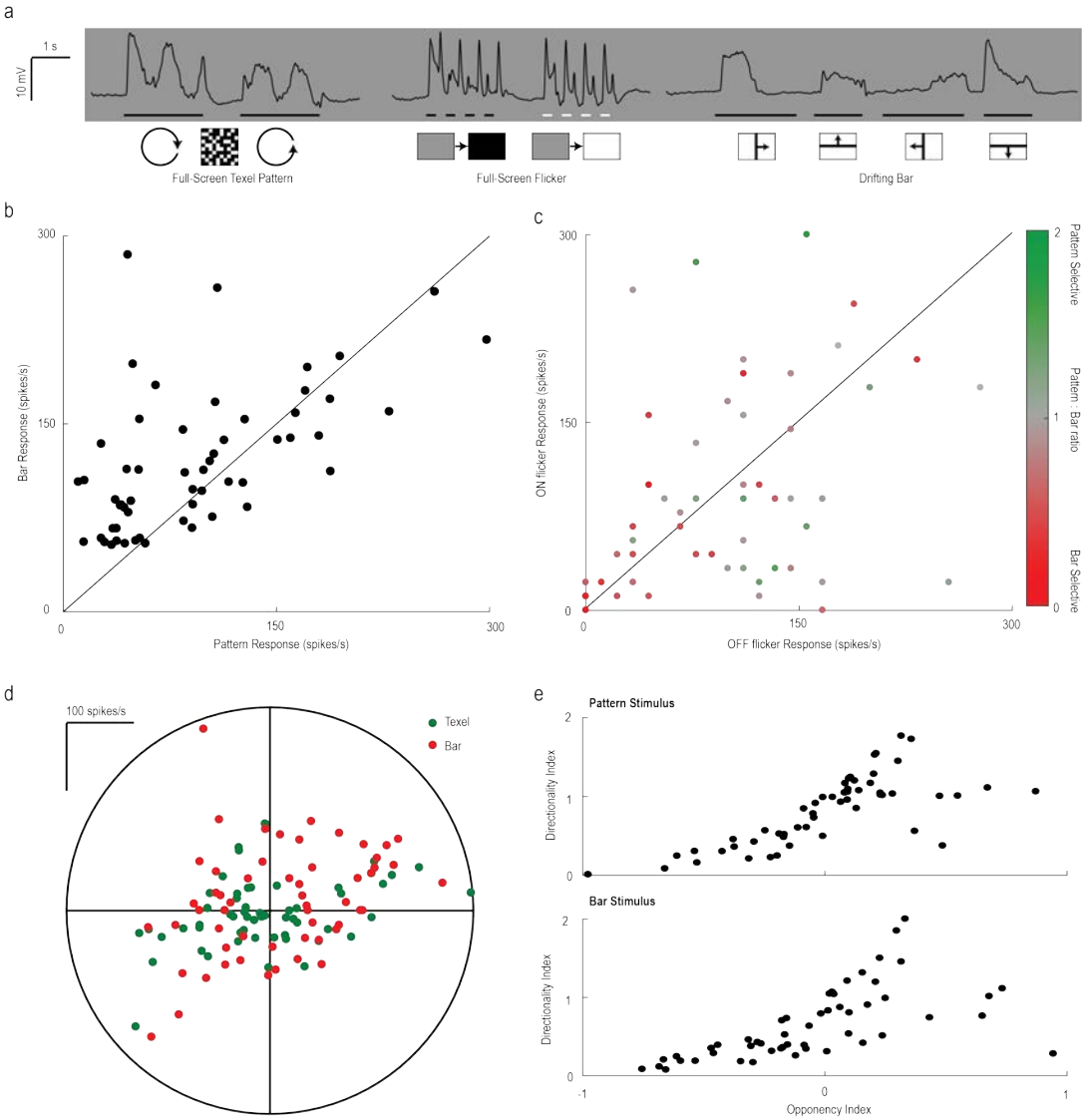

Figure 7-2: The diverse physiological properties of bar-sensitive neurons. a) 56 bar-sensitive neurons were presented with a series of stimuli including circular texel pattern motion, full-screen flicker and drifting bars. Stimulus bars represent peristimulus duration. b) Responses of each neuron to single bars and full screen texel patterns drifting in their preferred direction. c) A scatterplot showing the responses of each cell to the ON and OFF components of a full screen flicker. Data points are color-coded based on the ratio of their responses to a bar and full-screen texel pattern (b). d) The direction tuning of each cell in response to bars and patterns. Points represent the optimal direction, and the magnitude of responses to stimuli presented in that direction. This was performed in each cell with a single 2x86° bar (red points), and a full-screen texel pattern (green points). e) The direction opponency and direction selectivity indexes for each cell, measured with a texel pattern (top) and bar (bottom).

Next we investigated the responses of bar-sensitive neurons to bars drifting at different velocities and widths. STMD neurons are tuned to target velocity, with optimal responses observed for targets that drift at approximately 80°/s (Geurten et al. 2007). The velocity tuning of an STMD neuron is thought to be a result of the temporal delay filter in individual Elementary Small Target Motion Detector (ESTMD) units (Wiederman and O'Carroll 2008; Dunbier et al. 2011). For this reason velocity tuning in STMD neurons varies with target width (Geurten et al. 2007). However the ESTMD model produces inherently weak responses to elongated bars, due to the strong surround suppression from neighbouring units. Therefore it is more likely that bar-sensitive neurons have EMD-like inputs. Similarly to an ESTMD, the velocity tuning of an EMD is dependent on the temporal delay filter (Reichardt 1961). This means that cells with EMD-like inputs are also velocity tuned, with optimal velocities of approximately 100°/s (Dror et al. 2001).

Bars were drifted across the entire width of a LCD monitor at a series of different velocities and widths (figure 3a). Unlike most motion sensitive neurons reported in the insect visual system, the responses of bar-sensitive neurons steadily increases with increasing velocity. Neurons encoded velocity over the entire range presented, from 6°/s to more than 900°/s (figure 3b). Given the display refresh rate of 165 Hz, the maximum velocity presented already jumped 5.8° per frame. For this reason we did not attempt to increase bar velocity further to find the velocity at which response is optimal. However, it is clear that these neurons respond strongly to velocities that should not elicit a robust response in an EMD. It is possible that these neurons could integrate the outputs of many local flicker detectors that display fast temporal adaptation and lack spatial surround inhibition. However given that these neurons are commonly direction selective (figure 2e), such a model would require additional processing stages. It should also be noted that while the overwhelming majority of cells displayed extremely high velocity sensitivity, we did observe at least one cell in this dataset that displayed velocity tuning with an optimal of 100°/s, more suited to an EMD network (figure 3c). It is likely that this neuron had a fundamentally different input circuit, and may be better classified as a wide-field sensitive neuron.

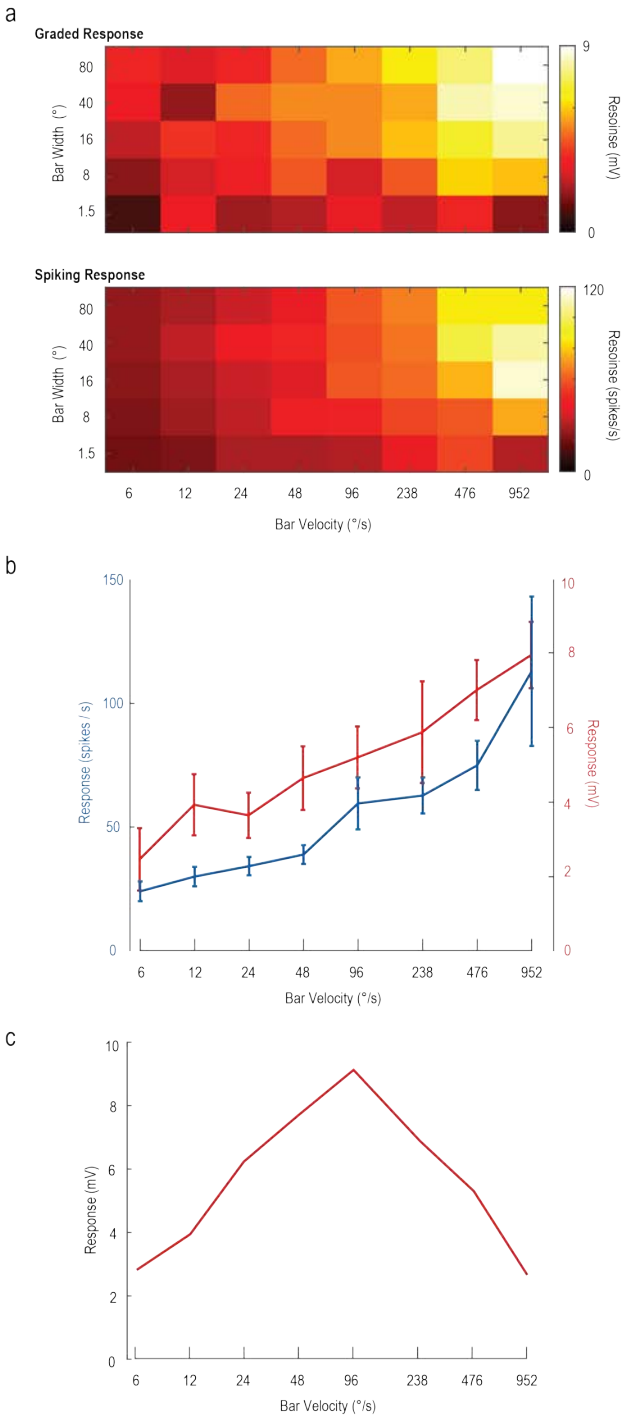

Figure 7-3: Responses to bars of different velocity and width. a) The mean responses of 18 bar-sensitive neurons to bars of different width drifting through the receptive field in the preferred direction at a series of velocities. Both graded (top) and spiking (bottom) responses are displayed for the dataset. b) An individual slice through (a) displaying the velocity sensitivity for a 16° wide bar. c) While most cells provided responses that increase with velocity, one individual cell display more usual velocity tuning profiles, with reduced response at high velocities.

Finally we invested the responses of bar-sensitive neurons to bars of different contrast. The contrast sensitivity functions of 4 bar-sensitive neurons are displayed, measured by drifting bars of different intensity against a mean background luminance (figure 4a). Cells 1-3 display relatively consistent and normal contrast sensitivity functions, although there was some minor variability in their sensitivity to different contrast polarities. However the sensitivity of cell 4 to bars of varying contrast were highly abnormal. Responses to both positive and negative contrasts peak at approximately 0.4, before a significant reduction in responses as contrast is increased further. In this paradigm the leading and trailing edges of a drifting bar represent two contrast boundaries of opposite polarity. This could potentially mask the underlying polarity sensitivity of individual cells. To separate this effect we compared the responses of a single neuron to bars and individual edges of different polarities. A drifting ON bar elicits a stronger response than an OFF bar (figure 4b). However this difference is exaggerated when we present ON and OFF edges. A single ON edge elicits a large and continuous response, which is only interrupted when the leading edge of the stimulus leaves the receptive field. Conversely, responses to an OFF edge drifting through the receptive field have a transient, bimodal appearance. Responses adapt rapidly, but build again shortly thereafter. Interestingly this second response peak occurs in a location that was not sensitive to ON edges, suggesting that the receptive field may contain separate and imperfectly aligned ON and OFF components. We observed similar results when the trailing edge of our ‘edge’ stimuli enters the receptive field with opposite polarity approximately 3 seconds into the trial. Interestingly the initiation of this second peak in response to an OFF stimulus correlates in time with the moment the edge leaves the ON sensitive component of the receptive field. Further data is required to identify whether this is simply a coincidence, or whether the fast adaptation of the OFF response may be a result of inhibitory interactions from ON sensitive pathways.

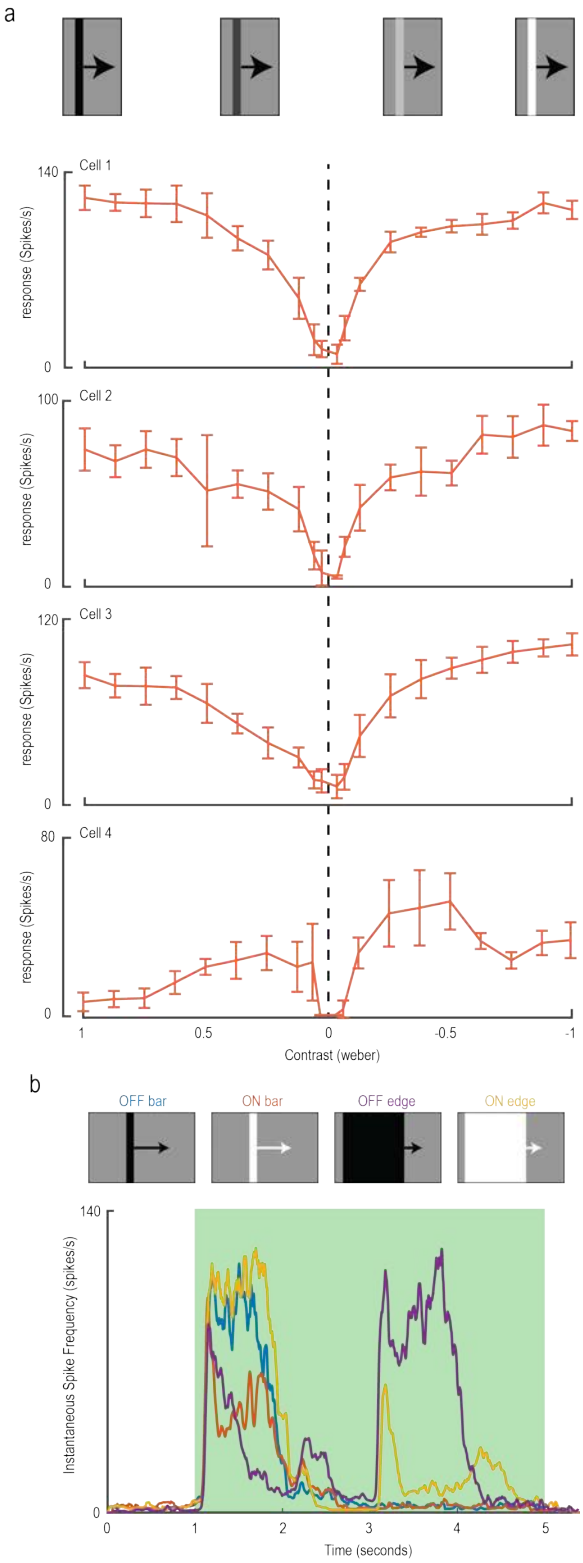

Figure 7-4: Responses to bars and edges of different contrast. a) The responses of four different cells to a 5° bar of different contrasts, both positive and negative. Data represents the mean ± SD across 4-7 trials within each cell. b) The response time-course of a bar-sensitive neuron presented with bars and edges of different contrast polarities.

7.4 Conclusions

The data presented here demonstrates that bar-sensitive neurons are a highly diverse cell class. Most neurons presented in this chapter display stronger responses to a discreet feature than a wide-field texel pattern, but the distinction between bar-sensitive and wide-field motion sensitive neurons is much less clear than we previously believed. One of the few consistent traits of these neurons is their abnormally fast velocity tuning. While our display technology prevented us from observing their true velocity optimum, it is at least 4 times faster than a male hoverfly HS cell (Barnett et al. 2010). Preliminary data also shows some interesting differences in response properties to ON and OFF edges, although a more comprehensive experiment is needed across more cells.

8 References

1. Albrecht, D. G., Geisler, W. S., Frazor, R. A., and Crane, A. M. (2002). Visual cortex of monkeys and cats: temporal dynamics of the contrast response function. *Journal of Neurophysiology* 88, 888–913.

2. Aptekar, J. W., Keles, M. F., Lu, P. M., Zolotova, N. M., and Frye, M. A. (2015). Neurons Forming Optic Glomeruli Compute Figure-Ground Discriminations in *Drosophila*. *Journal of Neuroscience* 35, 7587-7599.

3. Avidan, G., Harel, M., Hendler, T., Ben-Bashat, D., Zohary, E., and Malach, R. (2002). Contrast Sensitivity in Human Visual Areas and Its Relationship to Object Recognition. *Journal of Neurophysiology* 87, 3102-3116.

4. Barnett, P. D., Nordström, K., and O'Carroll, D. C. (2007). Retinotopic organization of small-field-target-detecting neurons in the insect visual system. *Current Biology* 17, 569-578

5. Barnett, P. D., Nordström, K., and O'Carroll., D. C. (2010). Motion Adaptation and the Velocity Coding of Natural Scenes. *Current Biology* 20, 994-999.

6. Bausenwein, B., Dittrich, A. P. M., and Fischbach, K, F. (1992). The optic lobe of *Drosophila* melanogaster. *Cell and Tissue Research* 267, 17-28.

7. Bennett, S. J., and Barnes, G. R. (2003). Human Ocular Pursuit During the Transient Disappearance of a Visual Target. *Journal of Neurophysiology* 90, 2504-2520.

8. Berry, M. J., Brivanlou, I. H., Jordan, T. A., and Meister, M. (1999). Anticipation of moving stimuli by the retina. *Nature* 398, 334-338.

9. Bolzon, D. M., Nordström, K., and O'Carroll, D. C. (2009). Local and Large-Range Inhibition in Feature Detection. *Journal of Neuroscience* 29, 14143-14150.

10. Brandt, R., Rohlfing, T., Rybak, J., Krofczik, S., Maye, A., Westerhoff, M., Hege, H., and Menzel, H. (2005). Three-Dimensional Average-Shape Atlas of the

Honeybee Brain and Its Applications. *Journal of Comparative Neurology* 492, 1-19.

11. Cajal, S. R., and Sanchez D (1915). Contribucion al conocimiento de los centros nerviosos de los insectes. *Trab Lab Invest Biol Univ Madrid* 13, 1-168.

12. Carrasco, M., Penpeci-Talgar, C., and Eckstein, M. (2000). Spatial covert attention increases contrast sensitivity across the CSF: support for signal enhancement. *Vision Research* 40, 1203-1215.

13. Chen, E. Y., Chou, J., Park, J., Schwartz, G., and Berry, M. J. (2014). The neural circuit mechanisms underlying the retinal response to motion reversal. *Journal of Neuroscience* 34, 15557-75.

14. Corbet, P. S. (1999). Dragonflies: Behavior and Ecology of Odonata. Ithaca: Cornell Univ Press.

15. Combes, S. A., Salcedo, M. K., Pandit, M. M., and Iwasaki, J. M. (2013). Capture success and efficiency of dragonflies pursuing different types of prey. *Integrative and comparative biology* 53, 787-798.

16. DeVoe, R. D., Kaiser, W., Ohm, J., and Stone, L. S. (1982). Horizontal movement detectors of honeybees: Directionally-selective visual neurons in the lobula and brain. *Journal of Comparative Physiology* 147, 155-170.

17. Dreyer, D., Vitt, H., Dippel, S., Goetz, B., el Jundi, B., Kolimann, M., Huetteroth, W., and Schachtner, J. (2010). 3D standard brain of the red flour beetle *Tribolium castaneum*: a tool to study metamorphic development and adult plasticity. *Frontiers in Systems Neuroscience* 4, 3.

18. Dror, R. O., O'Carroll., D. C., and Laughlin, S. B. (2001). Accuracy of velocity estimation by Reichardt correlators. *Journal of the Optical Society of America A* 18, 241-252.

19. Dunbier, J. R., Wiederman, S. D., Shoemaker, P. A., and O'Carroll, D. C. (2012). Facilitation of dragonfly target-detecting neurons by slow moving features on continuous paths. *Frontiers in neural circuits* 29, 6:79

20. el Jundi, B., Huetteroth, W., Kurylas, A.E., and Schachtner, J. (2009). Anisometric brain dimorphism revisited: implementation of a volumetric 3D standard brain in *Manduca sexta*. *Journal of Comparative Neurology* 517, 210–225.

21. El Jundi, B., Pfeiffer, K., Heinze, S., and Homberg, U. (2014). Integration of polarization and chromatic cues in the insect sky compass. *Journal of Comparative Physiology A* 200, 575-589.

22. Fischbach, K. F., and Dittrich, A. P. M. (1989). The optic lobe of *Drosophila melanogaster*. I: A. Golgi analysis of wild-type structure. *Cell and Tissue Research* 258, 441–475.

23. Geurten, B. R. H., Nordström, K., Sprayberry, J. D. H., Bolzon, D. M., and O'Carroll., D. C. (2007). Neural mechanisms underlying target detection in a dragonfly centrifugal neuron. *Journal of Experimental Biology* 210, 3277-3284.

24. Gilbert, C., and Strausfeld, N. J. (1991). The functional organization of male-specific visual neurons in flies. *Journal of Comparative Physiology A* 169, 395-411.

25. Gonzalez-Bellido PT, Peng H, Yang J, Georgopoulos AP, and Olberg RM. (2013). Eight pairs of descending visual neurons in the dragonfly give wing motor centers accurate population vector of prey direction. *Proceedings of the National Academy of Science U S A* 8, 696-701.

26. Gonzalez-Bellido, P. T., and Wardill, T. J. (2012). Labeling and Confocal Imaging of Neurons in Thick Invertebrate Tissue Samples. *Cold Spring Harbor Protocols.*

27. Guo A, and Reichardt W. (1987). An estimation of the time constant of movement detectors. *Naturwissenschaften* 74, 91-92

28. Harris, R. A., O'Carroll, D. C., and Laughlin, S. B. (2000). Contrast Gain Reduction in Fly Motion Adaptation. *Neuron* 28, 595-606.

29. Hassenstein, B., and Reichardt, W. (1956). Systemtheoretische Analyse Der Zeit, Reihenfolgen Und Vorzeichenauswertung Bei Der Bewegungsperzeption Des Rüsselkäfers Chlorophanus. *Zeitschrift für Naturforschung B* 11, 513-524.

30. Hausen, K. (1982). Motion Sensitive Interneurons in the Optopmotor System of the Fly. I. The Horizontal Cells: Structure and Signals. *Biological Cybernetics* 45, 143-156.

31. Heinze, S, and Reppert, S. M. (2012). Anatomical basis of sun compass navigation I: the general layout of the monarch butterfly brain. *Journal of Comparative Neurology* 520, 1599–1628.

32. Horridge, G. A. (1978). The separation of visual axes in apposition compound eyes. *Philosophical Transactions of the Royal Society London B Biological Sciences* 285, 1-59.

33. Ibbotson, M. R. (1991). Wide-field motion-sensitive neurons tuned to horizontal movement in the honeybee, *Apis mellifera*. *Journal of Comparative Physiology A* 168, 91-102.

34. Immonen, E., Dacke, M., Heinze, S., el Jundi, B. (2017). Anatomical organization of the brain of a diurnal and a nocturnal dung beetle. *Journal of Comparative Neurology* 525, 1879–1908.

35. Ito, K., Shinomiya, K., Ito, M., Armstrong, J. D., Boyan, G., Hartenstein, V., Harzsch, S., Heisenberg, M., Homberg, U., Jenett, A., Keshishian, H., Restifo, L. L., Rössler, W., Simpson, J. H., Strauss, R., Vosshall, L. B., et al. (2014). Insect Brain Name Working Group. A systematic nomenclature for the insect brain. *Neuron* 19, 755-65.

36. Kastner, D. B, and Baccus, S. A. (2013). Spatial Segregation of Adaptation and Predictive Sensitization in Retinal Ganglion Cells. *Neuron* 79, 541-554.

37. Keleş, M. F. and Frye, M. A., (2017). Object-detecting neurons in Drosophila. *Current Biology 27*, 680-687.

38. Kinoshita, M., Shimohigasshi, M., Tominaga, T., Arikawa, K., and Homberg, U. (2015). Topographically Distinct Visual and Olfactory Inputs to the Mushroom Body in the Swallowtail Butterfly, *Papilio xuthus*. *Journal of Comparative Neurology* 523, 162-182.

39. Klagges, B. R., Heimbeck, G., Godenschwege, T. A., Hofbauer, A., Pflugfelder, G. O., Reifegerste, R., Reisch, D., Schaupp, M., Buchner, S., and Buchner, E. (1996). Invertebrate synapsins: a single gene codes for several isoforms in *Drosophila*. *Journal of Neuroscience* 16, 3154–3165.

40. Kvello, P., Løfaldli, B., Rybak, J., Menzel, R., and Mustaparta, H. (2009). Digital, three-dimensional average shaped atlas of the *Heliothis virescens* brain with integrated gustatory and olfactory neurons. *Frontiers in Systems Neuroscience* 3, 14.

41. Land, M. F, and Collett, T. S. (1974). Chasing behaviour of houseflies (*Fannia canicularis*). *Journal of Comparative Physiology* 89, 331-357.

42. Lee, J., and Maunsell, J. H. R. (2010). The effect of attention on neuronal responses to high and low contrast stimuli. *Journal of Neurophysiol*ogy 104, 960–971.

43. Letch, H., Gottsberger, B., and Ware, J. L. (2016). Not going with the flow: a comprehensive time-calibrated phylogeny of dragonflies (Anisoptera: Odonata: Insecta) provides evidence for the role of lentic habitats on diversification. *Molecular Ecology* 25, 1340-1353.

44. Lin, H. T., and Leonardo, A. (2017). Heuristic Rules Underlying Dragonfly Prey Selection and Interception. *Current Biology* 27, 1124-1137.

45. Maddess, T., and Yang, E. (1997). Orientation-sensitive Neurons in the Brain of the Honey Bee (Apis mellifera). *Journal of Insect Physiology* 43, 329-336.

46. Maisak, M. S., Haag, J., Ammer, G., Serbe, E., Meier, M., Leonhardt, A., Schilling, T., Bahl, A., Rubin, G. M., Nern, A. and Dickson, B. J. (2013). A directional tuning map of *Drosophila* elementary motion detectors. *Nature* 500, 212-216.

47. Mischiati, M., Lin, H., Herold, P., Imler, E., Olberg, R., and Leonardo, A. (2015). Internal models direct dragonfly interception steering. *Nature* 517, 333-338.

48. Misof, B., Liu, S., Meusemann, K., Peters, R. S., Donath, A., Mayer, C., Frandsen,

P. B., Ware, J., Flouri, T., Beute, R.G. et al. (2014). Phylogenomics resolves the timing and pattern of insect evolution. *Science* 346, 763-767.

49. Montgomery, S. H., and Ott, S, R. (2015). Brain Composition in *Godyris zavaleta*, a Diurnal Butterfly, Reflects an Increased Reliance on Olfactory Information. *Journal of Comparative Neurology* 523, 869–891.

50. Moran, J., and Desimone, R. (1985). Selective attention gates visual processing in the extrastriate cortex. *Science* 229, 782-784.

51. Mysore, S. P., Asadollahi, A., and Knudsen, E. I., (2011). Signaling of the strongest stimulus in the owl optic tectum. *The Journal of Neuroscience* 31, 5186-5196.

52. Mysore, S. P., and Knudsen, E. I. (2013). A shared inhibitory circuit for both exogenous and endogenous control of stimulus selection. *Nature Neuroscience* 16, 473-478.

53. Nässel, D. R. and Klemm, N. K. (1983). Serotonin-like immunoreactivity in the optic lobes of three insect species. *Cell and Tissue Research* 232, 129-140.

54. Nordström, K., and O'Carroll, D. C. (2009). Feature detection and the hypercomplex property in insects. *Trends in Neurosciences* 32, 383-391.

55. Nordström, K., Bolzon, D. M., and O'Carroll, D. C. (2011). Spatial facilitation by a high-performance dragonfly target-detecting neuron. *Biology Letters* 7, 588-592.

56. O'Carroll, D. C. (1993). Feature-detecting neurons in dragonflies. *Nature* 362, 541-543.

57. Olberg, R. M. (1986). Identified target-selective visual interneurons descending form the dragonfly brain. *Journal Comparative Physiology A* 159, 827-840.

58. Okamura, J-Y and Strausfeld, N. J. (2007). Visual system of calliphorid flies: Motion- and orientation-sensitive visual interneurons supplying dorsal optic glomeruli. *Journal of Comparative Neurology* 500, 189–208.

59. O'Shea, M., and Rowell, C. H. F. (1975). Protection from habituation by lateral inhibition. *Nature* 254, 53-55.

60. Ott, S. R. (2008). Confocal microscopy in large insect brains: Zinc-formaldehyde fixation improves synapsin immunostaining and preservation of morphology in whole-mounts. *Journal of Neuroscience Methods* 172, 220-230.

61. Pestilli, F., and Carrasco, M. (2005). Attention enhances contrast sensitivity at cued and impairs it at uncued locations. *Vision Research* 45 1867-1875.

62. Polat, U., Mizobe, K., Pettet, M. W., Kasamatsu, T., and Norcia, A. M. (1998). Collinear stimuli regulate visual responses depending on cell's contrast threshold. *Nature* 391, 580-584.

63. Posner, M. I., and Cohen, Y. (1984). Components of visual orienting. *Attention and Performance X: Control of Language Processes* 32, 531–556.

64. Preibisch, S., Saalfeld, S., and Tomancak, P. (2009) Globally optimal stitching of tiled 3D microscopic image acquisitions. *Bioinformatics* 25, 1463-1465.

65. Pritchard, G. (1966). On the morphology of the compound eyes of dragonflies (Odonata: Anisoptera), with special reference to their role in prey capture. *Physiological Entomology* 41, 1-8.

66. Rao, R. P. N., and Ballard, D. H. (1999). Predictive coding in the visual cortex: a functional interpretation of some extra-classical receptive-field effects. *Nature Neuroscience* 2, 79-87.

67. Rein, K., Zöckler, M., Mader, M.T., Grübel, C., and Heisenberg, M. (2002). The drosophila standard brain. *Current Biology* 3, 227-231.

68. Reynolds, J. H., Pasternak, T., and Desimone, R. (2000). Attention Increases Sensitivity of V4 Neurons. *Neuron* 26, 703-714.

69. Ribi, W. A., and Scheel, M. (1981). The second and third optic ganglia of the worker bee. *Cell and Tissue Research* 221, 17-43.

70. Rigosi, E., Wiederman, S. D., and O'Carroll., D. C. (2017). Photoreceptor signalling constrains the detection of small, moving targets in four flying insect species. *Journal of Experimental Biology*, under review.

71. Rosner, R., von Haldeln, J., Salden, T., and Homberg, U. (2017). Anatomy of the lobula complex in the brain of the praying mantis compared to the lobula complexes of the locust and cockroach. *Journal of Comparative Neurology* 525, 2343-2357.

72. Schwartz, G., Harris, R., Shrom, D., and Berry, M. J. (2007). Detection and prediction of periodic patterns by the retina. *Nature Neuroscience* 10, 552-554.

73. Shinomiya, K., Takemura, Shin-ya., Rivlin, P. K., Plaza, S. M., Scheffer, L. K., and Meinertzhagen, I, A. (2015). A common evolutionary origin for the ON-and OFF-edge motion detection pathways of the Drosophila visual system. *Frontiers in Neural Circuits* 9, 33.

74. Slagter, H. A., Prinssen, S., Reteig, L. C., and Mazaheri, A. (2016). Facilitation and inhibition in attention: Functional dissociation of pre-stimulus alpha activity, P1, and N1 components. *NeuroImage* 125, 25-35.

75. Strausfeld, N. (2009). Brain organization and the origin of insects: an assessment. *Proceedings of the Royal Society B* 276, 1929-1937.

76. Strausfeld, N. (1970). Golgi studies on insects. Part II. The optic lobes of diptera. *Philosophical Transactions of the Royal Society of London Series B, Biological Sciences* 258, 135–223.

77. Strausfeld, N. (2005). The evolution of crustacean and insect optic lobes and the origins of chiasmata. *Athropod Structure and Development* 34, 235-256.

78. Stöckl, A., Heinze, S., Charalabidis, A., el Jundi, B., Warrant, E., and Kelber, A. (2016). Differential investment in visual and olfactory brain areas reflects behavioural choices in hawk moths. *Scientific Reports* 6, 26041.

79. Sztarker, J., Strausfeld, N. J., and Tomsic, D. (2005) Organization of optic lobes that support motion detection in a semiterrestrial crab. *Journal of Comparative*

Neurology 493, 396-411.

80. Takemura, S. Y., Bharioke, A., Lu, Z., Nern, A., Vitaladevuni, S., Rivlin, P. K., Katz, W. T., Olbris, D. J., Plaza, S. M., Winston, P., and Zhao, T. (2013). A visual motion detection circuit suggested by *Drosophila* connectomics. *Nature* 500, 175-181.

81. Vitzthum, H., Müller, M., and Homberg, U. (2002). Neurons of the Central Complex of the Locust *Schistocerca gregaria* are Sensitive to Polarised Light. *Journal of Neuroscience* 22, 1114-1125.

82. Watamaniuk, S. N. J., and McKee, S. P. (1995). Seeing motion behind occluders. *Nature* 377, 729-730.

83. Watamaniuk, S. N. J., McKee, S. P., and Grzywacs, N. M. (1995). Detecting a Trajectory Embedded in Random direction Motion Noise. *Vision Research* 35, 65-77.

84. Wendt, B, and Homberg, U. (1992). Immunocytochemistry of dopamine in the brain of the locust Schistocerca gregaria. *Journal of Comparative Neurology* 321, 387–403.

85. Wiederman, S. D., Fabian, J. M., Dunbier, J. R., and O'Carroll., D. C. (2017). A predictive focus of gain modulation encodes target trajectories in insect vision. *eLife* 6, e26478.

86. Wiederman, S. D., Shoemarker, P. A., and O'Carroll, D. C. (2008). A model for the detection of moving targets in visual clutter inspired by insect physiology. *PLOS ONE* 3, e2784

87. Wiederman, S. D., and O'Carroll, D. C. (2011). Discrimination of features in natural scenes by a dragonfly neuron. *Journal of Neuroscience* 31, 7141-7144

88. Wiederman, S. D., Shoemaker, P. A., and O'Carroll, D. C. (2013). Correlation between OFF and ON channels underlies dark target selectivity in an insect visual system. *Journal of Neuroscience* 33, 13225-13232

89. Wiederman, S. D, and O'Carroll, D. C. (2013). Selective Attention in an Insect Visual Neuron. *Current Biology* 23, 156-161.

90. Wiederman SD, Dunbier JR, Fabian JM, Evans BJE, O'Carroll DC. 2017. Stimulus scripts and sequences. https://github.com/swiederm/predictive-gain

91. Zawarzin, A. (1914). Histologische Studien über Insekten. IV. Die optischen Ganglien der Aeschna- Larven. *Zeitschrift fur wissenschaftliche Zoologie* 108, 175-257

92. Zirnsak, M., Steinmetz, N. A., Noudoost, B., Xu, K. Z., and Moore, T. (2014). Visual space is compressed in prefrontal cortex before eye movements. *Nature* 507, 504 – 507.

9 Conclusions

9.1 The organization of optic lobe of dragonflies

Prior to this work the organisation of the dragonfly optic lobe was poorly understood. The most detailed investigation was more than 100 years old, and more recent reports in the literature were inconsistent with the original description (Zawarzin. 1914; Strausfield. 2005; Ito et al. 2014). Despite knowing little about its organisation, neurons in the dragonfly lobula complex have been studied in detail over the last 25 years. The results presented in chapter 3 represent the first modern detailed description of the dragonfly optic lobe. This data identifies 6 different subunits within the lobula complex, and characterised the physiological functions of several neuron classes found in different subunits. These neuron classes include multiple classes of STMD neurons, as well as a class of neurons analogous to the LPTCs in diptera. This provides a framework that will aid our future investigations into the neuronal circuitry underlying both target detection and motion detection in the dragonfly. Furthermore, this data may have significant implications into our understanding of the evolution of visual neuropil in the insect lobula complex. Strausfield (2005) has stated that the sublobula of the bee is supplied by homologues of T4 neurons, and is homologous with the lobula plate in diptera. This idea was supported by the fact that no insect had been found to have both a lobula plate and sublobula. However now that we have shown that the dragonfly does contain both structures, the evolutionary origins of the sublobula and its homology with the lobula plate may need to be revisited.

9.2 Predictive gain modulation in STMD neurons

In the years leading up to this project significant progress was made in our understanding of the physiological properties of STMD neurons. The key findings were the identification and basic characterisation of a neuronal facilitation mechanism in CSTMD1 (Nordström et al. 2011; Dunbier et al. 2011; Dunbier et al. 2012), and the description of competitive selection of a single target when presented with multiple alternatives (Wiederman and O'Carroll. 2013). The key objective of my project was to expand our understanding of neuronal facilitation, and identify whether it represented a mechanism of selective attention. In chapter 4 I demonstrated that this facilitation was significantly more complex than initially proposed. A target that drifts

on a continuous trajectory produces local increase in sensitivity, combined with a global suppression of response to targets presented elsewhere. Because of this we use the more general term gain modulation. This work also demonstrated that this modulation generated strong direction selectivity that matched a targets direction of motion, and resulted in a large improvement in contrast sensitivity. These observations are remarkably similar to findings in mammalian neurons when attention is cued for a particular region of space (Reynolds et al. 2000). While physiological responses of responses to a single target in the absence of any attentional cue cannot be interpreted as attention, the combination of local contrast gain surrounded by global suppression did hint of a relationship with attention.

While previous work provided detailed descriptions of how a particular primer affects probes of different locations, contrasts or directions, we still knew very little about what makes a primer strong or weak. In chapter 5 I characterised how different primer parameters affect the strength of gain increases, and the position and propagation of the focus across time following occlusions. I showed that primers moving at velocities close to CSTMD1's optimal range were the most effective at enhancing responses to the probes that follow. This was despite each primer covering different total distances, across different periods of time. Previous work had characterised facilitation as a process that was primarily dependent on the duration of a trajectory, reporting a t50 of approximately 160 ms (Nordström et al. 2011). However this work suggests that duration is just one of multiple parameters that determine the strength of gain, and thus the t50 would be expected to vary with different stimulus velocities, sizes or directions.

9.3 Selective attention and predictive gain modulation

When presented with multiple targets within the receptive field, one target elicits a response whilst the other is ignored (Wiederman and O'Carroll. 2013). Attention is commonly described as a spotlight, where stimuli within an 'attentional spotlight' are detected while stimuli outside this spotlight are ignored. A drifting primer produces gain modulation across the receptive field that resembles such a spotlight, leading us to hypothesise that this gain modulation may represent a mechanism of target selection. In chapter 6 we found that in most cases, an unattended priming target still resulted in predictive gain modulation. This is strong evidence against predictive gain modulation representing a major mechanism underlying selective attention.

9.4 Bar-sensitive neurons in the dragonfly lobula

Small targets represent just one of multiple classes of features. The ability to detect the velocity low frequency patterns in a scene could be highly beneficial to an animal that flies at high speed through hazardous environments. Bar-sensitive neurons of dragonflies are an understudied and poorly understood cell type. In chapter 7 I described physiological properties of a population of bar-sensitive neurons. These neurons showed diverse responses to many stimuli paradigms, and encoded stimulus velocity over an enormously broad range. These cells may represent part of a circuit that computes the velocity of ego-motion. While more work is needed, this data has provided substantial insight into this system that will help in the design of future experiments.

9.5 Limitations of this work

The majority of the work presented here are results of presenting immobilised dragonflies with classical visual stimuli in a dark, unrealistic visual environment. The target-detecting circuits of the dragonfly brain evolved for performance in nature, where a behaving dragonfly is able to interact with the visual stimuli that they detect. At this time technology does not permit us to perform long and healthy electrophysiological recordings from STMD neurons in a behaving animal. While we can present classical stimuli in a controlled environment and characterise the responses of neurons, we cannot know how these responses might differ in nature. We know that in flies the gain and velocity tuning of motion sensitive visual neurons change during locomotion (Maimon et al. 2010; Chiappe et al. 2010; Jung et al. 2011). There is also evidence that motor behaviour such as body saccades affect the responses of target selective neurons (Kim et al. 2015). In the future it may be possible to investigate how similar behaviours modulate STMD neuron responses in the dragonfly.

Similarly, in several chapters of this thesis I refer to ‘natural’ or ‘realistic’ target trajectories. These statements are based on several assumptions, some of which are yet to be rigorously tested. Thanks to recent work from Mischiati et al (2015) and Lin and Leonardo (2017) we have reasonably detailed knowledge about the movements of a target across the retina during pursuit. However the initial detection and selection of

a target must occur at an earlier stage, before pursuit is initiated. The target detection and target pursuit stages of dragonfly prey capture represent completely different tasks, and the characteristics of 'natural' target trajectories will differ considerably between the two. Both STMDs in the lobula, and TSDNs in the ventral nerve cord require a target to drift across the retina, however during prey pursuit a targets position on the retina is relatively stable (O'Carroll. 1993; Olberg, 1986; Mischiati et al. 2015). Therefore these systems are most likely involved in the target detection stage of pursuits, and are less suited to playing a significant role during the final pursuit of a target.

9.6 Future Directions

The work presented in this thesis answers several questions regarding the dragonfly visual system, but raises many more. Perhaps the most obvious question raised by this work relates to the physiological function of different layers and subunits in the dragonfly optic lobe. While recent progress into the connectomics of visual pathways in the fruit fly is extremely exciting for invertebrate vision science, the 21 layers in the dragonfly medulla and a lobula complex formed of 6 subunits represents an entire new frontier.

As for predictive gain modulation, this thesis has provided a substantial amount of data regarding increases in gain. However some of the most fundamental questions regarding these effects remain largely unanswered. One obvious question is how long does this effect last after target motion terminates? We know that gain at the last seen target position decreases over time following target termination (See chapters 4 and 5), but we have never presented a pause long enough to observe sensitivity returning to the unfacilitated state. Additionally, while we studied gain increases in detail, the corresponding surrounding inhibition has received much less attention (no pun intended). We have limited knowledge of the mechanisms that build this inhibition, or how long it persists. Experiments including backwards jumps and target reversals in chapters 4 and 5 give us a foundation that should inform future experimental designs.

There are also interesting follow-up experiments regarding interactions between gain modulation and selective attention. While it is unlikely that gain modulation is the mechanism of selective attention, it is still possible that gain modulation from a prior trajectory could bias target selection in the future. Furthermore, detailed comparisons

between the gain produced by selected and unselected targets could be informative for pinpointing the position in the visual pathway where this gain modulation occurs.

Finally, the data from bar-sensitive neurons presented in chapter 7 leaves many questions unanswered. Future work should model different motion sensitive pathways that could account for the velocity encoding properties of these bar-sensitive neurons. In addition, my data suggests that a detailed characterisation of the temporal dynamics of responses to ON and OFF contrast boundaries may be of interest.

9.7 References

1. Chiappe, M. E., Seelig, J. D., Reiser, M. B., and Jayaraman, V. (2010). Walking modulates speed sensitivity in *Drosophila* motion vision. *Current Biology* 20, 1470-1475.

2. Dunbier, J. R., Wiederman, S. D., Shoemaker, P. A., and O'Carroll, D. C. (2012). Facilitation of dragonfly target-detecting neurons by slow moving features on continuous paths. *Frontiers in neural circuits, 6.*

3. Dunbier, J. R., Wiederman, S. D., Shoemaker, P. A., and O'Carroll, D. C. (2011). Modelling the temporal response properties of an insect small target motion detector. *Intelligent Sensors, Sensor Networks and Information Processing* 125-130.

4. Ito, K., Shinomiya, K., Ito, M., Armstrong, J. D., Boyan, G., Hartenstein, V., Harzsch, S., Heisenberg, M., Homberg, U., Jenett, A., Keshishian, H., Restifo, L. L., Rössler, W., Simpson, J. H., Strauss, R., Vosshall, L. B., et al. (2014). Insect Brain Name Working Group. A systematic nomenclature for the insect brain. *Neuron* 19, 755-65.

5. Jung, S. N., Borst, A., and Haag, J. (2011). Flight Activity Alters Velocity Tuning of Fly Motion-Sensitive Neurons. *The Journal of Neuroscience* 31, 9231-9237.

6. Kim, A. J., Fitzgerald, J. K., and Maimon, G (2015). Cellular evidence for efference copy in *Drosophila* visuomotor processing. *Nature Neuroscience* 18, 1247-1255.

7. Lin, H. T., and Leonardo, A. (2017). Heuristic Rules Underlying Dragonfly Prey Selection and Interception. *Current Biology* 27, 1124-1137.

8. Maimon, G., Straw, A. D., and Dickinson, M. H. (2010). Active flight increases the gain of visual motion processing in *Drosophila*. *Nature Neuroscience* 13, 393-399.

9. Mischiati, M., Lin, H., Herold, P., Imler, E., Olber, R., and Leonardo, A.

(2014). Internal models direct dragonfly interception steering. *Nature* 517, 333-338.

10. Nordström, K., Bolzon, D. M., and O'Carroll, D. C. (2011). Spatial facilitation by a high-performance dragonfly target-detecting neuron. *Biology Letters. 7*, 588-592.

11. O'Carroll, D. C. (1993). Feature-detecting neurons in dragonflies. N*ature* 362, 541-543.

12. Olberg, R. M., (1986). Identified target-selective visual interneurons descending from the dragonfly brain. *Journal of Comparative Physiology A* 159, 827-840.

13. Reynolds, J. H., Pasternak, T., and Desimone, R. (2000). Attention Increases Aensitivity of V4 Neurons. *Neuron* 26, 703-714.

14. Strausfeld, N. (2005). The evolution of crustacean and insect optic lobes and the origins of chiasmata. *Athropod Structure and Development* 34, 235-256.

15. Wiederman, S. D., and O'Carroll, D. C., (2013). Selective attention in an insect neuron. *Current Biology* 23, 156-161.

16. Zawarzin, A. (1914). Histologische Studien über Insekten. IV. Die optischen Ganglien der Aeschna- Larven. *Zeitschrift fur wissenschaftliche Zoologie* 108, 175-257.